UNIVERSITÉ DU QUÉBEC À MONTRÉAL

EVALUATING AND FORECASTING DROUGHT-INDUCED TREE MORTALITY AND ITS IMPACTS ON CARBON DYNAMICS OF CANADA'S BOREAL FOREST

THESIS

PRESENTED IN PARTIAL

FULFILLMENT OF THE REQUIREMENT FOR

THE DOCTORAL DEGREE IN ENVIRONMENTAL SCIENCES

BY

QIUYU LIU

DECEMBER 2022

UNIVERSITÉ DU QUÉBEC À MONTRÉAL

ÉVALUATION ET PRÉVISION DE LA MORTALITÉ DES ARBRES CAUSÉE PAR LA SÉCHERESSE ET SES IMPACTS SUR LA DYNAMIQUE DU CARBONE DE LA FORÊT BORÉALE DU CANADA

THÈSE

PRÉSENTÉE

COMME EXIGENCE PARTIELLE

DU DOCTORAT EN SCIENCES DE L'ENVIRONNEMENT

PAR
QIUYU LIU

DÉCEMBRE 2022

ACKNOWLEDGEMENTS

This work was financially supported by the Fonds de recherche du Québec (FQRNT) program and the Natural Sciences and Engineering Research Council of Canada (NSERC) Discover Grant. I would also like to thank China Scholarship Council for funding my living expenses during my Ph.D. study.

I would like to gratefully and sincerely thank my supervisor, Dr. Changhui Peng, for his guidance, patience, and understanding during my Ph.D. study at the Université du Québec à Montréal (UQAM). I wish to thank my co-supervisor Dr. Daniel Kneeshaw. His academic guidance and assistance were very important to my Ph.D. research. I want to thank Dr.Robert Schneider, Dr. Dominic Cyr. As my Ph.D. committee members, they gave me great guidance and help during the past four years. At the same time, Dr. Nate G. McDowell has given me a lot of constructive comments, suggestions, and help during my Ph.D. research. I am very grateful for his work and input. I also appreciate the friendship and support of members of the Laboratory of Ecological Modelling and Carbon Science. I am thankful to numerous colleagues for their discussion and manuscript comments. I also would like to thank the entire Institut des Sciences de l'Environnement, UQAM, for providing an outstanding academic environment and supporting efforts.

Last but not least, I would like to thank my parents and my dear wife Ms. Hui Zhang. During the past four years of doctoral study, their support and encouragement have been my biggest motivation. I also want to thank my good friends Mr. Mingxi Du, and Ms. Beibei Sun for their care and encouragement, which helped me overcome many difficulties. In addition, I would like to thank my colleague and good friend David Grenier-Héon for his great help in my life in Canada over the past few years.

PREFACE

This dissertation is comprised of five chapters (three main articles) that present and discuss the simulation and forecasting of drought-induced tree mortality and its impacts on the carbon dynamics of Canada's boreal forest. All three papers involved in the dissertation are original contributions to my Ph.D. in Environmental Sciences at the Université du Québec à Montréal.

Chapters I and V are the general introduction and general conclusion, respectively. Chapters II to IV are correspondingly based on the following three publications:

1. **Liu, Qiuyu**, Changhui Peng, Robert Schneider, Dominic Cyr, Zelin Liu, Xiaolu Zhou, and Daniel Kneeshaw. "TRIPLEX-Mortality model for simulating drought-induced tree mortality in boreal forests: Model development and evaluation." *Ecological Modelling*. 455 (2021): 109652.
2. **Liu, Qiuyu**, Changhui Peng, Robert Schneider, Dominic Cyr, Nate G. McDowell and Daniel Kneeshaw. "Drought-induced increase in tree mortality and corresponding decrease in the carbon sink capacity of Canada's boreal forests from 1970 to 2020". G*lobal Change Biology.* (2022). (Under review)
3. **Liu, Qiuyu,** Changhui Peng, Robert Schneider, Dominic Cyr, Nate G. McDowell and Daniel Kneeshaw. "Forecasting drought-induced tree mortality and its impact on the biomass carbon sink of Canada's boreal forest by the end of the twenty-first century". (To be submitted)

Appendix I is the result of my Ph.D. comprehensive exam, which is a requirement for Ph.D. candidates and answers a topical question indirectly related to their dissertation. This paper is:

4. **Liu, Qiuyu,** Changhui Peng, Robert Schneider, Dominic Cyr, Zelin Liu, Xiaolu Zhou, Mingxi Du, Peng Li, Zihan Jiang, Nate G. McDowell and Daniel Kneeshaw. "Vegetation browning: Global drivers, impacts, and feedbacks" *Trends in Plant Science*. (2022). (Under review)

With the guidance of my Ph.D. supervisor, Dr. Changhui Peng, and co-supervisor Dr. Daniel

Kneeshaw, I developed all hypotheses and designed the new drought-induced tree mortality sub-model (TRIPLEX-Mortality) based on the TRIPLEX 1.0. I conducted the model validation and wrote the first article. After the model development, I applied the model, conducted model forecasting, and wrote the second and third articles. Dr. Robert Schneider and Dr. Dominic Cyr constantly advised and discussed with me about my Ph.D. project and commented on early versions of the manuscripts in this dissertation. Dr. Zelin Liu and Dr. Xiaolu Zhou helped to explain the TRIPLEX 1.0 model and discussed the programming problems. Dr. Nate G. McDowell substantially discussed and commented on the content of Chapter III and Chapter IV. All co-authors contributed comments and suggestions, greatly improving the quality of the articles.

TABLE OF CONTENTS

LIST OF FIGURES

LIST OF TABLES

RESUME

Les sécheresses associées aux changements globaux ont causé un accroissement important des taux de mortalité des arbres à travers la forêt boréale du Canada, générant des impacts profonds sur ses fonctions écosystémiques et son bilan du carbone. Ces impacts devraient augmenter en raison des sécheresses plus fréquentes, plus intenses et plus longues prévues dans le cadre des futurs changements climatiques. Étant donné le rôle critique de la forêt boréale du Canada dans l'albédo de surface et du bilan de carbone de la Terre, l'évaluation et la prévision de la mortalité des arbres induite par la sécheresse et de ses impacts sur la dynamique du carbone de cet écosystème ont suscité un intérêt considérable de la part des scientifiques et des décideurs dans les dernières décennies.

L'objectif général de cette recherche est d'améliorer notre compréhension et notre capacité à quantifier les impacts de la mortalité des arbres induite par la sécheresse sur la dynamique du carbone boréal au Canada. Plus précisément, cette étude vise à (1) développer un nouveau modèle basé sur le processus de mortalité des arbres boréaux induit par la sécheresse (TRIPLEX-Mortality); (2) Utiliser le modèle TRIPLEX-Mortality pour caractériser les changements spatio-temporels des taux de mortalité des arbres boréaux induits par la sécheresse et en quantifier les impacts sur le puits de carbone de la biomasse de 1970 à 2020; (3) Utiliser le modèle TRIPLEX-Mortality pour prévoir les taux de mortalité de ces arbres induits par la sécheresse et les impacts correspondants sur la dynamique du carbone dans le cadre du changement climatique futur.

Un nouveau sous-modèle TRIPLEX-Mortality piloté par les données climatiques a été développé sur la base du mécanisme avancé (défaillance hydraulique et carence de carbone). La validation du modèle de mortalité TRIPLEX par rapport aux observations tirées des parcelles d'échantillonnage permanentes a confirmé sa capacité fiable à simuler la mortalité induite par la sécheresse dans les forêts boréales du Canada. De 1970 à 2020, nous avons révélé qu'il y a une tendance à la hausse de la mortalité des arbres induite par la sécheresse avec une accélération depuis 2002, ainsi qu'un taux annuel moyen de mortalité des arbres est de 2.7 %. Environ 43 % des forêts boréales du Canada ont connu une augmentation significative de la mortalité des arbres (dont 71 % sont situés dans la

région ouest du pays). Cette augmentation a entraîné une perte de carbone significative à un taux approximatif de 1.51 ± 0.29 MgC ha^{-1} an^{-1} (intervalle de confiance à 95 %) avec une perte totale approximative de 0.46 ± 0.09 PgC par an (intervalle de confiance à 95 %) de 1970 à 2020. Il s'agit d'un énorme flux de carbone qui équivaut à environ 210 % des émissions annuelles totales de carbone du Canada. Nous prévoyons que la mortalité des arbres induite par la sécheresse (4.2 % ± 0.4 % ~ 7.2 % ± 0.4 %) et la réduction de la capacité en carbone de la biomasse (0.7 ± 0.06 Pg C an^{-1} ~1.29 ± 0.05 Pg C an^{-1}) causées par la mortalité devraient augmenter selon les différents scénarios de changement climatique. L'étendue spatiale de l'augmentation de la mortalité des arbres induite par la sécheresse augmente avec l'augmentation du forçage radiatif pour les scénarios SSP, en particulier pour la région de l'Ouest du Canada. Si les changements climatiques futurs suivent la trajectoire de forçage le plus pessemiste (scénario SSP5-8.5), la région de l'est de la forêt boréale du Canada risque également de perdre son rôle de puits de carbone.

Dans l'ensemble, le modèle TRIPLEX-Mortality est fiable pour estimer la mortalité des arbres induite par la sécheresse ainsi que pour évaluer leurs impacts sur la dynamique du carbone. Les sécheresses peuvent entraîner une augmentation continue de la mortalité et une perte importante de la capacité de carbone de la biomasse de la forêt boréale du Canada. La forêt boréale canadienne pourrait perdre son rôle de puits de carbone robuste, exacerbant le réchauffement climatique. Ce résultat pourrait fournir; a la fois une base solide pour orienter les stratégies de gestion forestière pour la santé de la forêt boréale du Canada et fournir de nouvelles perspectives sur la compréhension de la dynamique du carbone de la forêt boréale du Canada dans un monde en évolution.

ABSTRACT

Global-change-type drought has caused widespread tree mortality events in Canada's boreal forest, generating profound impacts on the function of ecosystems and carbon balance. These impacts are expected to increase due to more frequent, more intense, and longer droughts projected under future climate change. Given the critical role of Canada's boreal forest in Earth's surface albedo and global carbon budget, evaluating and forecasting drought-induced tree mortality and its impacts on the carbon dynamics of Canada's boreal forests has elicited considerable interest from scientists and policymakers.

The overall objective of this research is to improve our quantitative understanding of the impact of drought-induced tree mortality on Canada's boreal carbon dynamics. Specifically, (1) a novel drought-induced tree mortality process-based model (TRIPLEX-Mortality) was developed; (2) the TRIPLEX-Mortality model was used to characterize spatiotemporal changes in drought-induced tree mortality rates and quantify its impacts on the biomass carbon sink from 1970 to 2020; (3) the TRIPLEX-Mortality model was used to forecast drought-induced tree mortality rates and corresponding impacts on carbon dynamics under future climate change.

A new TRIPLEX-Mortality submodel driven by climate data was developed based on mechanisms advanced in the literature (hydraulic failure and carbon starvation). The validation of the model against observations derived from permanent sample plots confirmed the reliability of the TRIPLEX-mortality model in simulating drought-induced mortality in Canada's boreal forests and thus demonstrated that the model captured well the drought-induced mechanisms of mortality. From 1970 to 2020, we estimated that there is an increasing trend in drought-induced tree mortality with an acceleration since 2002, and an average annual tree mortality rate of 2.7%. Approximately 43% of Canada's boreal forests experienced a significant trend of increasing tree mortality (71% of which are located in the western region of the country). This increase in tree mortality has resulted in a significant carbon loss at an approximate rate of 1.51 ± 0.29 MgC ha^{-1} $year^{-1}$ (95%

confidence interval) with an approximate total loss of 0.46 ± 0.09 PgC per year (95% confidence interval) from 1970 to 2020. This is a huge carbon flux which is equivalent to approximately 210% of Canada's total annual carbon emissions. I forecast that drought-induced tree mortality (4.2 % ± 0.4 % ~ 7.2 % ± 0.4 %) and the reduction in biomass carbon capacity (0.7 ± 0.06 Pg C $year^{-1}$ ~1.29 ± 0.05 Pg C $year^{-1}$) caused by mortality are projected to increase across different climate change scenarios. The spatial extent of increased drought-induced tree mortality increases with the increase in radiative forcing for SSP scenarios, especially for the western region of Canada. If future climate change follows the high-end forcing pathway (SSP5-8.5 scenario), the eastern region of Canada's boreal forest also has a significant risk to lose its role as a robust sink of carbon.

Overall, the TRIPLEX-Mortality model is reliable to estimate drought-induced tree mortality and further evaluate the corresponding impacts on carbon dynamics. Droughts have and will continue to lead to an ongoing increase in mortality and significant loss in the biomass carbon capacity of Canada's boreal forest. Canadian boreal forest may lose their role as a sink of carbon, leading to significant positive climate feedback that exacerbates global warming. These results provide a solid basis to guide forest management strategies to maintain Canada's boreal forest health and provide new insights into the understanding of carbon dynamics of Canada's boreal forest in a changing world.

CHAPTER I

GENERAL INTRODUCTION

1.1. Background

1.1.1. Climate change, droughts and forest mortality

According to the sixth assessment report of the Intergovernmental Panel on Climate Change (IPCC, 2021), global surface temperature has increased by around 0.99 °C from 1850–1900 to the first two decades of the 21st century (2001–2020) and by around 1.09 °C from 1850–1900 to 2011–2020 (Fig. 1. 1 a and b) (IPCC, 2021; Arias et al., 2021). Compared with 1850-1900, the global mean surface temperature for the period 2081-2100 was projected to be nearly 1.4ºC higher under the low forcing scenario (i.e., shared socioeconomic pathway; SSP1-2.6), and about 4.5°C higher under the high forcing scenario SSP5-8.5 (IPCC, 2021; Arias et al., 2021). Rising temperatures associated with global warming will almost certainly exacerbate the effects of future droughts; when droughts occur, they will occur more quickly and with greater intensity (Cook et al., 2020; Trenberth et al., 2014). As mentioned in the assessment report of the Intergovernmental Panel on Climate Change (IPCC), "in general terms, drought is a prolonged absence or significant deficiency of precipitation, a 'deficiency of precipitation that results in a water shortage for some activity or for some group' or a 'period of abnormally dry weather sufficiently prolonged for the lack of precipitation to cause a serious hydrological imbalance" (IPCC, 2021).

Globally, drought is considered to be one of the most important stress factors affecting the carbon sink function of terrestrial ecosystems at both regional and global scales (Ciais et al., 2005; Zscheischler et al., 2014). From long-term positioning observations (Knapp et al., 2002; Phillips et al., 2009), field control experiments (Jentsch et al., 2011), carbon flux observations (Jentsch et al., 2011; Schwalm et al., 2010), and large-scale remote sensing observations (Zhao & Running, 2010), as well as model simulations (Zscheischler et al., 2014), a relatively consistent conclusion has been drawn that drought significantly

weakened the carbon sink function of ecosystems, and in some cases caused forests to become carbon sources. For instance, the 2003 droughts in Europe caused their forest ecosystems to release 0.5 Pg (petagram, 10^{15}g) of carbon into the atmosphere, offsetting the total sequestration in the previous four years (Ciais et al., 2005). Significant declines in forest carbon sink capacity caused by droughts have also been detected in boreal (Ma et al., 2012; Michaelian et al., 2011) and tropical forests (Yang et al., 2018).

The decrease in carbon sequestration and increase in carbon emissions from increased decomposition following tree mortality events will significantly impact the carbon cycle. One of the significant aspects of the impact of drought on the carbon cycle is region scale drought-induced tree mortality events, which can kill millions of trees in a short period of time. Canopy loss associated with tree mortality is expected to lead to sharp declines in carbon sequestration. In addition, the decomposition of standing and fallen aboveground biomass and underground roots from dead and dying forests leads to significant carbon emissions (Kurz et al., 2008). Widespread tree mortality events caused by drought are not limited to specific regions. For example, in Texas (Asner et al., 2016; Moore et al., 2016) and California (Asner et al., 2016), droughts have respectively led to the death of 300 million and over 100 million trees. In Australia, droughts in 2015 led to the death of more than 7000 ha of mangrove forests (Duke et al., 2017). Some drought-induced tree mortality events in Asia have been reported by Nakagawa et al., (2000) and Van et al., (2005). Drought-induced tree mortality events in tropical rainforests such as in 2005 in the Amazon, led to a noticeable increase in stem mortality (Phillips et al., 2009). The first global assessment of recent tree mortality attributed to drought and heat stress was presented by Allen et al., (2010) with this assessment showing the potential for amplified tree mortality due to drought impacts on forests worldwide. To date, drought-induced tree mortality events have been detected in boreal (Michaelian et al., 2011; Peng et al., 2011; Sánchez-Pinillos et al., 2022), tropical (Aleixo et al., 2019; Davidson et al., 2012; Monteiro et al., 2014; Zhou et al., 2014) and temperate forests (Carnicer et al., 2011; Matusick et al., 2013; Van Mantgem et al., 2009; Williams et al., 2013).

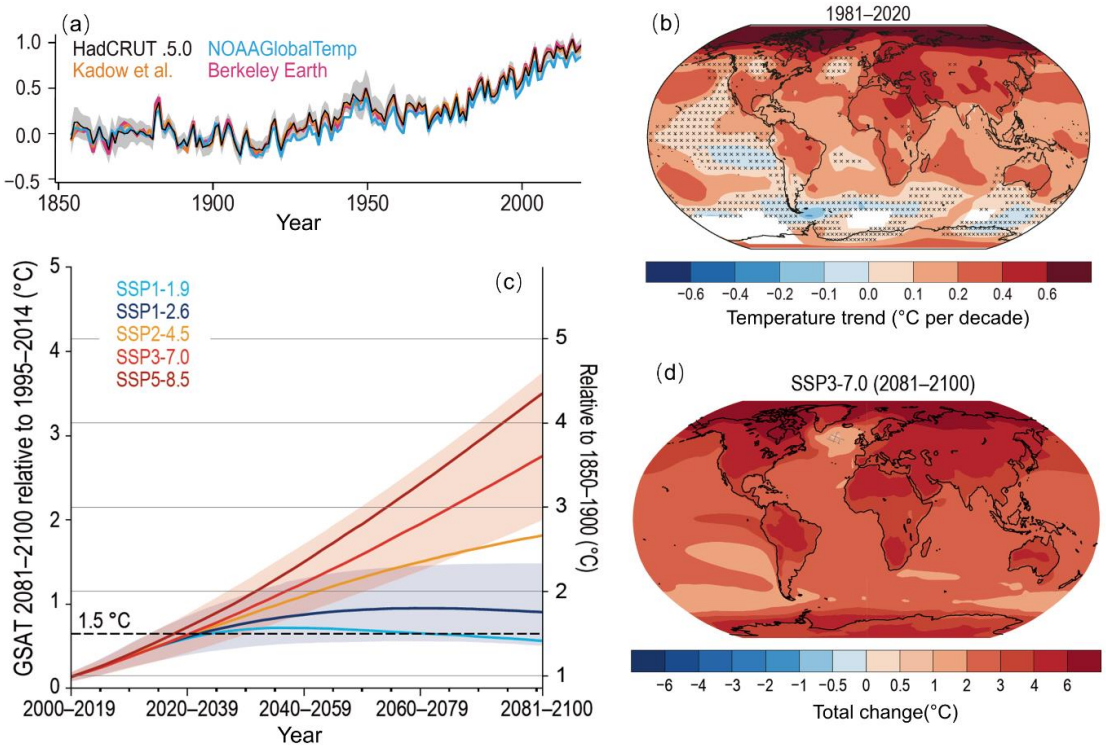

Figure 1. 1. Earth's surface temperature history and future. This figure was redrawn from the IPCC report, in 2021 (Arias et al., 2021). HadCRUT5 in (a) is Met Office Hadley Centre/Climatic Research Unit global surface temperature anomalies, version 5. NOAAGlobalTemp in (a) is the temperature derived from National Oceanic and Atmospheric Administration. GSAT in (c) is global surface air temperature.

1.1.2. Drought-induced tree mortality in Canada's boreal forests

Among all forest ecosystem types, boreal forests, are especially vulnerable to drought, due to the longevity of trees and the extent of the expected climate change within their life span (Goulden et al., 1998). To date, drought-induced tree die-off events in boreal forests have been widely reported (Hogg et al., 2008; Lenton et al., 2008; Michaelian et al., 2011; Peng et al., 2011; Sánchez-Pinillos et al., 2022). These events can substantially influence ecological regime shifts and ecosystem functioning of boreal forests at multiple scales (Adams et al., 2010; Ma et al., 2012; Michaelian et al., 2011; Wang et al., 2012). Although most boreal forests are resilient to extreme climate changes such as drought that are currently taking place, the predicted speed and extent of climate change are expected to be unprecedented. Subsequently, it will pose a significant threat to the tree communities and

ultimately to the health of this vital forest ecosystem (Gauthier et al., 2015). Canadian boreal forests, which occupy about 77% of Canada's total forest land, play a critical role in the Earth's surface albedo (Bonan, 2008) and global carbon budget (Kurz et al., 2008, 2013). The possibility of increased tree mortality in boreal forests is of particular interest because boreal forests have been identified as a critical "tipping element" in the Earth's climate system (Lenton et al., 2008) and are considered to be sensitive to drought impacts (Soja et al., 2007). Consequently, evaluating drought-induced mortality and its impacts on the carbon dynamics of Canada's boreal forests is of significant concern.

Recent progress on the impacts of drought on Canada's boreal forests includes detected massive trembling aspen (*Populus tremuloides*) mortality in western Canada using a combination of remote sensing and ground surveys (Michaelian et al., 2011). This massive mortality of aspen resulted in about 15 Tg carbon loss, which is equivalent to roughly 7% of Canada's annual anthropogenic carbon emissions (Michaelian et al., 2011). Using long-term forest permanent sampling plots, (Peng et al., 2011) revealed that drought-induced tree mortality rates experienced an increased trend from 1963 to 2008. Consequently, the huge reduction in the biomass carbon sink of Canada's boreal forests detected in long-term forest permanent sampling plots, suggests that Canada's boreal forests may lose their role as a robust sink of carbon (Ma et al., 2012). Despite such progress based on the plot-scale approaches, considerable uncertainty could appear when extrapolating data from plot-scale inventories to the entire Canadian boreal forest region (Huntingford et al., 2013). There is thus little empirical information available on spatiotemporal changes in tree mortality and associated impacts on biomass carbon dynamics in Canada's boreal forests. More importantly, given that many future droughts will almost certainly be worse under future climate change, little is known about how tree mortality and carbon sink capacity will be affected.

1.1.3. Simulating drought-induced tree mortality and its impact on carbon dynamics

Model simulation is an important tool that could help people fill the gaps in knowledge about the quantification information of drought-induced tree mortality and corresponding impacts on forest carbon dynamics, especially to fill these gaps under future climate

change. The two endpoints of the theoretical continuum of modeling approaches are the empirical model and the process-based model. All process-based models contain some empirical information (for example, in the selection of relevant mechanisms), while correlations on which empirical models are based are assumed to capture relevant processes (Mäkelä et al., 2000). To date, some attempts have used mortality observation data and extreme climate events to simulate or predict mortality based on empirical models (Gustafson & Sturtevant, 2013; Mitchell et al., 2016). Empirical models rely on correlations, that should be consistent with mechanical understanding, and thus do not fully describe system behavior and interactions (Adams et al., 2013). In contrast, process-based approaches focus on simulating detailed physical or biological processes that explicitly describe the behavior of a system at a given scale (Korzukhin et al., 1996). Process-based models can be more comprehensive and explicitly based on mechanisms, whereas empirical approaches are generally simpler and mechanistically implicit. In an empirical approach, model uncertainty may be reduced, but when extrapolating correlations beyond observed variability, the exclusion of important mechanisms may result in significant bias. Empirical relationships may also fail where long-term shifts toward a novel, drier climate is occurring (Choat et al., 2018). In contrast, process-based models can better include new or non-simulated responses that may occur under future conditions (Williams & Jackson, 2007). To date, some progress has also been made in the use of process-based models to simulate tree mortality. For example, in the Community Land Model (Bonan et al., 2012), vegetation represented by plant functional types was established according to biogeographical rules based on temperature thresholds and a minimum precipitation requirement. Annual mortality occurs in the model due to light, competition, fire, growth efficiency, and heat-stress tolerance. The ecosystem demography model has been updated with algorithms for tree carbon resources and xylem cavitation to represent carbon starvation and hydraulic failure mechanisms (Fisher et al., 2010). The TREES model simulates mortality from the gas exchange, soil-plant hydraulics, and carbohydrate dynamics (Loranty et al., 2010; Mackay et al., 2012; McDowell et al., 2013). Gustafson and Sturtevant (Gustafson & Sturtevant, 2013) used LANDIS - II (a forest succession model) to predict mortality from drought duration and intensity. Hendrik and Maxime (2017) described how physiological process-based models can be used to assess tree

mortality risk under climate change and highlighted that physiological process-based models can be of high interest to determine the factors predisposing and inducing tree death. Despite field studies demonstrating that hydraulic failure and carbon starvation (Hartmann et al., 2015; McDowell et al., 2008) are the primary mechanisms for tree mortality during drought events, no model has yet been developed to integrate these mechanisms for simulating drought-induced mortality in boreal forests so far. For better quantifying and forecasting drought-induced tree mortality and its impacts on carbon dynamics of Canada's boreal forest under climate change, reliable process-based models that can simulate drought-induced tree mortality are thus needed (Adams et al., 2013; Choat et al., 2018).

1.2. General questions and hypotheses

In summary, three primary knowledge gaps remain in the evaluation of drought impacts on tree mortality and the corresponding carbon sink capacity of Canada's boreal forests. These knowledge gaps can be addressed by answering the following questions:

1. Can the proposed mechanisms that cause drought-induced mortality be integrated into a process-based tree mortality model?
2. What are the spatiotemporal changes in drought-induced tree mortality and the associated impacts on biomass carbon dynamics in Canada's boreal forests over the past several decades?
3. Under future climate change, what would be the potential risk of drought-induced tree mortality and the corresponding loss of the carbon sink capacity of Canada's boreal forests?

In this dissertation, I hypothesize that (1) based on a robust forest dynamics model (TRIPLEX 1.0), it is possible to develop a new drought-induced tree mortality submodel by combining the existing advanced mechanisms of drought-induced tree mortality with field observation data to calibrate the model. (2) Over the past several decades, the overall tree mortality rate and the loss of carbon capacity may be higher than expected. The mortality rate and associated loss of carbon sink capacity have increased over time and

exhibited spatial heterogeneity, particularly in eastern and western Canada. (3) The potential risk of tree mortality and loss of carbon sink capacity will increase under future climate change. Under the extreme emissions scenario, Canada's boreal forests may be at significant risk to lose their role as a carbon sink.

1.3. Objectives and thesis structure

To address the above questions and fill in knowledge gaps, the overall objective of this dissertation is to simulate and forecast drought-induced tree mortality and its impacts on the biomass carbon sink capacity of boreal forests in the face of climate change.

Specifically, I propose to:

1. Develop a novel process-based drought-induced tree mortality model: TRIPLEX-Mortality;
2. Quantify drought-induced tree mortality and its impacts on the biomass carbon sink capacity of Canada's boreal forest over the past 50 years;
3. Forecast risks and uncertainties of drought-induced tree mortality changes and corresponding impacts on the biomass carbon sink capacity of Canada's boreal forest under future climate change;

This dissertation is organized such that each chapter addresses an objective suitable for a stand-alone publication (or is an already published) article. The Introduction provides the research background, objectives, and dissertation structure. Chapter II addresses objective 1, where a new process-based drought-induced tree mortality model (TRIPLEX-Mortality) integrating advanced mechanisms of drought-induced tree mortality was developed and successfully validated against observed data from long-term forest permanent sampling plots. This Chapter was published in the journal *Ecological Modelling* (*Liu, Qiuyu et al. "TRIPLEX-Mortality model for simulating drought-induced tree mortality in boreal forests: Model development and evaluation." Ecological Modelling. 455 (2021): 109652.*). Chapter III addresses objective 2, in which the TRIPLEX-Mortality model was used to quantify spatiotemporal changes in drought-induced tree mortality and associated impacts

on biomass carbon dynamics in Canada's boreal forests from 1970 to 2020. This Chapter is under review for publishing by the journal *Global Change Biology (Liu, Qiuyu et al. "Drought-induced increase in tree mortality and corresponding decrease in the carbon sink capacity of Canada's boreal forests from 1970 to 2020")*. Chapter IV addresses objective 3, in which I use a forecast from the TRIPLEX-Mortality model to evaluate changes in drought-induced tree mortality risk and corresponding impacts on biomass carbon sink capacity of Canada's boreal forest under future climate change. This Chapter will be submitted to the journal *Earth's Future (Liu, Qiuyu et al. Forecasting drought-induced tree mortality and its impact on the biomass carbon sink of Canada's boreal forest by the end of the twenty-first century")*. Chapter V includes the conclusions of the dissertation and potential future research.

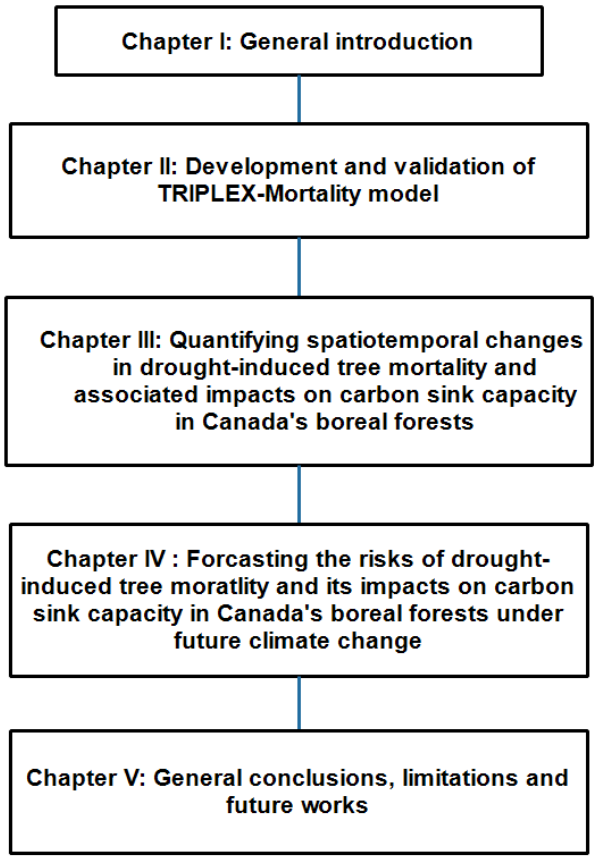

Figure 2. 2. Structure of dissertation.

Note: This thesis is written as a collection of published or submitted peer-reviewed journal articles. Consequently, there is little overlap between the General Introduction, General

Conclusion, and the main body of the Chapters.

1.4. References

Adams, H. D., Macalady, A. K., Breshears, D. D., Allen, C. D., Stephenson, N. L., Saleska, S. R., Huxman, T. E., & McDowell, N. G. (2010). Climate-induced tree mortality: Earth system consequences. Eos, Transactions American Geophysical Union, 91(17), 153–154. https://doi.org/https://doi.org/10.1029/2010EO170003

Adams, H. D., Williams, A. P., Xu, C., Rauscher, SaraA., Jiang, X., & McDowell, N. G. (2013). Empirical and process-based approaches to climate-induced forest mortality models. Frontiers in Plant Science, 4(11), 1–5. https://doi.org/10.3389/fpls.2013.00438

Aleixo, I., Norris, D., Hemerik, L., Barbosa, A., Prata, E., Costa, F., & Poorter, L. (2019). Amazonian rainforest tree mortality driven by climate and functional traits. Nature Climate Change, 9(5), 384–388. https://doi.org/10.1038/s41558-019-0458-0

Allen, C. D., Macalady, A. K., Chenchouni, H., Bachelet, D., McDowell, N., Vennetier, M., Kitzberger, T., Rigling, A., Breshears, D. D., Hogg, E. H. (Ted), Gonzalez, P., Fensham, R., Zhang, Z., Castro, J., Demidova, N., Lim, J. H., Allard, G., Running, S. W., Semerci, A., & Cobb, N. (2010). A global overview of drought and heat-induced tree mortality reveals emerging climate change risks for forests. Forest Ecology and Management, 259, 660–684. https://doi.org/10.1016/j.foreco.2009.09.001

Arias, P., Bellouin, N., Coppola, E., Jones, R., Krinner, G., Marotzke, J., Naik, V., Palmer, M., Plattner, G.-K., & Rogelj, J. (2021). Climate Change 2021: The Physical Science Basis. Contribution of Working Group14 I to the Sixth Assessment Report of the Intergovernmental Panel on Climate Change; Technical Summary.

Asner, G. P., Brodrick, P. G., Anderson, C. B., Vaughn, N., Knapp, D. E., & Martin, R. E. (2016). Progressive forest canopy water loss during the 2012–2015 California drought. Proceedings of the National Academy of Sciences, 113(2), 249–255. https://doi.org/10.1073/pnas.1523397113

Bonan, G. B. (2008). Forests and Climate Change: Forcings, Feedbacks, and the Climate Benefits of Forests. Science, 320(5882), 1444–1449. https://doi.org/10.1126/science.1155121

Bonan, G. B., Oleson, K. W., Fisher, R. A., Lasslop, G., & Reichstein, M. (2012). Reconciling leaf physiological traits and canopy flux data: Use of the TRY and

FLUXNET databases in the Community Land Model version 4. Journal of Geophysical Research: Biogeosciences, 117(2), 1–19. https://doi.org/10.1029/2011JG001913

Carnicer, J., Coll, M., Ninyerola, M., Pons, X., Sanchez, G., & Penuelas, J. (2011). Widespread crown condition decline, food web disruption, and amplified tree mortality with increased climate change-type drought. Proceedings of the National Academy of Sciences, 108(4), 1474–1478. https://doi.org/10.1073/pnas.1010070108

Choat, Brendan., Brodribb, T. J., Brodersen, C. R., Duursma, R. A., López, Rosana., & Medlyn, B. E. (2018). Triggers of tree mortality under drought. Nature, 558(7711), 531–539. https://doi.org/10.1038/s41586-018-0240-x

Ciais, P., Reichstein, M., Viovy, N., Granier, A., Ogée, J., Allard, V., Aubinet, M., Buchmann, N., Bernhofer, C., Carrara, A., Chevallier, F., De Noblet, N., Friend, A. D., Friedlingstein, P., Grünwald, T., Heinesch, B., Keronen, P., Knohl, A., Krinner, G., … Valentini, R. (2005). Europe-wide reduction in primary productivity caused by the heat and drought in 2003. Nature, 437(7058), 529–533. https://doi.org/10.1038/nature03972

Clinton, B. D., Boring, L. R., & Swank, W. T. (1993). Canopy Gap Characteristics and Drought Influences in Oak Forests of the Coweeta Basin. Ecology, 74(5), 1551–1558. https://doi.org/10.2307/1940082

Cook, B. I., Mankin, J. S., Marvel, K., Williams, A. P., Smerdon, J. E., & Anchukaitis, K. J. (2020). Twenty-First Century Drought Projections in the CMIP6 Forcing Scenarios. Earth's Future, 8(6), 1–20. https://doi.org/10.1029/2019EF001461

Davidson, E. A., de Araújo, A. C., Artaxo, P., Balch, J. K., Brown, I. F., Bustamante, M. M., Coe, M. T., DeFries, R. S., Keller, M., Longo, M., & Munger, J. W. (2012). The Amazon basin in transition. Nature, 481(7381), 321–328. https://doi.org/10.1038/nature10717

Duke, N. C., Kovacs, J. M., Griffiths, A. D., Preece, L., Hill, D. J. E., van Oosterzee, P., Mackenzie, J., Morning, H. S., & Burrows, D. (2017). Large-scale dieback of mangroves in Australia's Gulf of Carpentaria: a severe ecosystem response, coincidental with an unusually extreme weather event. Marine and Freshwater Research, 68(10), 1816–1829.

Fisher, R., McDowell, N., Purves, D., Moorcroft, P., & Sitch, S. (2010). Assessing uncertainties in a second-generation dynamic vegetation model caused by ecological scale limitations. (Special Issue: Amazonian rain forests and drought.). New

Phytologist; 2010, 187(3), 666–681.

Gauthier, S., Bernier, P., Kuuluvainen, T., Shvidenko, A. Z., & Schepaschenko, D. G. (2015). Boreal forest health and global change. Science, 349(6250), 819–822. https://doi.org/10.1126/science.aaa9092

Goulden, M. L., Wofsy, S. C., Harden, J. W., Trumbore, S. E., Crill, P. M., Gower, S. T., Fries, T., Daube, B. C., Fan, S. M., Sutton, D. J., Bazzaz, A., & Munger, J. W. (1998). Sensitivity of boreal forest carbon balance to soil thaw. Science, 279(5348), 214–217. https://doi.org/10.1126/science.279.5348.214

Gustafson, E. J., & Sturtevant, B. R. (2013). Modeling Forest Mortality Caused by Drought Stress: Implications for Climate Change. Ecosystems, 16(1), 60–74. https://doi.org/10.1007/s10021-012-9596-1

Hendrik, D., & Maxime, C. (2017). Assessing drought-driven mortality trees with physiological process-based models. Agricultural and Forest Meteorology, 232, 279–290. https://doi.org/10.1016/j.agrformet.2016.08.019

Hogg, E. H. (Ted), Brandt, J. P., & Michaelian, M. (2008). Impacts of a regional drought on the productivity, dieback, and biomass of western Canadian aspen forests. Canadian Journal of Forest Research, 38(6), 1373–1384. https://doi.org/10.1139/X08-001

Huntingford, C., Zelazowski, P., Galbraith, D., Mercado, L. M., Sitch, S., Fisher, R., Lomas, M., Walker, A. P., Jones, C. D., Booth, B. B. B., Malhi, Y., Hemming, D., Kay, G., Good, P., Lewis, S. L., Phillips, O. L., Atkin, O. K., Lloyd, J., Gloor, E., … Cox, P. M. (2013). Simulated resilience of tropical rainforests to CO2 -induced climate change. Nature Geoscience, 6(4), 268–273. https://doi.org/10.1038/ngeo1741

Jentsch, A., Kreyling, J., Elmer, M., Gellesch, E., Glaser, B., Grant, K., Hein, R., Lara, M., Mirzae, H., Nadler, S. E., Nagy, L., Otieno, D., Pritsch, K., Rascher, U., Schädler, M., Schloter, M., Singh, B. K., Stadler, J., Walter, J., … Beierkuhnlein, C. (2011). Climate extremes initiate ecosystem-regulating functions while maintaining productivity. Journal of Ecology, 99(3), 689–702. https://doi.org/10.1111/j.1365-2745.2011.01817.x

Knapp, A. K., Fay, P. A., Blair, J. M., Collins, S. L., Smith, M. D., Carlisle, J. D., Harper, C. W., Danner, B. T., Lett, M. S., & McCarron, J. K. (2002). Rainfall variability, carbon cycling, and plant species diversity in a mesic grassland. Science, 298(5601), 2202–2205. https://doi.org/10.1126/science.1076347

Korzukhin, M. D., Ter-Mikaelian, M. T., & Wagner, R. G. (1996). Process versus empirical models: which approach for forest ecosystem management? Canadian Journal of Forest Research, 26(5), 879–887.

Kurz, W. A., Dymond, C. C., Stinson, G., Rampley, G. J., Neilson, E. T., Carroll, A. L., Ebata, T., & Safranyik, L. (2008). Mountain pine beetle and forest carbon feedback to climate change. Nature, 452(7190), 987–990. https://doi.org/10.1038/nature06777

Kurz, W. A., Shaw, C. H., Boisvenue, C., Stinson, G., Metsaranta, J., Leckie, D., Dyk, A., Smyth, C., & Neilson, E. T. (2013). Carbon in Canada's boreal forest — A synthesis. Environmental Reviews, 21(4), 260–292.

Lenton, T. M., Held, H., Kriegler, E., Hall, J. W., Lucht, W., Rahmstorf, S., & Joachim, H. (2008). Tipping elements in the Earth's climate system. Proceedings of the National Academy of Sciences, 105(6), 1786–1793. https://doi.org/10.1073/pnas.0705414105

Loranty, M. M., MacKay, D. S., Ewers, B. E., Traver, E., & Kruger, E. L. (2010). Competition for light between individual trees lowers reference canopy stomatal conductance: Results from a model. Journal of Geophysical Research: Biogeosciences, 115(4). https://doi.org/10.1029/2010JG001377

Ma, Z., Peng, C., Zhu, Q., Chen, H., Yu, G., Li, W., Zhou, X., Wang, W., & Zhang, W. (2012). Regional drought-induced reduction in the biomass carbon sink of Canada's boreal forests. Proceedings of the National Academy of Sciences, 109(7), 2423–2427. https://doi.org/10.1073/pnas.1111576109

Mackay, D. S., Ewers, B. E., Loranty, M. M., Kruger, E. L., & Samanta, S. (2012). Bayesian analysis of canopy transpiration models: A test of posterior parameter means against measurements. Journal of Hydrology, 432–433, 75–83. https://doi.org/10.1016/j.jhydrol.2012.02.019

Mäkelä, A., Landsberg, J., Ek, A. R., Burk, T. E., Ter-Mikaelian, M., Ågren, G. I., Oliver, C. D., & Puttonen, P. (2000). Process-based models for forest ecosystem management: Current state of the art and challenges for practical implementation. Tree Physiology, 20(5–6), 289–298. https://doi.org/10.1093/treephys/20.5-6.289

Mark G. L. Van Nieuwstadt, & Douglas Sheil. (2005). Drought, fire and tree survival in a Borneo rain forest, East Kalimantan, Indonesia. Journal of Ecology, 93, 191–201. https://doi.org/10.1111/j.1365-2745.2005.00954.x

Matusick, G., Ruthrof, K. X., Brouwers, N. C., Dell, B., & Hardy, G. S. J. (2013). Sudden forest canopy collapse corresponding with extreme drought and heat in a

mediterranean-type eucalypt forest in southwestern Australia. European Journal of Forest Research, 132(3), 497–510. https://doi.org/10.1007/s10342-013-0690-5

McDowell, N., Fisher, R., Chonggang, X., Sperry, J. S., Boutz, A., Dickman, L., Gehres, N., Limousin, J. M., Macalady, A., Pangle, R. E., Rasse, D. P., Ryan, M. G., Sevanto, S., Waring, R. H., Williams, A. P., Yepez, E. A., & Pockman, W. T. (2013). Evaluating theories of drought-induced vegetation mortality using a multimodel – experiment framework. New Phytologist, 200, 304–321. https://doi.org/10.1111/nph.12465

Michaelian, M., Hogg, E. H., Hall, R. J., & Arsenault, E. (2011). Massive mortality of aspen following severe drought along the southern edge of the Canadian boreal forest. Global Change Biology, 17(6), 2084–2094. https://doi.org/10.1111/j.1365-2486.2010.02357.x

Mitchell, P. J., O'Grady, A. P., Pinkard, E. A., Brodribb, T. J., Arndt, S. K., Blackman, C. J., Duursma, R. A., Fensham, R. J., Hilbert, D. W., Nitschke, C. R., Norris, J., Roxburgh, S. H., Ruthrof, K. X., & Tissue, D. T. (2016). An ecoclimatic framework for evaluating the resilience of vegetation to water deficit. Global Change Biology, 22(5), 1677–1689. https://doi.org/10.1111/gcb.13177

Monteiro, P., Balch, J. K., Nepstad, D. C., Morton, D. C., & Putz, F. E. (2014). Abrupt increases in Amazonian tree mortality due to drought – fire interactions. Proceedings of the National Academy of Sciences, 111(17), 6347–6352. https://doi.org/10.1073/pnas.1305499111

Moore, G. W., Edgar, C. B., Vogel, J. G., Washington-Allen, R. A., March, R. G., & Zehnder, R. (2016). Tree mortality from an exceptional drought spanning mesic to semiarid ecoregions. Ecological Applications, 26(2), 602–611. https://doi.org/10.1890/15-0330

Nakagawa, M., Tanaka, K., Nakashizuka, T., Ohkubo, T., Kato, T., Maeda, T., & Sato, K. (2000). Impact of severe drought associated with the 1997–1998 El Niño in a tropical forest in Sarawak. Journal of Tropical Ecology, 16(03), 355–367.

Peng, C., Ma, Z., Lei, X., Zhu, Q., Chen, H., Wang, W., Liu, S., Li, W., Fang, X., & Zhou, X. (2011). A drought-induced pervasive increase in tree mortality across Canada's boreal forests. Nature Climate Change, 1(9), 467–471. https://doi.org/10.1038/nclimate1293

Peñuelas, J., Lloret, F., & Montoya, R. (2001). Severe drought effects on mediterranean woody flora in Spain. Forest Science, 47(2), 214–218. https://doi.org/10.1093/forestscience/47.2.214

Phillips, O. L., Lewis, S. L., Lloyd, J., López-González, G., Peacock, J., Quesada, C. A., Van Der Heijden, G., Baker, T. R., Feldpausch, T. R., Gloor, E., Patiño, S., Schwarz, M., Chao, K.-J., Keeling, H., Aragão, L. E. O. C., Fisher, J. B., Malhi, Y., Morel, A., Silva, J., … Terborgh, J. (2009). Drought sensitivity of the amazon rainforest. Science, 323(5919), 1344–1347. https://doi.org/10.1126/science.1164033

Phillips, O. L., Phillips, O. L., Aragão, L. E. O. C., Lewis, S. L., Fisher, J. B., Lloyd, J., López-gonzález, G., Malhi, Y., Monteagudo, A., Peacock, J., Quesada, C. A., Heijden, G. Van Der, Almeida, S., Amaral, I., Arroyo, L., Aymard, G., Baker, T. R., Bánki, O., Blanc, L., … Keeling, H. (2009). Drought Sensitivity of the Amazon Rainforest. Science, 323, 1344–1348. https://doi.org/10.1126/science.1164033

Sánchez-Pinillos, M., D'Orangeville, L., Boulanger, Y., Comeau, P., Wang, J., Taylor, A. R., & Kneeshaw, D. (2022). Sequential droughts: A silent trigger of boreal forest mortality. Global Change Biology, 28(2), 542–556. https://doi.org/10.1111/gcb.15913

Schwalm, C. R., Williams, C. A., Schaefer, K., Arneth, A., Bonal, D., Buchmann, N., Chen, J., Law, B., Lindroth, A., Luyssaert, S., Reichstein, M., & Richardson, A. D. (2010). Assimilation exceeds respiration sensitivity to drought: A FLUXNET synthesis. Global Change Biology, 16(2), 657–670. https://doi.org/10.1111/j.1365-2486.2009.01991.x

Soja, A. J., Tchebakova, N. M., French, N. H. F., Flannigan, M. D., Shugart, H. H., Stocks, B. J., Sukhinin, A. I., Parfenova, E. I., Chapin, F. S., & Stackhouse, P. W. (2007). Climate-induced boreal forest change: Predictions versus current observations. Global and Planetary Change, 56(3–4), 274–296. https://doi.org/10.1016/j.gloplacha.2006.07.028

Trenberth, K. E., Dai, A., Schrier, G. Van Der, Jones, P. D., Barichivich, J., Briffa, K. R., & Sheffield, J. (2014). Global warming and changes in drought. Nature Climate Change, 4(1), 17–22. https://doi.org/10.1038/NCLIMATE2067

Van Mantgem, P. J., Nathan L, S., John C, B., Lori D, D., Jerry F, F., Peter Z, F., Mark E, H., Andrew J, L., Jeremy M, S., Alan H, T., & Thomas T, V. (2009). Widespread increase of tree mortality rates in the western United States. Science, 323(5913), 521–524. https://doi.org/10.1126/science.1165000

Voelker, S. L., Muzika, R., & Guyette, R. P. (2008). Individual Tree and Stand Level Influences on the Growth, Vigor, and Decline of Red Oaks in the Ozarks. Forest Science, 54(1), 8–20.

Wang, W., Peng, C., Kneeshaw, D. D., Larocque, G. R., & Luo, Z. (2012). Drought-induced

tree mortality: ecological consequences, causes, and modeling. Environmental Reviews, 20(2), 109–121. https://doi.org/10.1139/a2012-004

Williams, A. P., Allen, C. D., Macalady, A. K., Griffin, D., Woodhouse, C. A., Meko, D. M., Swetnam, T. W., Rauscher, S. A., Seager, R., Grissino-Mayer, H. D., Dean, J. S., Cook, E. R., Gangodagamage, C., Cai, M., & Mcdowell, N. G. (2013). Temperature as a potent driver of regional forest drought stress and tree mortality. Nature Climate Change, 3(3), 292–297. https://doi.org/10.1038/nclimate1693

Williams, J. W., & Jackson, S. T. (2007). Novel climates, no-analog communities, and ecological surprises. Frontiers in Ecology and the Environment, 5(9), 475–482. https://doi.org/10.1890/070037

Yang, Y., Saatchi, S. S., Xu, L., Yu, Y., Choi, S., Phillips, N., Kennedy, R., Keller, M., Knyazikhin, Y., & Myneni, R. B. (2018). Post-drought decline of the Amazon carbon sink. Nature Communications, 9(1). https://doi.org/10.1038/s41467-018-05668-6

Zhao, M., & Running, S. W. (2010). Drought-Induced Reduction in Global Terrestrial Net Primary Production from 2000 Through 2009. Science, 329(5994), 940–943. https://doi.org/10.1126/science.1192666

Zhou, L., Tian, Y., Myneni, R. B., Ciais, P., Saatchi, S., Liu, Y. Y., Piao, S., Chen, H., Vermote, E. F., Song, C., & Hwang, T. (2014). Widespread decline of Congo rainforest greenness in the past decade. Nature, 508(7498), 86–90. https://doi.org/10.1038/nature13265

Zscheischler, J., Mahecha, M. D., Von Buttlar, J., Harmeling, S., Jung, M., Rammig, A., Randerson, J. T., Schölkopf, B., Seneviratne, S. I., Tomelleri, E., Zaehle, S., & Reichstein, M. (2014). A few extreme events dominate global interannual variability in gross primary production. Environmental Research Letters, 9(3). https://doi.org/10.1088/1748-9326/9/3/035001

Zscheischler, J., Michalak, A. M., Schwalm, C., Mahecha, M. D., Huntzinger, D. N., Reichstein, M., Berthier, G., Ciais, P., Cook, R. B., El-Masri, B., Huang, M., Ito, A., Jain, A., King, A., Lei, H., Lu, C., Mao, J., Peng, S., Poulter, B., … Zeng, N. (2014). Impact of large-scale climate extremes on biospheric carbon fluxes: An intercomparison based on MsTMIP data. Global Biogeochemical Cycles, 28(6), 585–600. https://doi.org/10.1002/2014GB004826

CHAPTER II

TRIPLEX-MORTALITY MODEL FOR SIMULATING DROUGHT-INDUCED TREE MORTALITY IN BOREAL FORESTS: MODEL DEVELOPMENT AND EVALUATION

Liu, Qiuyu, Changhui Peng, Robert Schneider, Dominic Cyr, Zelin Liu, Xiaolu Zhou, and Daniel Kneeshaw

Article published in *Ecological Modelling*. 455 (2021): 109652

2.1. Resume

À l'échelle mondiale, l'augmentation des taux de mortalité des arbres induite par la sécheresse dans le cadre des changements climatiques devrait avoir des effets considérables sur les écosystèmes forestiers. Parmi ces systèmes forestiers, la forêt boréale est considérée comme un ‘élément de basculement’ du système climatique de la Terre. Tout en étant très sensible au stress hydrique, ce biome forestier joue un rôle essentiel dans les services, les structures et les fonctions écosystémiques. Bien que les modèles basés sur les processus soient des outils importants pour la recherche en écologie, très peu peuvent actuellement intégrer des mécanismes physiologiques avancés pour simuler la mortalité induite par la sécheresse dans les forêts boréales. Pour palier ce manque, cette étude introduit le nouveau sous-module TRIPLEX-Mortalité, basée sur le modèle original TRIPLEX, pour les forêts boréales canadiennes au niveau du peuplement, qui intègre pour la première fois avec succès deux mécanismes physiologiques avancés menant à la mortalité mortalité induits par la sécheresse. Pour calibrer et valider le modèle, 73 placettes d'échantillonnage permanentes ont été sélectionnées dans au sein de la forêt boréale du Canada. Les résultats confirment un bon accord entre la mortalité simulée et observée ($R^2 = 0.79$; $P < 0.01$; IA = 0.94), démontrant une bonne performance du modèle dans la simulation de la mortalité induite par la sécheresse dans les forêts boréales. L'analyse de sensibilité a indiqué que la sensibilité des paramètres augmentait à mesure que la sécheresse s'intensifiait, et le paramètre de forme (c) pour calculer le pourcentage de perte de conductivité était le paramètre le plus sensible pour simuler la mortalité des arbres. En outre, les résultats de l'analyse de sensibilité des entrées du modèle ont également montré que celui-ci peut capturer les changements de mortalité dans différents scénarios de sécheresse. Par conséquent, notre modèle est adapté pour simuler la mortalité induite par la sécheresse dans les forêts boréales et fournit de nouvelles informations sur l'amélioration des modèles de simulation pour la mortalité des arbres et ses conséquences sur la dynamique du carbone dans un monde progressivement plus chaud et plus sec.

2.2. Abstract

Globally, increasing drought-induced tree mortality rates under climate change are

projected to have far-reaching effects on forest ecosystems. Among these forest systems, the boreal forest is considered a 'tipping element' of the Earth's climate system. This forest biome plays a critical role in ecosystem services, structures, and functions while being highly sensitive to drought stress. Although process-based models are important tools in ecological research, very few have yet been developed that integrate advanced physiological mechanisms to simulate drought-induced mortality in boreal forests. Accordingly, based on the process-based TRIPLEX model, this study introduces the new TRIPLEX-Mortality submodule for the Canadian boreal forests at the stand level, that for the first time successfully incorporates two advanced drought-induced physiological mortality mechanisms (i.e., hydraulic failure and carbon starvation). To calibrate and validate the model, 73 permanent sample plots (PSPs) were selected across Canada's boreal forests. Results confirm a good agreement between simulated mortality and mortality observations (R^2 = 0.79; P < 0.01; IA = 0.94), demonstrating good model performance in simulating drought-induced mortality in boreal forests. Sensitivity analysis indicated that parameter sensitivity increased as drought intensified, and the shape parameter (c) for calculating percentage loss of conductivity (PLC) was the most sensitive parameter (average SI = -3.51) to simulate tree mortality. Furthermore, the results of the model input sensitivity analysis also showed that the model can capture changes in mortality under different drought scenarios. Consequently, our model is suitable for simulating drought-induced mortality in boreal forests while also providing new insight into improving model simulations for tree mortality and associated carbon dynamics in a progressively warmer and drier world.

2.3 Introduction

Global change, associated with increasing and intensifying extreme drought, has caused widespread tree mortality events across the globe biomes (Brouwers et al., 2015; Goulden and Bales, 2019; Lewis et al., 2011; Liu et al., 2014; Peng et al., 2011; Reichstein et al., 2007). Increased drought-induced tree mortality can potentially trigger an abrupt and irreversible change in forest ecosystem structure, function, biodiversity and services (Allen et al., 2015; Anderegg et al., 2019, 2013; Choat et al., 2018; Suarez and Kitzberger, 2008).

Among all forest ecosystem types, the boreal forest, which is considered to be a critical "tipping element" of the Earth's climate system (Lenton et al., 2008), represents approximately 30% of the total global forest area (Brandt et al., 2013), containing more surface freshwater than any other biome (Burton et al., 2010) and accounting for approximately 20% of all forest carbon sequestration (Pan et al., 2011). However, recent studies indicated that boreal forests are very sensitive to drought and have suffered from widespread drought-induced tree die-off events (Hogg et al., 2008; Lenton et al., 2008; Michaelian et al., 2011; Peng et al., 2011). For example, ground observations showed that drought-induced tree mortality rates of Canadian boreal forests have increased by an average of 4.7% per year from 1963 to 2008 (Peng et al., 2011). The southern edge of the Canadian boreal forest suffered massive mortality of aspen trees 4 years after a severe drought (2001-2002), and dead biomass increased by about 29Mt (Michaelian et al., 2011). Such unexpected impacts could substantially influence ecological regime shifts and ecosystem functioning of boreal forests at multiple scales (Adams et al., 2010; Wang et al., 2012a). Although most boreal forests are resilient to extreme climate changes such as drought that are currently taking place, the predicted speed and extent of climate change is expected to be unprecedented and subsequently will pose a significant threat to the tree communities and ultimately to the health of this vital forest ecosystem (Gauthier et al., 2015). Consequently, evaluating the impacts caused by drought-induced mortality in boreal forests is of significant concern.

Compared with traditional observation and experimental approaches, models can quantify the dynamics of drought-induced mortality over a long-term and at a large spatial-scale. These can thus help us better understand and predict terrestrial climate forcing and future climate change (Choat et al., 2018; Friedlingstein et al., 2006; Purves and Pacala, 2008; Sitch et al., 2003). However, drought-induced tree mortality is complex and a number of interdependent mechanisms play important roles in this process, therefore, the parameterization of the tree mortality process in models remains a considerable challenge (Choat et al., 2018; McDowell et al., 2013, 2008). Previous attempts have been made based on empirical models that were designed to incorporate observed mortality records and meteorological data to model or predict mortality (Gustafson and Sturtevant, 2013; Mitchell et al., 2016). Although these attempts have provided insight into the drivers of

drought-induced mortality, their functional reliability under future climatic conditions remains uncertain given that such conditions have yet to occur (Adams et al., 2013; O'sullivan et al., 2017). Dynamic global vegetation models (DGVMs) can represent the biogeochemical and hydrological processes of vegetation dynamics. However, tree mortality algorithms in most current DGVMs are still unable to adequately simulate drought-induced mortality because, under drought stress, they represent neither the advanced understanding of the internal state of carbon and water nor the interactions between hydraulic architecture and carbon allocation in plants (McDowell, 2011a; Mencuccini et al., 2015; Moorcroft, 2006; Powell et al., 2013; Xu et al., 2013). There is thus an urgent need to integrate more mechanistic mortality algorithms into DGVMs to better predict the ecological consequences of climate change and climate–biosphere feedbacks (Wang et al., 2012a).

Process-based models that integrate physiological mechanisms are the most promising for simulating drought-induced tree mortality (Adams et al., 2013; Choat et al., 2018; McDowell et al., 2008, 2016). Recent studies on physiological mechanisms of drought-induced mortality have identified both hydraulic failure (HF) and carbon starvation (CS) as the major pathways with recent research suggesting that it is a combination of both (Adams et al., 2017; McDowell et al., 2013, 2011, 2008; McDowell and Sevanto, 2010). Death by HF is due to partial or complete loss of xylem function caused by embolisms that inhibit water transport through the vessels or tracheids. Mortality by CS is caused by partial or complete depletion of nonstructural carbon content in the plant resulting in an inability to meet growth, metabolic and defensive carbon needs, due to an imbalance between carbohydrate demand and supply from photosynthesis (Hartmann et al., 2013; McDowell et al., 2016, 2013, 2011, 2008; O'Brien et al., 2014; Sala et al., 2010; Sevanto et al., 2014). To date, the assessment of HF is generally conducted by the percentage loss of conductivity (PLC), whereas CS is mostly quantified by the dynamics of non-structural carbohydrate (NSC) concentrations (Hartmann et al., 2013; O'Brien et al., 2014; Piper and Fajardo, 2016; Quirk et al., 2013; Sevanto et al., 2014). Research suggests that HF and CS mechanisms can be influenced by tree height and DBH (diameter at breast height), and that multiple interactions between HF and CS processes may occur during mortality and may vary with tree species (McDowell, 2011a; Olson et al., 2018; Stovall et al., 2019). By

integrating new evidence from the research field, McDowell et al., (2011) concluded that most of these mechanisms and their interdependencies are expected to be amplified under a warmer, drier climate. Given that recent projections (Trenberth et al., 2014) indicate longer and more intense droughts due to land surface climate warming, accurate simulations and predictions of the effects of drought on forest ecosystems are thus highly desirable.

Simulations that exploit both HF and CS have been used to establish the importance of each physiological process involved in drought-induced tree mortality. Based on the CASTANEA model and observed mortality rates, Hendrik and Maxime, (2017) simulated the functional development over time of trees with different ontogenetic and phenotypic characteristics (e.g. age and leaf area index) and growing under different site conditions (e.g. altitude, soil water content). They determined the physiological carbon and hydraulic thresholds of key plant traits and indicated the significant importance of CS in drought-induced mortality. They also highlighted that the factors which predispose and induce tree death can be identified using process-based models. However, their model only uses simplified resistance and capacitance mechanisms between soil and leaves to simulate water potential. The ability to translate meteorological data (e.g., precipitation or evaporative demands) into plant water content or xylem tension is key for simulating drought induced-mortality using process-based models (Blackman et al., 2016). McDowell et al., (2013) compared model simulations from FINNSIM (Hölttä et al., 2006), Sperry (Sperry et al., 1998), TREES (Mackay et al., 2012), MuSICA (Domec et al., 2012; Ogée et al., 2003), ED(X) (Fisher et al., 2010; Xu et al., 2012) and CLM(ED) (Bonan et al., 2012) process-based models on tree mortality events in the USA. The predictions from these models show that the mortality of all species in their study was caused by both HF and CS. They subsequently suggest that integrating the latest information on physiological mechanisms that drive drought-induced mortality into vegetation models and comparing predictions against observations could result in an improved capacity to predict drought-induced mortality. The main strengths of the study by McDowell et al., (2013) are not only the insights it provided in evaluating different tree species using both isohydric and anisohydric strategies, but also in the improved understanding, it provided for the physiological processes involved in drought-induced mortality across different species.

However, the results from their study do not sufficiently account for the influence of spatial variability in tree communities and soil characteristics as well as the effect of temperature on plant growth rates and the interaction between CS and HF (Mao et al., 2013). Consequently, these models may not be suitable for application in Canadian boreal forests at a regional scale. Additionally, most Canadian carbon models, such as InTEC (Chen et al., 2000; Chen et al., 2000), CLASS (Verseghy, 2000), CTEM (Arora, 2003; Arora and Boer, 2005; Melton and Arora, 2016), CLASSIC (Melton et al. 2020), CBM-CFS3 (Kurz et al., 2009, 1992) and Ecosys (Grant and Nalder, 2000), have been successfully used to simulate carbon dynamics. However, due to the lack of physiological processes involved in drought-induced tree mortality, these models are unable to explicitly represent the dynamics of drought-induced tree mortality under a changing climate. Despite recent progress, drought-induced tree mortality has not yet been well represented in current process-based models. Accordingly, a robust process-based model that provides the best possible understanding of drought-induced mortality is still highly desirable (Adams et al., 2013; Choat et al., 2018).

TRIPLEX 1.0 is a generic hybrid model that simulates the key processes of forest growth and carbon cycle. As the TRIPLEX 1.0 model integrates the advantages of both process-based and empirical models, it bridges the gap between empirical forest growth and yield, as well as process-based carbon balance models (Peng et al., 2002). In addition, TRIPLEX effectively considers the effect of spatial variability in tree stands and soil characteristics through the using of forest and soil information such as tree species, age, stocking percent, soil carbon, and texture from each simulated plot as input to the model. To date, the TRIPLEX 1.0 model has been successfully calibrated and validated for different forest ages (Peng et al., 2002; Zhou et al., 2006), tree species (Sun et al., 2008; Zhou et al., 2004), harvest disturbance and climate change (Wang et al., 2012b, 2011), as well as insect disturbance (Liu et al., 2019, 2018) in boreal forest ecosystems. TRIPLEX 1.0 can therefore be applied to simulate both short and long-term forest growth and carbon dynamics of boreal forests.

Given the wide availability and high reliability of the TRIPLEX model in the boreal forest ecosystems, this study intends to develop a new mortality submodule for the TRIPLEX process-based model (TRIPLEX-Mortality) that incorporates physiological CS and HF

processes to better quantify drought-induced mortality in boreal forests at the stand level. The specific objectives of this study are (1) to provide the best possible understanding of the physiological processes associated with drought-induced mortality into a process-based model; (2) to calibrate and validate the model using permanent sampling plots (PSPs) from Canada's boreal forests; and (3) to conduct parameter and climate input sensitivity analyses to identify the most sensitive parameters under different drought conditions.

2.4. Methods

2.4.1. Model description

TRIPLEX-Mortality (Fig. 2. 1) was developed from TRIPLEX1.0 (Peng et al., 2002), which is a hybrid model that incorporates forest growth as well as carbon and nitrogen dynamics. TRIPLEX1.0 (Fig. 2. 1) is based on three well-established models: 3-PG (Landsberg & Waring, 1997), TREEDYN3.0 (Bossel, 1996) and CENTURY4.0 (Parton et al., 1993). This hybrid model combines physical, biological and biogeochemical processes that control the dynamics of carbon, nitrogen and water and can predict growth and yield of a forest stand (Peng et al., 2002; Zhou et al., 2005). TRIPLEX 1.0 mainly includes the following six submodules: (1) Photosynthetically active radiation (PAR), which is calculated as a function of solar constant, radiation fraction, solar altitude, and atmospheric absorption. Forest production, carbon and nitrogen dynamics are primarily driven by solar radiation. (2) Gross primary production (GPP): It is estimated as a function of the monthly mean air temperature, stand age, soil water content, nitrogen limitation, the percentage of frost days during a period of a month and the leaf area index. (3) Net primary productivity (NPP), which is the difference between GPP and respiration (maintenance and autotrophic respiration). (4) Forest growth and yield (FGY). The primary variables in the FGY submodule include tree diameter and height increment, calculated using a function of the stem wood biomass increment equations developed by Bossel, (1996). (5) Soil carbon and nitrogen (SCN). The SCN is developed from the CENTURY soil decomposition submodule (Parton et al., 1993). This submodule effectively estimates both carbon and nitrogen mineralization rates for Canadian boreal forest ecosystems. A function of maximum decomposition rates, soil moisture effects, and soil temperature is used to

calculate soil carbon decomposition rates for each pool. (6) Soil water submodule (SW). Monthly water loss is calculated using the function of transpiration, evaporation, soil and snow water content. This submodule requires precipitation as an input and outputs transpiration, evaporation, and leached water to other submodules. A more detailed description of the TRIPLEX 1.0 model was published by Peng et al., (2002) and Liu et al., (2002).

A drought-induced mortality submodule that incorporates HF and CS and its links with TRIPLEX 1.0 are presented in Fig. 2. 1, while details on the modelling of key processes and equations of HF and CS pathway are described below as well as provided in Appendix A.1.

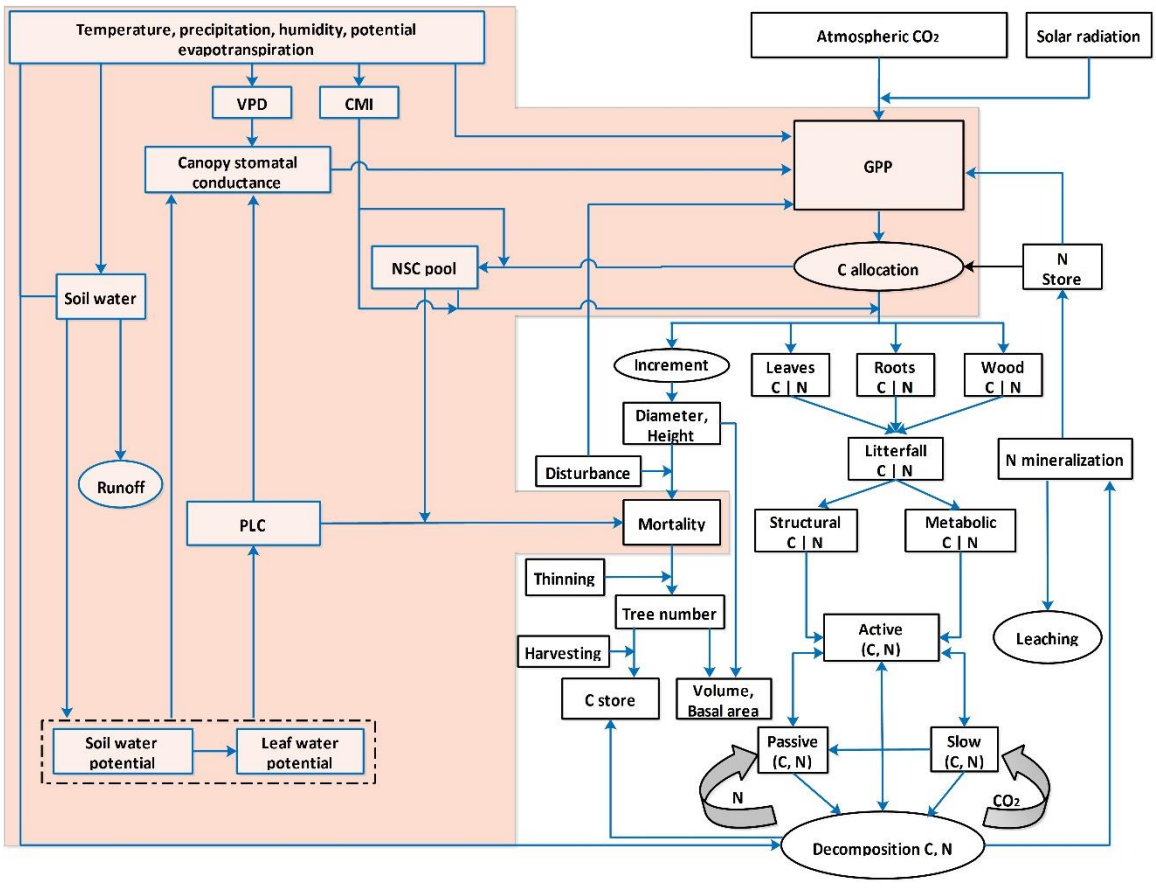

Figure 2. 1. Basic structural concept of the TRIPLEX-Mortality model (modified from Peng et al., (2002)). Shaded areas show the related processes involved in drought-induced mortality. CMI, PLC, NSC and GPP represent the climate moisture index, the percentage loss of conductivity, non-structural carbohydrate, and the gross primary production,

respectively.

2.4.1.1. Hydraulic failure (HF)

The TRIPLEX-Mortality model is designed to simulate soil water pools that account for monthly water loss through transpiration and evaporation, soil water content and snow water content. When monthly mean air temperature is less than 0°C, total monthly precipitation is designated as snow (Parton et al., 1987 and 1993). The water balance (L_w) is calculated as a function of water inputs and outputs as follows (Peng et al., 2002):

$$\Delta L_w = R - T - E - L \quad (2.\ 1)$$

R is rainfall (cm), and T, E and L represent transpiration (cm), evaporation (cm) and leached water (cm), respectively.

The physiological HF mechanism represents the complete loss of water transport to the canopy resulting from xylem embolism. During drought events, as transpiration persists, the soil water potential (SWP, in MPa) dramatically declines below the air entry pressure. The hydraulic connection between roots and soil is consequently severed, and HF subsequently takes place (Plaut et al., 2012). Based on soil water conditions, SWP is calculated using the reference soil water potential of saturated soil ($swps$, in MPa), the volumetric saturation (vs) in soil pores and the soil attribution parameter (λ) as follows (Oleson et al., 2010):

$$SWP = swps * vs^{-\lambda} \quad (2.\ 2)$$

Based on the Community Land Model (CLM) (Oleson et al., 2010), Eq. 2. 3 is used to calculate vs, where t is the thickness of the topsoil layer; s (mm^3) is the saturated volumetric water content of the topsoil layer; P_{liq} is the density of liquid water; and W_{liq} is the mass of liquid water of the topsoil layer.

$$vs = \frac{1}{ts}\left[\frac{W_{liq}}{P_{liq}}\right] \quad (2.\ 3)$$

The $swps$ is correlated to the soil organic matter fraction (f), the saturated organic matter matric potential (swp_{om}) and the saturated mineral soil matric potential (swp_{sat}) as follows:

$$swps = (1 - f)swp_{sat} + fswp_{om} \quad (2.\ 4)$$

The loss of xylem conductivity along with a decrease in the xylem water potential is represented by the PLC index, which is plotted against pressure and fitted to a Weibull function to generate a vulnerability curve (Neufeld et al., 1992; Rosner et al., 2019). Based on the research by Plaut et al., (2012), the root water potential is assumed to be equal to the SWP.

$$PLC = 100\left(1 - e^{\left(-\frac{-swp}{b}\right)^c}\right) \quad (2.\ 5)$$

where b is the critical SWP that results in a 63% reduction in conductivity, and c is a shape parameter (Neufeld et al., 1992; Pammenter and Van der Willigen, 1998; Sperry and Tyree, 1988).

2..4.1.2. Carbon starvation (CS)

Plants must regulate multiple demands on stomatal control during drought events where a decrease in water availability will promote HF. And a decrease in stomatal conductance (G_s) will reduce the risk of HF but subsequently limit CO_2 assimilation into leaves increasing the risk of CS (Damour et al., 2010; Plaut et al., 2012). The response of G_s to drought varies across the isohydric-anisohydric continuum of hydraulic strategies (Martínez-Vilalta et al., 2014). For this hydraulic strategy continuum, the canopy scale (G_s) simulation has been adapted based on models developed by Buckley et al., (2003) and Gao et al., (2002) as follows:

$$G_s = (1 - PLC)/(VPD * p)(SWP - \Psi_l) \quad (2.\ 6)$$

where Ψ_l (MPa) is the leaf water potential (LWP), VPD (mb) is the vapor pressure deficit of the canopy and p is a coefficient. Eq. 2. 6 indicates that mortality may increase when drought causes a sustained decrease in the soil water potential, while an increase in VPD can potentially be considered the greatest threat to survival because increasing global temperatures are driving a chronic increase in the VPD despite concurrent increases in specific humidity (Williams et al., 2013).

In TRIPLEX1.0, gross primary productivity (GPP, in t ha^{-1}) is calculated as a function of

the received photosynthetically active radiation (PAR) modified by the leaf area index (LAI), forest age (f_a), monthly mean air temperature (f_t), soil drought (f_w) and the percentage of frost days within a period of a month (f_d). k is a conversion constant (Peng et al., 2002). Stomatal conductance (G_s) is used as a limiting factor of GPP.

$$GPP = kI_m LAI f_a f_t f_w f_d G_s \quad (2.\ 7)$$

We adapted the original NSC submodel from the RHESSys process-based model (Tague et al., 2013) and then integrated this model into the TRIPLEX-Mortality model to estimate dynamic NSC pools (Fig. 2. 2). The NSC pool maintains a net balance between carbohydrate allocation and consumption. Under normal conditions, it is assumed that a portion of carbohydrates (α, see Table 2. S1) is allocated to the NSC pool until the total NSC reaches a threshold ($P_{threshold}$, see Table 2. S1) percentage of the total aboveground biomass (Fisher et al., 2010; Genet et al., 2009; Gruber et al., 2012). The remaining carbohydrate is then transferred to the structural carbon pool. During drought events, in conjunction with a rapid decline in productivity, if the ratio of leaves to aboveground carbon falls below 0.05, a value that derives from Callaway et al., (1994) and Tague et al., (2013) or if the climate moisture index (CMI, Eq. 2. 12) is less than -20, trees will access the NSC pool to maintain respiration requirements and restore their hydraulic function and leaf biomass.

$$NSC = NPP * \alpha - C_m - C_s \quad (2.\ 8)$$

where C_m represents the carbohydrate consumption from NSC to support basic metabolism, and C_s is the carbohydrate consumption from NSC that is transferred to structural carbon.

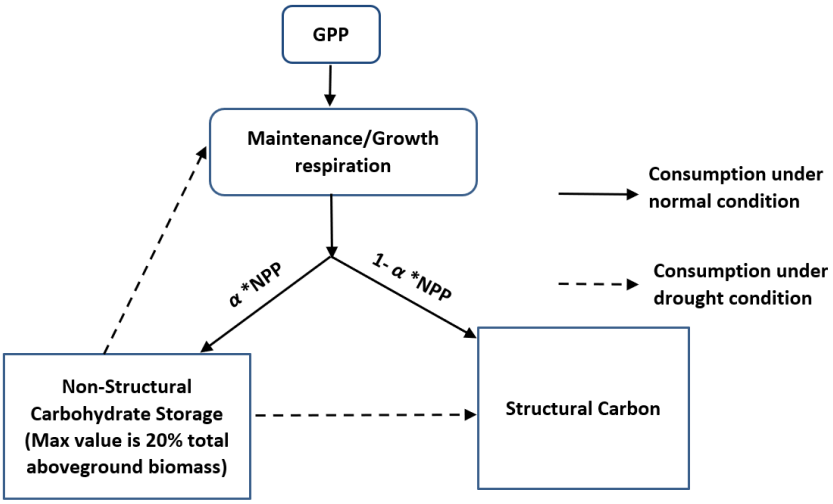

Figure 2. 2. The new carbon allocation mechanisms provided in the TRIPLEX-Mortality model. GPP, NPP and α represent gross primary production, net primary productivity and a percentage for the net primary productivity transfer to the non-structural carbon pool.

To calculate the mortality rate of each site, our study introduces the minimum factor limitation concept as follows:

$$Mortality = \frac{\sum_{i=1}^{n} Max(DMCS_{Mort}, DM_{Mort})}{n} \quad (2.\ 9)$$

where n is the number of modelling sites, and $DMCS_{Mort}$ and DM_{Mort} represent the tree mortality rate effectuated by CS and HF, respectively.

2.4.2. Study sites

Following the approach used by Peng et al., (2011), we selected 73 sites from long-term permanent sampling plots (PSPs) across Canada's boreal and hemiboreal regions (Fig. 2. 3, Table 2. S2). Of these plots, 57 were located across the drier western Canadian boreal ecozone including Alberta (AB), Saskatchewan (SK) and Manitoba (MB), and 16 were located in the moister eastern Canada boreal ecozone including Ontario (ON) and Quebec (QC). All selected sites had to meet the following criteria: (1) Sites are situated in a typically dry area for the region studies; (2) each site has to have at least three consecutive censuses that include complete tree recruitment and mortality records to obtain two

different time intervals to evaluate mortality rates, in addition, the DBH (diameter at 1.3 m above the ground) of trees was measured during the initial census; (3) to avoid errors created by potential disturbances on mortality rates, only plots for which there is no evidence of fire, flood, storm or insect disturbance and no evidence of forest management (such as thinning) for at least four decades were selected; (4) to avoid impacts of stand development and succession on mortality rates, stand age was ≥ 80 years in all plots, and (5) individual trees must have been clearly marked and repeatedly measured.

Plots aged between 80 and 218 years are dominated by black spruce (*Picea mariana*), white spruce (*Picea glauca*), trembling aspen (*Populus tremuloides*), balsam fir (*Abies balsamea*) and jack pine (*Pinus banksiana*). The elevation of all plots ranged from 101 to 2609 m and the spatial range spanned 53° in longitude and 9° in latitude (Table 2. S2). The monthly mean temperature and total precipitation from 1979 to 2004 ranged between -5.1 and 5.9°C and between 278.5 and 1392.5 mm, respectively.

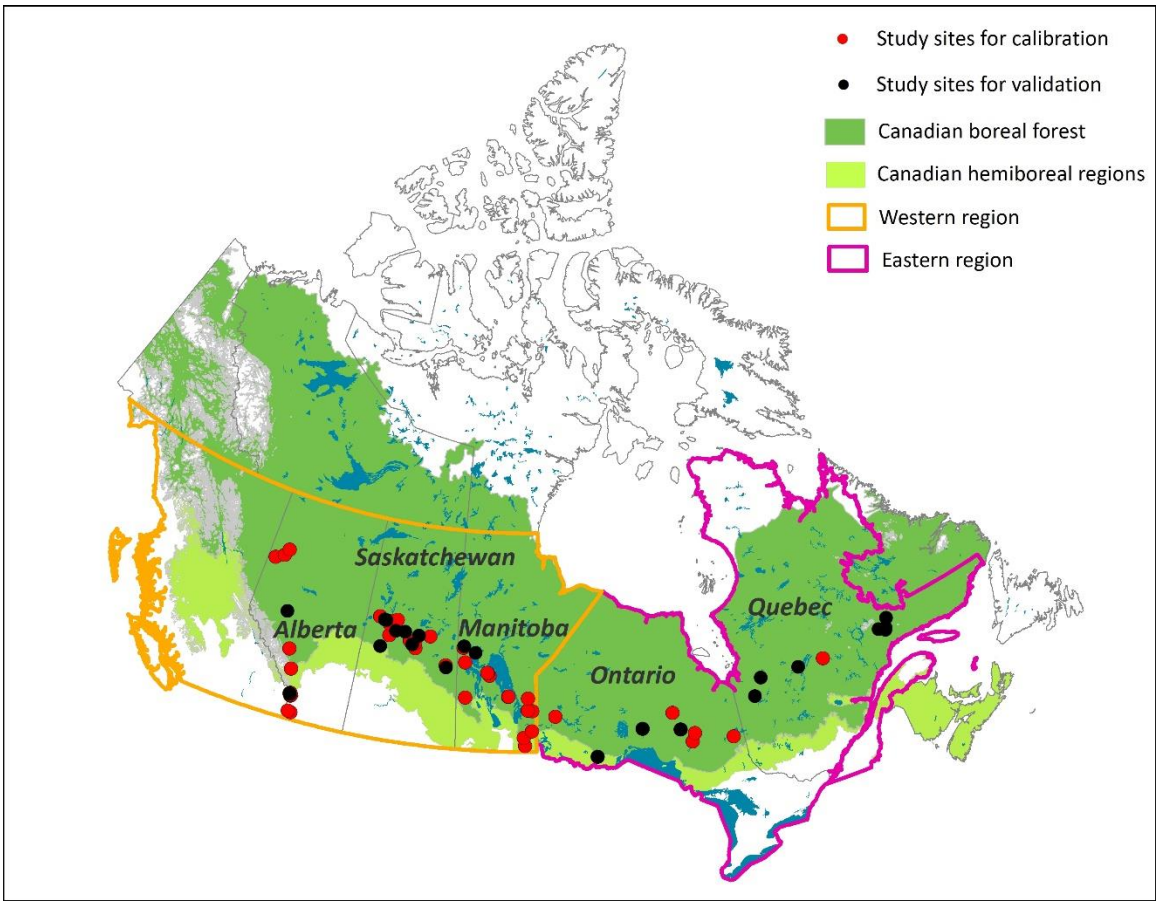

Figure 2. 3. Locations of the 73 study sites selected across Canada's boreal forests, the purple line denotes the eastern region, and the yellow line denotes the western ecozone. Red dots denote the 50 calibration sites and black dotes denote the 23 validation sites.

2.4.3. Input data

2..4.3.1. Climate data

As a driving force, climate variables of the TRIPLEX-Mortality model primarily include mean monthly temperature, monthly precipitation, potential evapotranspiration and monthly mean relative humidity. These climate variables were interpolated between the different sites for the years 1900–2008 (Fig. 2. 3) using the BioSIM model (Régnière, 1996). Data from a network of weather stations under the auspice of Environment Canada (ftp://ftp.cfl.scf.rncan.gc.ca/regniere/Data/Weather/Daily/.) were used to generate daily climate variables. Daily climate data were interpolated from the eight closest weather

stations, adjusted for differences in latitude, longitude and elevation (Fig. 2. 3 and Table 2. S2) between the data sources and the study site locations and averaged using a $1/d^2$ weight, where d represents distance. The average or sum of daily data was used to generate monthly means or totals. For this procedure, the number of matched weather stations that were used to generate weather data was kept constant through time (Régnière, 1996). It should be noted that the uncertainty of past climate records is greater than present climate records due to the overall increase in weather stations over time.

2.4.3.2. Forest stands and soil information

The model requires data on forest stand type, forest type, tree age and tree species for the simulation of each stand. This information was obtained from PSPs across Canada (Table 2. S2) to initialize the TRIPLEX-Mortality model at each study site. Soil information at each site is also required for model initialization. The soil organic carbon data used in model initialization was obtained from the dataset generated by Tarnocai and Lacelle, (1996). We also used a soil property dataset generated by Batjes, (2012), which contains soil texture information (i.e., soil clay, sand and the silt fraction) to initialize the TRIPLEX-Mortality model.

2.4.4. Model calibration and validation

In this study, 50 sites (70% of the total) were randomly selected for model calibration. Tree density and mean DBH in each site were selected as calibration targets at each site by performing multiple interactions of modifications to the initial parameters. Based on simulated PLC and NSC_{ratio} (the ratio of NSC and the initial NSC pool) as well as their corresponding theoretical thresholds (PLC = 1, NSC_{ratio} = 0), we used a similar theory of the law of the minimum (Liebig & Playfair, 1843) to determine the major CS or HF pathways that caused tree mortality in each site. Specifically, the mortality pathway was the pathway with the smallest difference between HF (or CS) and its corresponding to the theoretical threshold (Eq.2. 10). According to observed mortality rates and the corresponding simulated PLC (HF pathway plots) and NSC_{ratio} (CS pathway plots), we used the Levenberg–Marquardt iteration algorithm (Levenberg, 1944; Moré, 1978) with

400 iterations to fit the equations which were used to calculate tree mortality (see Section 3.1), respectively.

$$A = Min\ (1 - PLC, NSC_{ratio} - 0) \quad (2.\ 10)$$

where A represents the major pathway that causes tree mortality in each plot.

For validation, we selected tree density, mean quadratic DBH and the mortality rate (the ratio of the number of dead trees to the total number of trees in a quadrat) derived from 23 sites (30% of the total) to evaluate model performance. We evaluated model performance using the coefficient of determination (R^2) and the index of agreement (IA) (Willmott, 1981), where $IA = 1$ when predictions are equal to observations (Willmott, 1981). IA is calculated as follows:

$$IA = 1 - \frac{\sum_{i=1}^{n}(S_i - O_i)^2}{\sum_{i=1}^{n}(|Si - \bar{O}| + |Oi - \bar{O}|)^2} \quad (2.\ 11)$$

where S_i is the ith simulated value; O_i is the ith observed value; n is the number of data; and $\bar{O}$ is the average observed value.

2.4.5. Sensitivity analysis

2.4.5.1. Parameter sensitivity analysis

Identifying the most sensitive parameter is critical for model simulation. In this study, the drought intensity of each site was estimated (see Eq. 2. 12) along with the monthly CMI index (E. H. Hogg et al., 2013) from 1990 to 2008 at each site in order to investigate parameter sensitivity under different drought levels.

$$CMI = Prec - PET \quad (2.\ 12)$$

where $Prec$ and PET are monthly precipitation (mm) and potential evapotranspiration (mm), respectively.

Based on the CMI, we selected three typical sites (QC17, ON9 and SK19) to represent drought gradients as either being light (CMI = 51), moderate (CMI = 23) or severe drought (CMI = -2.4) levels (see Fig. 2. 8). Among the major parameters involved in mortality-related processes (Table 2. S1), the adopted values of some of them such as *a*, *b*, and *c* have

been fully discussed and supported in previous studies (see Table 2. S1). Therefore, seven parameters (Table 2. 1) were selected for sensitivity analysis. Sensitivity is typically expressed as the ratio between a relative change in a model output and a relative change in a parameter value. Initial parameter values varied from +20% and -20%. We obtained corresponding modelling outputs for sensitivity analysis. We then used the sensitivity index (SI) (Lenhart et al., 2002) to quantify parameter sensitivity, where higher absolute SI values indicate higher parameter sensitivity.

$$SI = \frac{1}{n}\sum_{j=1}^{n}\left\{\frac{(y_{2j}-y_{1j})/y_{0j}}{2*\Delta x/x_0}\right\} \quad (2.\ 13)$$

where SI is the sensitive index; y_0 is the modelling output; x_0 is an initial parameter value; y_2 and y_1 are corresponding values of the output based on + Δx (+20%) and - Δx (-20%), respectively; n is the number of sites used in the sensitivity analysis.

Table 2. 1. List of major sensitive analysis parameters

Parameters	Explanation	Values	Unit	Reference
t	coefficient for the thickness of the topsoil layer	0.1	m	This study
f	coefficient for the soil organic matter fraction	0.47	-	This study
s_{min}	coefficient for the porosity of mineral soil	1.088	-	(Farouki, 1981; Letts et al., 2000)
s_{om}	coefficient for the porosity of organic matter	0.9	-	(Farouki, 1981; Letts et al., 2000)
swp_{om}	saturated organic matter matric potential	-10.3	MPa	(Letts et al., 2000)

b	critical soil water potential value that leads to a 63% reduction in conductivity	-3.57	MPa	(Neufeld et al., 1992; Pammenter and Van der Willigen, 1998; Sperry and Tyree, 1988)
c	shape parameter to calculate percentage loss conductivity	4.07	-	(Neufeld et al., 1992; Pammenter and Van der Willigen, 1998; Sperry and Tyree, 1988)

2.4.5.2. Sensitivity to climate inputs

Sensitivity to climate inputs allowed us to systematically test model behavior while gaining insight into how the simulated system operates. Based on the setting of sensitivity scenarios in the previous study of Peng et al., (2002), we refined the scenarios setting to better explore the sensitivity of each climate input variable. In this study, the sensitivity scenarios involved applying a uniform 10%, 8%, 6%, 4% and 2% increase or decrease in each climate input variable (see Table 2. 2). To conduct this sensitivity analysis, we used the same three sites (QC17, ON9, SK19) as the parameter sensitivity analysis.

Table 2. 2. Sensitivity scenarios of selected key variables to climate change

Sensitivity scenarios	S1	S2	S3	S4	S5	S6	S7	S8	S9	S10
Temperature	-10%	-8%	-6%	-4%	-2%	+2%	+4%	+6%	+8%	+10%
Precipitation	+10%	+8%	+6%	+4%	+2%	-2%	-4%	-6%	-8%	-10%
Humidity	+10%	+8%	+6%	+4%	+2%	-2%	-4%	-6%	-8%	-10%
Potential evapotranspiration	-10%	-8%	-6%	-4%	-2%	+2%	+4%	+6%	+8%	+10%

2.5. Results

2.5.1. Model parameterization and calibration

Comparisons between calibrated tree density (R^2 = 0.96; IA = 0.96) and DBH (R^2 = 0.98; IA = 0.97) over 50 PSPs (see Table 2. S2) in conjunction with their corresponding observations showed a good agreement (Fig. 2. 4). Based on mortality observations, we calibrated equations (Eq. 2. 14 and Eq. 2. 15) to calculate mortality caused by HF and CS pathways, respectively (see Fig. 2. 5).

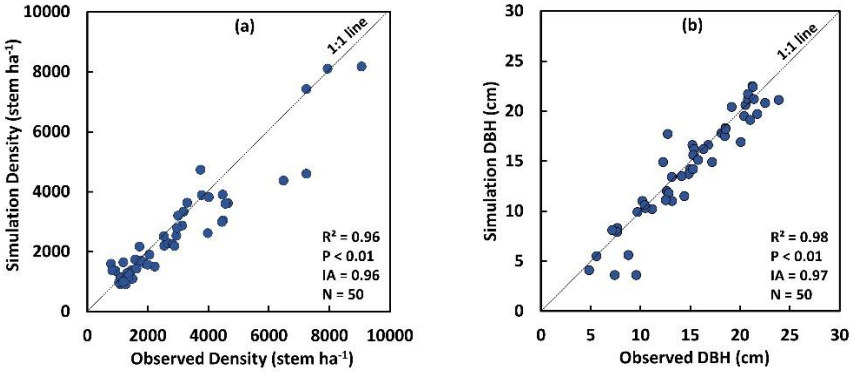

Figure 2. 4. Comparison between observed and calibrated simulations of density (a) and diameter at breast height (DBH in cm, b).

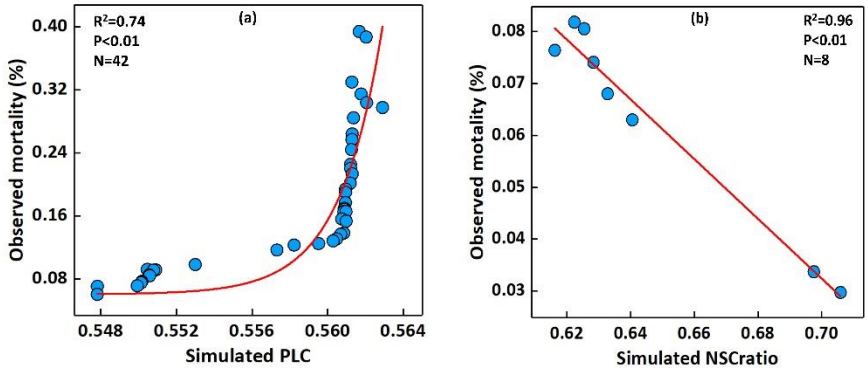

Figure 2. 5. Relationships between the simulated percentage loss of conductivity (PLC, a), the ratio of the NSC and the initial NSC pool (NSCratio, b) and observed mortality rates.

42 PSPs were identified as death caused by HF (see section 2.4), over these 42 PSPs, the PLC and observed mortality rates closely correlated (Fig. 2. 5a; R^2 = 0.74):

$$Mort = 0.0606 + 6.72363 * 10^{-5} * e^{\frac{PLC-0.54562}{0.00227}} + 9.71743 * 10^{-5} * e^{\frac{PLC-0.54562}{0.00226}} \quad if PLC \geq 0.54 \qquad (2.\ 14)$$

where $Mort$ is tree mortality caused by HF, and PLC represents the percentage loss of conductivity.

8 PSPs were identified as death caused by CS. The NSC_{ratio} and observed mortality rate in these 8 PSPs were close (Fig. 2. 5b, $R^2 = 0.96$) to the relationship as below:

$$Mortc = -0.57566 * NSC_{ratio} + 0.43536 \qquad if NSC_{ratio} \leq 0.7 \qquad (2.\ 15)$$

where $Mortc$ is tree mortality caused by CS.

2.5.2. Model validation

Being two critical parameters that can affect tree vulnerability under drought conditions, DBH and tree density were accurately represented (tree density: $R^2 = 0.75$ and IA = 0.99; DBH: $R^2 = 0.73$ and IA = 0.98) by the TRIPLEX-Mortality model during drought events (Fig. 2. 7b and c). Fig. 2. 6 provides annual cycles of monthly averaged water and carbon states (SWP, PLC and NSC_{ratio}) change respective to VPD, temperature and wet/dry month in four sites. Note that even though the absolute changes of each variable differed under the different drought conditions of each site, their trends were consistent and reasonable. During summer months (from June to September), both temperature and VPD gradually increased under the intensified drought conditions typical of these months, while they exhibited a decreasing tendency (see Fig. 2. 6e, f, g and h). Correspondingly, this situation led to a decrease in water potential, which in turn decreased hydraulic conductivity (see Fig. 2. 6a, b and c) and non-structural carbon storage (see Fig. 2. 6d).

Under different drought conditions, the TRIPLEX-Mortality model was able to accurately capture changes in mortality regardless of the region it was investigating (i.e., Western or Eastern Canada) (see Fig. 2. 7a). Simulated mortality results showed good agreement with mortality observations ($P < 0.01$; $R^2 = 0.79$ and IA = 0.94). Averaged simulated mortality

rates (Fig. 2. 7a) from 13 sites in Western Canada (18.5 %) were higher overall compared to 10 sites in Eastern Canada (11.5%). Mortality in four sites (QC 2, 4, 12 and 14) was caused by low non-structural carbon content (i.e., the CS pathway), whereas high percentage loss of conductivity (i.e., the HF pathway) was responsible for mortality in the other sites.

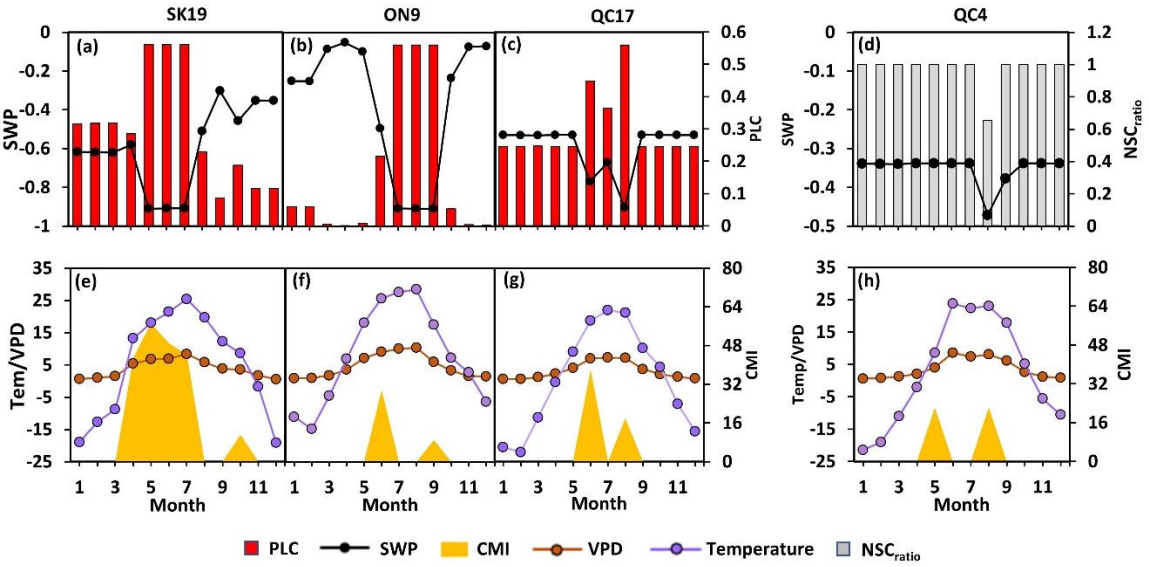

Figure 2. 6. Simulated monthly PLC, NSCratio, soil water potential (MPa), VPD (mb) and observed monthly temperature (°C) in the SK19, ON9, QC17 and QC4 plots. SK19, ON9 and QC17 represent drought gradients as either light (CMI = 51), moderate (CMI = 23) or severe drought (CMI = -2.4) levels and that tree mortality in these plots was caused by HF. Tree death in QC4 (CMI = 37) was caused by CS.

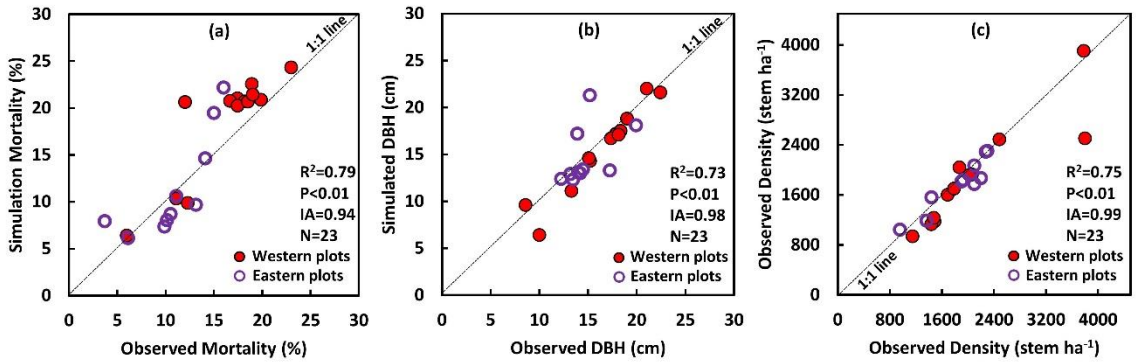

Figure 2. 7. Comparison between observed and modeled mean quadrat mortality (a), diameter at breast height (DBH in cm, b) and density (c). IA represents the index of

agreement, western plots include plots that located in the provinces of Alberta, Saskatchewan and Manitoba, while the eastern plots include plots that located in the provinces of Ontario and Quebec.

2.5.3. Sensitivity analysis

Among the selected parameters, the mean SI of each parameter varied from -4.99 to 2.48 (Fig. 2. 8). Compared to the mean values of each parameter, parameters *c*, *Smin*, *Som* and *b*, exhibiting either high or extremely high sensitivity to mortality rates and parameter *c* (average SI = -3.5) was the most sensitive of these parameters. Overall parameter sensitivity differed depending on drought intensity, for which the sensitivity of drought prone regions (Western Canada) was higher compared to moister regions (Eastern Canada).

Fig 2. 9 shows the results of sensitivity analysis under different drought scenarios. For the HF pathway, intensified drought resulted in a decrease in soil water (SW) and SWP and an increase in tree vulnerability to HF (i.e., an increase in PLC, see Fig. 2. 9), ultimately leading to higher mortality. Conversely, the opposite trend occurred as drought conditions alleviated. Similar to the HF pathway, more drought resulted in a decline in LWP due to a decrease in SW and SWP. In this case, stomatal conductance (SC, represented by G_s in this study), total primary productivity (GPP_D) under drought conditions and NSC decreased while tree mortality increased. Mortality exhibited a nonlinear response to both drought intensified and alleviated, indicating that each drought level has a specific plateau. As drought intensified, increased soil water content and decreased PLC were significantly lower in the QC17 site (i.e., the site with only a slight degree of drought) compared to sites with severe drought (SK19) and moderate drought (ON9). However, under intensified drought conditions, SWP and the LWP in the QC17 site were both much higher compared to the SK19 and ON9 sites. There was also a relatively significant impact on productivity in the SK19 site regardless of the drought condition (i.e., drought intensified or alleviated). As drought intensified, the SK19 site exhibited a significant decrease in NSC. Conversely, as drought intensified, the QC17 site exhibited a greater increase in both SC and NSC.

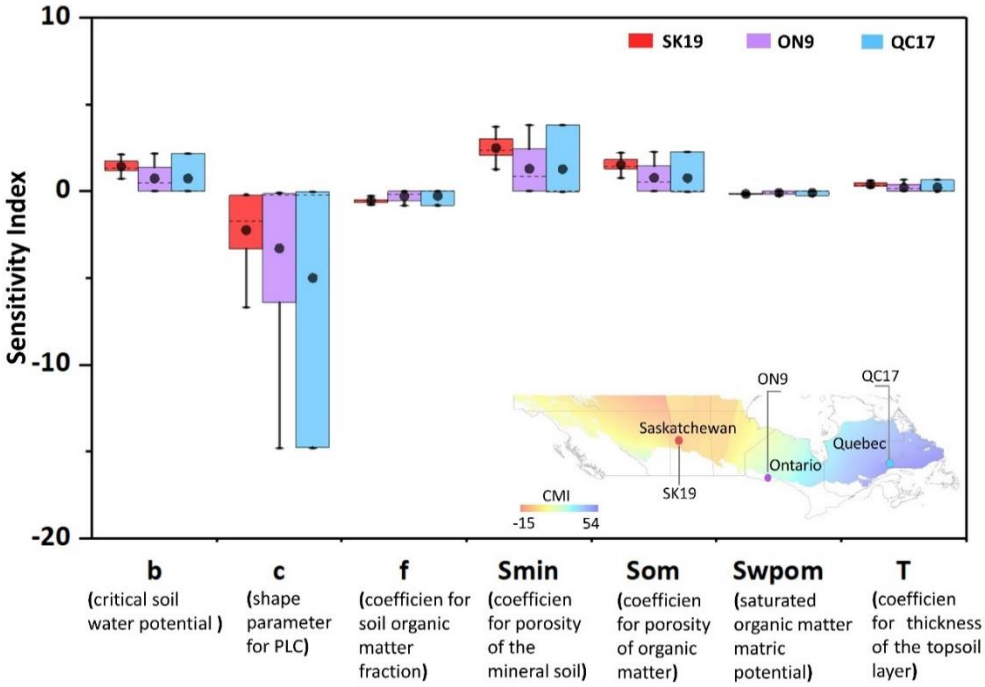

Figure 2. 8. Sensitivity index (SI) of the different parameters in the selected sites. CMI represents the climate moisture index; black dots represent the mean SI values of the parameters.

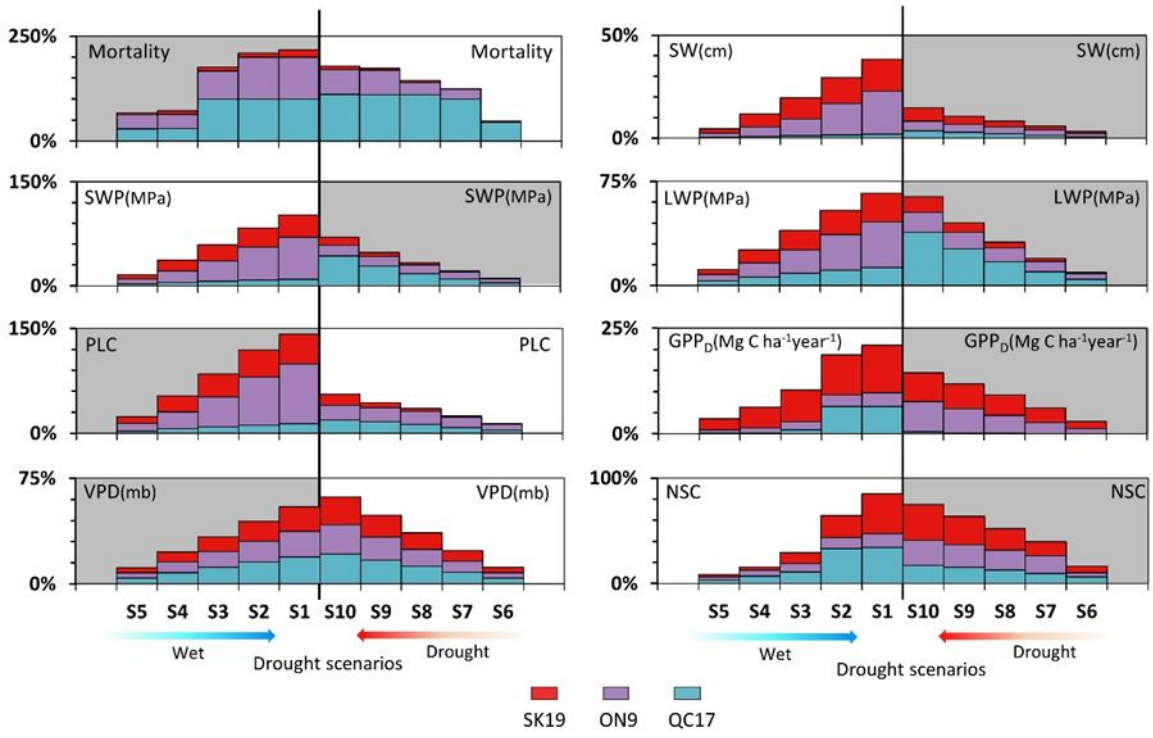

Figure 2. 9. Changes in simulated values of the major variables (compared to actual drought conditions) under the different drought scenarios (see Table 2. 2) within light (QC17), moderate (ON9) and severe drought (SK19) level sites. The white background shows the percentage increase, while the gray background shows the percentage decrease. Abbreviations are defined as follows: SW = soil water, SWP = soil water potential, LWP = leaf water potential, PLC = percentage loss of conductivity, GPPD = gross primary productivity under drought conditions, NSC = non-structural carbohydrate content, VPD = vapor pressure deficit.

2.6. Discussion

2.6.1. Key components and parameter settings for HF and CS pathways

The incorporation of drought-induced physiological mortality mechanisms (i.e., HF: hydraulic failure; CS: carbon starvation) into our new process-based TRIPLEX-Mortality model is critical for improving our quantitative understanding and ability to predict drought-induced mortality dynamics of boreal forest ecosystems. The integration of these two mechanisms to predict carbon dynamics under a changing climate is key improvement over other models that only consider one or neither of the carbon and water limitations under drought conditions at the stand level in the boreal forests.

To be able to evaluate the HF pathway, we developed a new soil-water balance submodule in TRIPLEX-Mortality based on TRIPLEX 1.0. We also developed a modelling approach for the PLC index, whose usefulness is both theoretical and practical for investigating HF with respect to different plant functional types (Choat et al., 2012; Maherali et al., 2004). Our development work thus permits the TRIPLEX-Mortality model to describe both hydraulic dynamics (i.e., soil water potential) and risks (i.e., PLC) at a stand level under various drought conditions.

A logical hypothesis is that 100% PLC is the threshold that causes tree mortality. However, Urli et al., (2013) found substantial differences in cavitation resistance between species, with P_{50} water potential values ranging from -2.36 to -5.52 MPa inducing a 50% PLC. Based on their multimodel-experiment framework, McDowell et al., (2013) found that PLC thresholds varied significantly between different species and models, while also

determining the mean PLC thresholds of different models (FINNSIM, Sperry, TREES, MuSICA, ED(X) and CLM(ED)) for pine trees (0.63) and for juniper trees (0.32). Adams et al., (2017) used a standardized physiological framework to analyze drought-induced tree mortality across species, and they recommended a threshold value of 0.6 or higher for PLC. Another way to identify a mortality threshold is to compare with empirical approaches based on mortality observations (De Kauwe et al., 2020). Anderegg et al., (2015), McDowell et al., (2016) and Mitchell et al., (2014) all defined reasonable mortality thresholds for their mortality simulation based on observational and experimental datasets. Similarly, in this study, we used tree mortality observations from 42 PSPs used to define the PLC threshold (see Table 2. S1) and established the relationship (see Eq. 2. 14) between PLC and mortality at a stand level across Canada's boreal forests.

In order to integrate the CS pathway into the TRIPLEX-mortality model, we improved the carbon allocation of TRIPLEX 1.0 and integrated a new NSC carbon pool into the TRIPLEX-Mortality model. However, it is still a big challenge to quantify the NSC threshold at which mortality begins (Gruber et al., 2012; McDowell, 2011). McDowell et al., (2013) reported mean NSC thresholds of six models for pine trees (0.51) and for juniper trees (0.45). Carbohydrate concentrations at death varied among factors, including tree species, tree tissue and canopy position; thus, these thresholds require empirical investigation (Adams et al., 2017b; Anderegg et al., 2015; McDowell et al., 2013; Oliva et al., 2014). To date, specific NSC survival or mortality thresholds have not been resolved adequately for drought events (Adams et al., 2017). We, therefore, used mortality observations derived from eight PSPs to define the NSC threshold (see Table 2. S1) and establish the relationship (see Eq. 2. 15) between NSC_{ratio} and mortality at a stand level across Canada's boreal forests.

2.6.2. Model calibration and sensitivity analysis

Based on mortality observations and threshold ranges from literature whose initial parameters were calibrated for different species, we defined thresholds (Table 2. S1) and calibrated mortality calculation equations (Eq. 2. 14 and Eq. 2. 15) at the stand level. Although such calibration methods achieved the desired results (comparable to observed mortality for a given drought condition), this procedure may induce potential uncertainties.

Because first of all, due to a lack of observed PLC and NSC from the stand level, our simulated PLC and NSC were not directly calibrated and independently validated. Second, during calibration, the main pathway for each site that caused tree mortality was simply determined based on the assumption of differences between theoretical thresholds (PLC (100%); NSC (0%)) and simulated values (PLC and NSC). Additionally, recent studies have shown the existence of a multitude of interactions between CS and HF that can accelerate or buffer mortality during drought (Flexas et al., 2006; Hummel et al., 2010; McDowell et al., 2011; Muller et al., 2011). In theory, many of these interactions should be captured by simulated PLC and NSC_{ratio}. However, further observations, experiments and modeling tests are still needed so that models can more reasonably simulate these interactions (McDowell et al., 2011). Therefore, in the TRIPLEX-mortality model, these interactions were simplified by accounting for hydraulic impacts on the simulation of stomatal conductance and subsequent effects on NSC dynamics.

Sensitivity analysis was used to identify relatively sensitive parameters. The results of the parameters sensitivity analysis indicated that the *c*, *Smin*, *Som* and *b* parameters were more sensitive than the other parameters. Moreover, parameters showed higher sensitivity under more severe drought conditions (Fig. 2. 8). This was mainly due to soil water potential, which can significantly influence hydraulic conductance (see section 2.1.1), and the fact that hydraulic conductance and water potential simultaneously regulate stomatal behavior (see Eq. 2. 6), which affects productivity and ultimately non-structural carbon dynamics (Adams et al., 2017). Under more severe drought conditions, specific water and carbon status are more likely to exceed their own threshold margins, and any slight change in them could consequently lead to significant changes in model outputs.

The results of our input sensitivity analysis indicated that the TRIPLEX-Mortality model can capture changes in tree mortality under both intensified and alleviated droughts (Fig. 2. 9). Although each variable within the different drought level plots (SK19, ON9 and QC17) exhibited a consistent changing trend, changes in magnitude differed. Mortality rates did not linearly correspond to changes in drought conditions, suggesting the existence of a plateau at each drought level. This is because PLC and NCSratio have thresholds that trigger death and not all changes in drought intensity are sufficient to trigger the mortality thresholds of PLC or NCS. Along with drought intensified, SWP and LWP were more

sensitive to changes in drought in the QC17 site compared to the SK19 and ON9 sites (Fig. 2. 9). A wetter condition may be responsible for this finding because the tolerance difference of variables to the threshold was greater compared to those under more serve drought conditions.

2.6.3. Model validation, limitation and uncertainties

This study presents for the first time two physiological drought-induced mortality mechanisms (HF and CS) that have been incorporated into a process-based model (TRIPLEX-Mortality) at a stand level across Canada's boreal forests. Results from validation and sensitivity analyses showed high confidence in the model's ability to reproduce drought-induced mortality, tree density and DBH (Fig. 2. 7). The good agreement between observations and simulation was likely due to (1) the ability of the TRIPLEX-Mortality model to accurately simulate forest dynamics (i.e., tree density and DBH), (2) the high number of PSPs used in model calibration and validation, (3) the ability of the TRIPLEX-Mortality model to capture hydraulic risk (PLC) and NSC dynamics under drought stress, and (4) the ability of the TRIPLEX-Mortality model to represent relationships between mortality and PLC and NSC, respectively, at a stand level.

Our model simulation results were in general agreement with existing results from previous studies on drought-induced mortality in Canada's boreal forests. For instance, Peng et al., (2011) estimated drought-induced tree mortality throughout Canada's boreal forests using data from the permanent sample plots and statistical models and indicated that tree mortality rate in the west is much higher than in the east. Michaelian et al., (2011) also reported that aspens in Southwestern Canada suffered from severe drought, which resulted in higher mortality rates and loss of biomass. Our simulated mortality rates 18.5% in the west and 11.5% in Eastern Canada are highly consistent with the above study results. Hogg et al., (2008) used tree-ring analysis and plot-based measurements to assess drought impacts on boreal forests in Western Canada, determining that western boreal forests are moisture limited. Model simulated average CMI (-31.4 mm) in western sites was lower compared to eastern sites (-24.6 mm), while the average VPD (7.87 mb) in western sites was higher compared to eastern sites (7.4 mb). These results indicated that during the simulation period, trees located in western sites underwent more severe and extensive

drought compared to trees located in eastern sites. Trees in west are more likely to suffer from water stress. Our work also shows, under a more severe drought condition, trees have a more positive response to drought stress, which is manifested by higher sensitivity of PLC and NSC to drought stress. The abundant precipitation, high soil moisture and lower temperatures in Eastern Canada may be the main reasons for these results. Moreover, our new tree mortality model considered both CS and HF and some of their interactions, which is more comprehensive and an advance on the work of Fisher et al., (2010) who only concentrated on CS. Drought-induced mortality mechanism may thus be better presented in our TRIPLEX-Mortality model.

Our efforts to model tree mortality represent the first step toward a new generation of process models that are capable of integrating key tree mortality processes into boreal forests. However, this study also has certain shortcomings. First, relationships between mortality in conjunction with hydraulic risk (PLC) and carbon dynamics (NSC) were fitted based on mortality observations, which only covered a range of quadrat mortality rates between 0 to 40%. This may reduce simulation accuracy in plots where mortality is greater than 40%. Another shortcoming of this study could potentially be the lack of in situ observed PLC and NSC data. Additionally, the influence of stomatal conductance on productivity and the interaction between HF and CS were simplified in our model.

2.6.4. Towards a better simulation of drought-induced tree mortality and future direction

Despite recent advances in drought-induced tree mortality modelling, there remain some gaps that need to be considered to improve the ability of our process-based model in simulating drought-induced mortality, including dynamics respective to canopy leaf area during drought events, coupling the hydraulic architecture with stomatal conductance and determining the plant water status dependence on the soil water potential vs on VPD (Choat et al., 2018; Hendrik & Maxime, 2017; Oogathoo et al., 2020). First, during drought events, many forest trees attempt to avoid drought stress on plant water content by leaf shedding (Limousin et al., 2010; Vilagrosa et al., 2003). However, due to the complex dynamics involved in leaf shedding, models have as yet poorly captured drought deciduousness (Dahlin et al., 2017). Second, despite recent progress in modelling relationships between

hydraulic architecture and stomatal conductance under drought conditions (Mackay et al., 2015), non-stomatal limitations to photosynthesis during drought should be incorporated into models to better simulate drought-induced mortality (Hendrik & Maxime, 2017). Finally, the relationship between soil and the status of plant water is the key component of the HF pathway. However, many models only simulate soil water content by using single water bucket technique, which does not fully capture these relationships. Future models need to incorporate vertical gradients into soil moisture potential, root distribution and soil-root resistance alterations caused by soil drying (Christoffersen et al., 2016; De Kauwe et al., 2015). Despite the abovementioned limitations and challenges, we remain confident that our TRIPLEX-Mortality model, which has been integrated with advanced physiological mechanisms and has been calibrated and validated against observed data at a stand scale. TRIPLEX-Mortality model offers far superior results in simulating drought-induced mortality dynamics and shows high potential in predicting the impacts of drought-induced mortality on carbon sinks and sources across boreal forests under future climate change conditions.

2.7. Conclusions

To the best of our knowledge, this study represents the first attempt to report on the successful integration of two important physiological tree mortality mechanisms by means of integrating hydraulic failure (HF) and carbon starvation (CS) components into a process-based model (TRIPLEX-Mortality) at a stand level. Results from model validation indicated that observed and simulated mortality rates were highly correlated ($R^2 = 0.79$; IA = 0.94), offering high confidence in applying this model across boreal forest ecosystems. Our results also confirmed that western Canada mortality rates are higher overall compared to eastern Canada mortality rates, which is consistent with previous studies. The model further suggests that hydraulic failure is the dominant driver of mortality in the drier western boreal forests of Canada and carbon starvation predominates as a cause of mortality in the eastern boreal forest of Canada. Results from sensitivity analysis indicated that the shape parameter (c) for calculating percentage loss of PLC was the most sensitive parameter to simulate tree mortality. Finally, the intent of the TRIPLEX-Mortality model is to contribute to the scientific modelling community by improving our quantitative

understanding of drought-induced mortality rates in boreal forests while also providing a new, groundbreaking approach for future Earth System Model development under a progressively changing climate.

2.8. Supplementary materials

2.8.1. Appendix A.1. The equations used in the hydraulic failure (HF) and carbon starvation (CS) pathway

2.8.1.1. Hydraulic failure pathway

λ (soil attribution parameter) is calculated as:

$$\lambda = 2.91 + 0.159 p_{clay} \quad \text{(S2. 1)}$$

where p_{clay} is the percentage of clay soil.

s (saturated volumetric water content of the topsoil layer) is calculated as a function of the soil organic matter fraction (f), the porosity of mineral soil (s_{min}) and the porosity of organic matter (s_{om}) (Eq. 2. 5). s_{min} is a function of the percentage of sand in soil ($Soil_{sand}$).

$$s = (1 - f) s_{min} + f s_{om} \quad \text{(S2. 2)}$$

$$s_{min} = 0.489 - 0.00126 \ (Soil_{sand}) \quad \text{(S2. 3)}$$

swp_{sat} is calculated as shown in Letts et al., (2000):

$$swp_{sat} = -10 * 10^{1.88 - 0.0131 (Soil_{clay})} \quad \text{(S2. 4)}$$

where $Soil_{clay}$ is the percentage of clay soil.

2.8.1.2. Carbon starvation pathway

To calculate Ψ_l(leaf water potential), we simplified the equation by Hendrik and Maxime, (2017) as follows:

$$\Psi_l = SWP(1 - r) - pet \quad \text{(S2. 5)}$$

where pet is potential transpiration (cm), and r is a coefficient representing the resistance

from soil to leaves.

NPP (net primary productivity) is then obtained from GPP as follows (Peng et al., 2002):

$$NPP = C_{NPP} GPP \quad \text{(S2. 6)}$$

Table 2. S1. List of major mortality-related process parameters

Parameters	Explanation	Values	Unit	Reference
t	coefficient for the thickness of the topsoil layer	0.1	m	This study
f	coefficient for the soil organic matter fraction	0.47	-	This study
SWP	Soil water potential	-	MPa	(Oleson et al., 2010)
s_{min}	coefficient for the porosity of the mineral soil	1.088	-	(Farouki, 1981; Letts et al., 2000)
s_{om}	coefficient for the porosity of organic matter	0.9	-	(Farouki, 1981; Letts et al., 2000)
swp_{om}	saturated organic matter matric potential	-10.3	MPa	(Letts et al., 2000)
swp_{sat}	saturated mineral soil matric potential	-	MPa	(Letts et al., 2000)
α	percentage for the net primary productivity transfer to the non-structural carbon pool	0.25~0.35	-	(Tague et al., 2013)
b	critical soil water potential value that leads to a 63% reduction in	-3.57	MPa	(Neufeld et al., 1992; Pammenter and Van der Willigen, 1998;

	conductivity			Sperry and Tyree, 1988)
c	shape parameter to calculate percentage loss conductivity	4.07	-	(Neufeld et al., 1992; Pammenter and Van der Willigen, 1998; Sperry and Tyree, 1988)
LWP	Leaf water potential	-	MPa	(Davi et al., 2017)
C_{NPP}	coefficient for the gross primary productivity transfer to net primary productivity	0.47	-	(Waring et al., 1998)
P_{cof}	empirical coefficient for the vapor pressure deficit	−0.05	-	(Waring et al., 1998)
VPD	vapor pressure deficit	-	mb	-
$P_{threshold}$	threshold percentage of structural plant carbon for the maximum non-structural carbon pool	0.2	-	(Tague et al., 2013)
$PLC_{threshold}$	threshold value for hydraulic failure to cause death	0.54	-	(McDowell., 2013)
$NSC_{r\_threshold}$	threshold value for the ratio of NSC and the initial NSC pool	0.7	-	This study

Table 2. S2. Information on selected forest plots used for model calibration and validation

Plots ID *	Plot size (ha)	Elevation (m)	Soil organic carbon * (t/ha)	Longitude (°W)	Latitude (°N)	(accounting year for year of mortality) First measurement	(accounting year for year of mortality) Last measurement	Stand age (Last measurement)	Density (stem ha^{-1}) (Last measurement)	DBH (cm) (Last measurement)	Observed mortality (%)	Dominant species	Application
SK30	0.08	1245	491	107.80	54.20	1980	1996	98	825	22.54	39	*Picea glauca*	Calibration
MB2	0.05	492	507	96.10	49.70	2001	2006	85	3980	13.19	39	*Genus cedrus*	Calibration
ON5	0.12	316	2111	80.30	48.50	1999	2006	92	783	20.80	33	*Populus tremuloides*	Calibration
SK13	0.08	2130	446	107.30	55.10	1979	1996	114	1350	18.55	31	*Picea glauca*	Calibration
MB5	0.05	366	515	95.80	51.70	2003	2008	88	1580	12.76	30	*Pinus banksiana*	Calibration
SK22	0.08	1692	581	108.90	55.10	1979	1996	119	1050	23.90	30	*Picea glauca*	Calibration
SK21	0.08	1700	469	107.90	54.80	1979	1996	134	1625	17.21	28	*Picea glauca*	Calibration
SK11	0.08	1958	419	107.70	55.00	1979	1996	103	2225	16.34	26	*Picea glauca*	Calibration
MB10	0.05	247	306	99.00	52.80	2000	2005	85	1720	12.28	24	*Populus tremuloides*	Calibration
MB4	0.05	426	794	95.50	50.00	1999	2004	112	7240	8.78	26	*Picea mariana*	Calibration
SK14	0.08	1692	581	108.90	55.10	1979	1996	125	1275	20.42	23	*Picea glauca*	Calibration
AB8	0.10	1435	44	114.20	49.30	1994	2003	95	3130	15.29	22	*Pinus contorta*	Calibration
SK2	0.08	1091	502	105.40	53.80	1979	1996	121	4450	10.50	21	*Picea mariana*	Calibration
AB21	0.16	747	132	118.30	57.10	1988	1993	175	9062	15.24	20	*Picea glauca*	Calibration
SK4	0.08	662	543	105.90	54.10	1979	1996	101	2963	10.44	19	*Picea mariana*	Calibration
SK1	0.08	1696	500	105.70	54.10	1979	1996	109	4013	13.17	19	*Picea mariana*	Calibration
AB20	0.40	815	80	119.30	56.60	1984	1989	103	3182	21.75	18	*Populus*	Calibration

											tremuloides	
MB16	0.05	273	142	101.30	54.10	2002	2007	117	6480	5.59	17	*Picea mariana*	Calibration
SK16	0.08	1353	321	105.50	54.10	1991	1994	91	1338	21.05	17	*Picea glauca*	Calibration
MB12	0.05	275	142	99.20	52.90	2000	2005	94	3740	7.66	17	*Pinus banksiana*	Calibration
MB13	0.05	285	142	101.10	53.40	2002	2007	108	7240	7.43	17	*Picea mariana*	Calibration
MB3	0.05	488	535	96.00	49.30	2001	2006	85	4480	11.19	16	*Picea mariana*	Calibration
MB7	0.05	397	122	95.50	51.00	2003	2008	157	4560	9.58	15	*Picea mariana*	Calibration
SK12	0.08	1700	469	107.90	54.80	1979	1996	105	1988	15.80	14	*Picea glauca*	Calibration
SK25	0.08	1392	622	102.70	53.10	1979	1996	144	1188	21.39	14	*Picea glauca*	Calibration
AB14	0.10	2010	34	114.60	50.20	1994	2003	120	2670	12.81	13	*Pinus contorta*	Calibration
AB9	0.10	1882	34	114.50	50.20	1994	2003	126	1090	20.55	13	*Pinus contorta*	Calibration
AB19	0.32	845	132	118.60	56.80	1988	1993	141	4648	21.26	13	*Pinus contorta*	Calibration
AB17	0.82	1501	65	115.70	52.40	1986	1998	102	4472	14.86	12	*Pinus contorta*	Calibration
AB16	0.10	1532	91	115.10	51.50	1994	2006	109	1370	19.16	12	*Pinus contorta*	Calibration
AB12	0.10	2010	34	114.60	50.30	1994	2002	126	2540	12.65	10	*Pinus flexilis*	Calibration
AB15	0.10	1903	34	114.60	50.30	1995	2007	141	2820	12.83	9	*Pinus contorta*	Calibration
AB7	0.10	1490	172	114.40	49.40	1994	2003	113	1310	15.39	9	*Pinus contorta*	Calibration
ON7	0.12	306	341	89.40	48.70	1997	2006	105	1458	16.80	9	*Picea mariana*	Calibration
QC10	0.04	590	83	72.00	50.90	1980	1995	135	2050	14.13	9	*Picea mariana*	Calibration
AB10	0.10	1903	34	114.60	50.30	1994	2003	107	1900	15.01	8	*Pinus contorta*	Calibration
ON1	0.12	349	149	93.60	50.70	1998	2006	94	1192	20.80	8	*Populus tremuloides*	Calibration
AB24	0.10	1882	34	114.50	50.10	1994	2002	211	1180	18.55	8	*Picea engelmanni*	Calibration

AB13	0.10	2010	34	114.60	50.20	1994	2002	157	1460	20.08	8	*Pinus contorta*	Calibration
ON4	0.12	267	0	83.10	49.10	2000	2006	98	933	21.30	7	*Populus tremuloides*	Calibration
SK5	0.08	1831	493	104.30	54.50	1980	1996	149	3000	9.70	7	*Picea mariana*	Calibration
MB6	0.05	394	174	95.80	51.10	2003	2008	155	3300	7.18	6	*Picea mariana*	Calibration
AB25	0.10	1882	34	114.50	50.20	1994	2002	216	1490	18.15	8	*Pinus contorta*	Calibration
AB26	0.10	1882	34	114.50	50.20	1994	2002	215	2880	14.42	8	*Pinus contorta*	Calibration
AB27	0.10	2448	34	114.50	50.20	1994	2002	220	1100	18.48	8	*Pinus contorta*	Calibration
ON6	0.12	101	615	90.50	50.30	1998	2004	159	2525	10.20	3	*Pinus banksiana*	Calibration
MB8	0.05	219	132	97.40	51.70	1999	2004	90	2940	12.54	7	*Picea mariana*	Calibration
MB1	0.05	680	159	100.90	51.60	1999	2004	126	7940	4.86	6	*Picea mariana*	Calibration
MB9	0.05	220	132	97.40	51.80	1999	2004	88	1780	15.31	3	*Picea mariana*	Calibration
MB11	0.05	275	1389	99.10	52.90	2000	2005	138	3780	7.67	7	*Picea mariana*	Calibration
AB11	0.10	2010	34	114.60	50.26	1994	2002	128	1870	15.22	12	*Pinus flexilis*	Validation
AB5	0.10	881	233	116.77	54.17	1993	2002	144	1490	17.94	17	*Picea mariana*	Validation
MB14	0.05	255	219	100.27	53.88	1994	2002	105	3780	8.60	11	*Picea mariana*	Validation
MB15	0.05	334	168	101.26	54.16	1994	2002	103	6380	10.00	6	*Pinus banksiana*	Validation
QC12	0.04	667	850	66.03	51.53	1989	2001	230	1900	14.02	10	*Picea mariana*	Validation
QC14	0.04	487	850	66.98	51.19	1989	2001	178	1925	14.49	11	*Picea mariana*	Validation
QC16	0.04	675	850	66.50	51.01	1989	2001	155	2100	17.24	11	*Abies balsamifera*	Validation
QC17	0.04	562	850	66.41	51.09	1989	2001	155	2200	14.21	14	*Picea mariana*	Validation
QC2	0.04	255	338	77.11	51.02	1990	1999	110	2300	13.20	4	*Picea mariana*	Validation
QC4	0.04	244	602	77.95	50.21	1990	1999	122	2100	13.46	13	*Picea mariana*	Validation

QC5	0.04	394	845	74.01	50.96	1990	1999	99	2275	12.25	10	*Picea mariana*	Validation
SK10	0.06	2025	1619	105.24	54.46	1992	1999	93	2483	15.09	17	*Picea mariana*	Validation
SK18	0.08	790	1619	105.24	54.45	1992	1999	103	1688	17.89	19	*Picea glauca*	Validation
SK19	0.08	1518	108	108.27	54.97	1979	1998	111	1788	18.35	20	*Picea glauca*	Validation
SK20	0.08	904	950	108.42	54.97	1979	1998	166	1150	22.44	18	*Picea glauca*	Validation
SK26	0.08	1626	559	102.64	53.03	1979	1998	101	2063	17.36	19	*Populus tremuloides*	Validation
SK27	0.08	1582	268	106.47	54.54	1979	1998	103	1438	21.03	23	*Populus tremuloides*	Validation
SK29	0.08	2609	288	108.35	53.62	1979	1998	114	2025	18.15	17	*Picea glauca*	Validation
SK3	0.08	829	257	107.27	54.52	1980	1992	112	3800	13.29	19	*Picea mariana*	Validation
SK31	0.08	1044	371	105.72	53.97	1984	1998	126	1475	19.01	12	*Pinus banksiana*	Validation
ON2	0.12	349	180	86.96	49.75	2000	2004	126	1367	19.94	6	*Pinus banksiana*	Validation
ON3	0.12	276	368	84.10	49.42	1997	2004	118	958	15.20	16	*Pinus banksiana*	Validation
ON9	0.12	445	260	90.60	48.60	2001	2004	100	1442	13.90	15	*Pinus banksiana*	Validation

Note: *AB, SK, MB, ON and QC represent the provinces of Alberta, Saskatchewan, Manitoba, Ontario and Quebec. Soil organic carbon data derived from the database generated from the study by Tarnocai and Lacelle., (1996).

2.9. Reference

Adams, H. D., Macalady, A. K., Breshears, D. D., Allen, C. D., Stephenson, N. L., Saleska, S. R., Huxman, T. E., & McDowell, N. G. (2010). Climate-induced tree mortality: Earth system consequences. Eos, Transactions American Geophysical Union, 91(17), 153–154. https://doi.org/https://doi.org/10.1029/2010EO170003

Adams, H. D., Williams, A. P., Xu, C., Rauscher, S., Jiang, X., & McDowell, N. G. (2013). Empirical and process-based approaches to climate-induced forest mortality models. Frontiers in Plant Science, 4(11), 1–5. https://doi.org/10.3389/fpls.2013.00438

Adams, H. D., Zeppel, M. J. B., Anderegg, W. R. L., Hartmann, H., Landhäusser, S. M., Tissue, D. T., Huxman, T. E., Hudson, P. J., Franz, T. E., Allen, C. D., Anderegg, L. D. L., Barron-Gafford, G. A., Beerling, D. J., Breshears, D. D., Brodribb, T. J., Bugmann, H., Cobb, R. C., Collins, A. D., Dickman, L. T., … McDowell, N. G. (2017). A multi-species synthesis of physiological mechanisms in drought-induced tree mortality. Nature Ecology and Evolution, 1(9), 1285–1291. https://doi.org/10.1038/s41559-017-0248-x

Allen, C. D., Breshears, D. D., & McDowell, N. G. (2015). On underestimation of global vulnerability to tree mortality and forest die-off from hotter drought in the Anthropocene. Ecosphere, 6(8), 1–55. https://doi.org/10.1890/ES15-00203.1

Anderegg, W. R. L., Anderegg, L. D. L., Kerr, K. L., & Trugman, A. T. (2019). Widespread drought-induced tree mortality at dry range edges indicates climate stress exceeds species' compensating mechanisms. Global Change Biology, gcb.14771. https://doi.org/10.1111/gcb.14771

Anderegg, W. R. L., Hicke, J. A., Fisher, R. A., Allen, C. D., Aukema, J., Bentz, B., Hood, S., Lichstein, J. W., Macalady, A. K., Mcdowell, N., Pan, Y., Raffa, K., Sala, A., Shaw, J. D., Stephenson, N. L., Tague, C., & Zeppel, M. (2015). Tree mortality from drought, insects, and their interactions in a changing climate. New Phytologist, 208(3), 674–683. https://doi.org/10.1111/nph.13477

Anderegg, W. R. L., Kane, J. M., & Anderegg, L. D. L. (2013). Consequences of widespread tree mortality triggered by drought and temperature stress. Nature Climate Change, 3(1), 30–36. https://doi.org/10.1038/nclimate1635

Anderegg, W. R. L., Schwalm, C., Biondi, F., Camarero, J. J., Koch, G., Litvak, M., Ogle, K., Shaw, J. D., Shevliakova, E., Williams, A. P., Wolf, A., Ziaco, E., & Pacala, S. (2015). Pervasive drought legacies in forest ecosystems and their implications for carbon cycle models. Science, 349(6247), 528–532. https://doi.org/10.1126/science.aab1833

Batjes, N. H. (n.d.). 2012. ISRIC-WISE derived soil properties on a 5 by 5 arc-minutes global grid (ver. 1.2) (No. 2012/01). ISRIC-World Soil Information. http://www.isric.org/data/isric-wise-derived-soil-properties-5-5-arc-minutes-global-grid-version-12

Blackman, C. J., Pfautsch, S., Choat, B., Delzon, S., Gleason, S. M., & Duursma, R. A. (2016). Toward an index of desiccation time to tree mortality under drought. Plant Cell and Environment, 39(10), 2342–2345. https://doi.org/10.1111/pce.12758

Bonan, G. B., Oleson, K. W., Fisher, R. A., Lasslop, G., & Reichstein, M. (2012). Reconciling leaf physiological traits and canopy flux data: Use of the TRY and FLUXNET databases in the Community Land Model version 4. Journal of Geophysical Research: Biogeosciences, 117(2), 1–19. https://doi.org/10.1029/2011JG001913

Bossel, H. (1996). TREEDYN3 forest simulation model. Ecological Modelling, 90(3), 187–227. https://doi.org/10.1016/0304-3800(95)00139-5

Brandt, J. P., Flannigan, M. D., Maynard, D. G., Thompson, I. D., & Volney, W. J. A. (2013). An introduction to Canada's boreal zone: Ecosystem processes, health, sustainability, and environmental issues. Environmental Reviews, 21(4), 207–226. https://doi.org/10.1139/er-2013-0040

Brouwers, N. C., Van Dongen, R., Matusick, G., Coops, N. C., Strelein, G., & Hardy, G. (2015). Inferring drought and heat sensitivity across a Mediterranean forest region in southwest Western Australia: A comparison of approaches. Forestry, 88(4), 454–464. https://doi.org/10.1093/forestry/cpv014

Buckley, T. N., Mott, K. A., & Farquhar, G. D. (2003). A hydromechanical and biochemical model of stomatal conductance. Plant, Cell and Environment, 26(10), 1767–1785. https://doi.org/10.1046/j.1365-3040.2003.01094.x

Burton, P. J., Bergeron, Y., Bogdanski, B. E., Juday, G. P., Kuuluvainen, T., McAfee, B. J., Ogden, A., Teplyakov, V. K., Alfaro, R. I., Francis, D. A., & Gauthier, Sb. (2010). Sustainability of boreal forests and forestry in a changing environment. IUFRO (International Union of Forestry Research Organizations).

Callaway, R. M., DeLucia, E. H., & Schlesinger, W. H. (1994). Biomass allocation of montane and desert ponderosa pine: An analog for response to climate change. Ecology, 75(5), 1474–1481. https://doi.org/10.2307/1937470

Choat, B., Brodribb, T. J., Brodersen, C. R., Duursma, R. A., López, R., & Medlyn, B. E. (2018). Triggers of tree mortality under drought. Nature, 558(7711), 531–539. https://doi.org/10.1038/s41586-018-0240-x

Choat, B., Jansen, S., Brodribb, T. J., Cochard, H., Delzon, S., Bhaskar, R., Bucci, S. J., Feild, T. S., Gleason, S. M., Hacke, U. G., Jacobsen, A. L., Lens, F., Maherali, H., Martínez-Vilalta, J., Mayr, S., Mencuccini, M., Mitchell, P. J., Nardini, A., Pittermann, J., … Zanne, A. E. (2012). Global convergence in the vulnerability of forests to drought. Nature, 491(7426), 752–755. https://doi.org/10.1038/nature11688

Christoffersen, B. O., Gloor, M., Fauset, S., Fyllas, N. M., Galbraith, D. R., Baker, T. R., Kruijt, B., Rowland, L., Fisher, R. A., Binks, O. J., Sevanto, S., Xu, C., Jansen, S., Choat, B., Mencuccini, M., McDowell, N. G., & Meir, P. (2016). Linking hydraulic traits to tropical forest function in a size-structured and trait-driven model (TFS v.1-Hydro). Geoscientific Model Development, 9(11), 4227–4255. https://doi.org/10.5194/gmd-9-4227-2016

Dahlin, K. M., Ponte, D. Del, Setlock, E., & Nagelkirk, R. (2017). Global patterns of drought deciduous phenology in semi-arid and savanna-type ecosystems. Ecography, 40(2), 314–323. https://doi.org/10.1111/ecog.02443

Damour, G., Simonneau, T., Cochard, H., & Urban, L. (2010). An overview of models of stomatal conductance at the leaf level. Plant, Cell and Environment, 33(9), 1419–1438. https://doi.org/10.1111/j.1365-3040.2010.02181.x

De Kauwe, M. G., Medlyn, B. E., Ukkola, A. M., Mu, M., Sabot, M. E. B., Pitman, A. J., Meir, P., Cernusak, L., Rifai, S. W., Choat, B., Tissue, D. T., Blackman, C. J., Li, X., Roderick, M., & Briggs, P. R. (2020). Identifying areas at risk of drought-induced tree mortality across South-Eastern Australia. Global Change Biology, 26(10), 5716–5733. https://doi.org/10.1111/gcb.15215

De Kauwe, M. G., Zhou, S. X., Medlyn, B. E., Pitman, A. J., Wang, Y. P., Duursma, R. A., & Prentice, I. C. (2015). Do land surface models need to include differential plant species responses to drought? Examining model predictions across a mesic-xeric gradient in Europe. Biogeosciences, 12(24), 7503–7518. https://doi.org/10.5194/bg-12-7503-2015

Domec, J. C., Ogée, J., Noormets, A., Jouangy, J., Gavazzi, M., Treasure, E., Sun, G., McNulty, S. G., & King, J. S. (2012). Interactive effects of nocturnal transpiration and climate change on the root hydraulic redistribution and carbon and water budgets of southern United States pine plantations. Tree Physiology, 32(6), 707–723. https://doi.org/10.1093/treephys/tps018

Fisher, J. B., Sitch, S., Malhi, Y., Fisher, R. A., Huntingford, C., & Tan, S.-Y. (2010). Carbon cost of plant nitrogen acquisition: A mechanistic, globally applicable model of plant nitrogen uptake, retranslocation, and fixation. Global Biogeochemical Cycles, 24(1). https://doi.org/10.1029/2009gb003621

Fisher, R., McDowell, N., Purves, D., Moorcroft, P., Sitch, S., Cox, P., Huntingford, C., Meir, P.,

& Woodward, F. I. (2010). Assessing uncertainties in a second-generation dynamic vegetation model caused by ecological scale limitations. New Phytologist, 187(3), 666–681. https://doi.org/10.1111/j.1469-8137.2010.03340.x

Flexas, J., Bota, J., Galme, J., Medrano, H. lito, & Ribas-Carbo, M. (2006). Keeping a positive carbon balance under adverse conditions: responses of photosynthesis and respiration to water stress. Physiologia Plantarum, 127(3), 343–352. https://doi.org/10.1111/j.1399-3054.2006.00621.x

Friedlingstein, P., Cox, P., Betts, R., Bopp, L., von Bloh, W., Brovkin, V., Cadule, P., Doney, S., Eby, M., Fung, I., Bala, G., John, J., Jones, C., Joos, F., Kato, T., Kawamiya, M., Knorr, W., Lindsay, K., Matthews, H. D., … Zeng, N. (2006). Climate-carbon cycle feedback analysis: Results from the C4MIP model intercomparison. Journal of Climate, 19(14), 3337–3353. https://doi.org/10.1175/JCLI3800.1

Gao, Q., Zhao, P., Zeng, X., Cai, X., & Shen, W. (2002). A model of stomatal conductance to quantify the relationship between leaf transpiration, microclimate and soil water stress. Plant, Cell and Environment, 25(11), 1373–1381. https://doi.org/10.1046/j.1365-3040.2002.00926.x

Gauthier, S., Bernier, P., Kuuluvainen, T., Shvidenko, A. Z., & Schepaschenko, D. G. (2015). Boreal forest health and global change. Science, 349(6250), 819–822. https://doi.org/10.1126/science.aaa9092

Genet, H., Bréda, N., & Dufrêne, E. (2009). Age-related variation in carbon allocation at tree and stand scales in beech (Fagus sylvatica L.) and sessile oak (Quercus petraea (Matt.) Liebl.) using a chronosequence approach. Tree Physiology, 30(2), 177–192. https://doi.org/10.1093/treephys/tpp105

Goulden, M. L., & Bales, R. C. (2019). California forest die-off linked to multi-year deep soil drying in 2012–2015 drought. Nature Geoscience. https://doi.org/10.1038/s41561-019-0388-5

Gruber, A., Pirkebner, D., Florian, C., & Oberhuber, W. (2012). No evidence for depletion of carbohydrate pools in Scots pine (Pinus sylvestris L.) under drought stress. Plant Biology, 14(1), 142–148. https://doi.org/10.1111/j.1438-8677.2011.00467.x

Gustafson, E. J., & Sturtevant, B. R. (2013). Modeling Forest Mortality Caused by Drought Stress: Implications for Climate Change. Ecosystems, 16(1), 60–74. https://doi.org/10.1007/s10021-012-9596-1

Hartmann, H., Ziegler, W., Kolle, O., & Trumbore, S. (2013). Thirst beats hunger - declining

hydration during drought prevents carbon starvation in Norway spruce saplings. New Phytologist, 200(2), 340–349. https://doi.org/10.1111/nph.12331

Hendrik, D., & Maxime, C. (2017). Assessing drought-driven mortality trees with physiological process-based models. Agricultural and Forest Meteorology, 232, 279–290. https://doi.org/10.1016/j.agrformet.2016.08.019

Hogg, E. H. (Ted), Brandt, J. P., & Michaelian, M. (2008). Impacts of a regional drought on the productivity, dieback, and biomass of western Canadian aspen forests. Canadian Journal of Forest Research, 38(6), 1373–1384. https://doi.org/10.1139/X08-001

Hogg, E. H., Barr, A. G., & Black, T. A. (2013). A simple soil moisture index for representing multi-year drought impacts on aspen productivity in the western Canadian interior. Agricultural and Forest Meteorology, 178–179, 173–182. https://doi.org/10.1016/j.agrformet.2013.04.025

Hölttä, T., Vesala, T., Sevanto, S., Perämäki, M., & Nikinmaa, E. (2006). Modeling xylem and phloem water flows in trees according to cohesion theory and Münch hypothesis. Trees, 20(1), 67–78. https://doi.org/10.1007/s00468-005-0014-6

Hummel, I., Pantin, F., Sulpice, R., Piques, M., Rolland, G., Dauzat, M., Christophe, A., Pervent, M., Bouteillé, M., Stitt, M., Gibon, Y., & Muller, B. (2010). Arabidopsis plants acclimate to water deficit at low cost through changes of carbon usage: An integrated perspective using growth, metabolite, enzyme, and gene expression analysis. Plant Physiology, 154(1), 357–372. https://doi.org/10.1104/pp.110.157008

Landsberg, J. J., & Waring, R. H. (1997). A generalised model of forest productivity using simplified concepts of radiation-use efficiency, carbon balance and partitioning. Forest Ecology and Management, 95(3), 209–228. https://doi.org/https://doi.org/10.1016/S0378-1127(97)00026-1

Lenhart, T., Eckhardt, K., Fohrer, N., & Frede, H.-G. (2002). Comparison of two different approaches of sensitivity analysis. Physics and Chemistry of the Earth, Parts A/B/C, 27(9–10), 645–654. https://doi.org/10.1016/S1474-7065(02)00049-9

Lenton, T. M., Held, H., Kriegler, E., Hall, J. W., Lucht, W., Rahmstorf, S., & Joachim, H. (2008). Tipping elements in the Earth's climate system. Proceedings of the National Academy of Sciences, 105(6), 1786–1793. https://doi.org/10.1073/pnas.0705414105

Letts, M. G., Comer, N. T., Roulet, N. T., Skarupa, M. R., & Verseghy, D. L. (2000). Parametrization of peatland hydraulic properties for the Canadian land surface scheme. Atmosphere - Ocean, 38(1), 141–160. https://doi.org/10.1080/07055900.2000.9649643

Levenberg, K. (1944). A method for the solution of certain non-linear problems in least squares. Quarterly of Applied Mathematics, 2(2), 164–168.

Lewis, S. L., Brando, P. M., Phillips, O. L., Heijden, V. Der, M.F., G., & Nepstad, D. (2011). The 2010 Amazon drought. Science, 331(6017), 554–554. https://doi.org/10.1126/science.1200807

Liebig, J., & Playfair, L. P. (1843). Organische Chemie in ihrer Anwendung auf Agricultur und Physiologie. English.

Limousin, J. M., Longepierre, D., Huc, R., & Rambal, S. (2010). Change in hydraulic traits of Mediterranean Quercus ilex subjected to long-term throughfall exclusion. Tree Physiology, 30(8), 1026–1036. https://doi.org/10.1093/treephys/tpq062

Liu, J., Peng, C., Dang, Q., Apps, M., & Jiang, H. (2002). A component object model strategy for reusing ecosystem models. Computers and Electronics in Agriculture, 35(1), 17–33. https://doi.org/10.1016/S0168-1699(02)00067-4

Liu, Z., Peng, C., De Grandpré, L., Candau, J. N., Work, T., Huang, C., & Kneeshaw, D. (2019). Simulation and Analysis of the Effect of a Spruce Budworm Outbreak on Carbon Dynamics in Boreal Forests of Quebec. Ecosystems, 22(8), 1838–1851. https://doi.org/10.1007/s10021-019-00377-7

Liu, Z., Peng, C., Louis, D. G., Candau, J. N., Zhou, X., & Kneeshaw, D. (2018). Development of a new TRIPLEX-insect model for simulating the effect of spruce budworm on forest carbon dynamics. Forests, 9(9), 1–17. https://doi.org/10.3390/f9090513

Mackay, D. S., Ewers, B. E., Loranty, M. M., Kruger, E. L., & Samanta, S. (2012). Bayesian analysis of canopy transpiration models: A test of posterior parameter means against measurements. Journal of Hydrology, 432–433, 75–83. https://doi.org/10.1016/j.jhydrol.2012.02.019

Mackay, D. S., Roberts, D. E., Ewers, B. E., Sperry, J. S., McDowell, N. G., & Pockman, W. T. (2015). Interdependence of chronic hydraulic dysfunction and canopy processes can improve integrated models of tree response to drought. Water Resources Research, 51(8), 6156–6176. https://doi.org/10.1002/2015WR017244

Maherali, H., Pockman, W. T., & Jackson, R. B. (2004). Adaptive variation in the vulnerability of woody plants to xylem cavitation. Ecology, 85(8), 2184–2199. https://doi.org/10.1890/02-0538

Mao, Z., Bonis, M. L., Rey, H., Saint-André, L., Stokes, A., & Jourdan, C. (2013). Which processes drive fine root elongation in a natural mountain forest ecosystem? Plant Ecology and

Diversity, 6(2), 231–243. https://doi.org/10.1080/17550874.2013.788567

Martínez-Vilalta, J., Poyatos, R., Aguadé, D., Retana, J., & Mencuccini, M. (2014). A new look at water transport regulation in plants. New Phytologist, 204(1), 105–115. https://doi.org/10.1111/nph.12912

McDowell, N., Fisher, R., Chonggang, X., Sperry, J. S., Boutz, A., Dickman, L., Gehres, N., Limousin, J. M., Macalady, A., Pangle, R. E., Rasse, D. P., Ryan, M. G., Sevanto, S., Waring, R. H., Williams, A. P., Yepez, E. A., & Pockman, W. T. (2013). Evaluating theories of drought-induced vegetation mortality using a multimodel – experiment framework. New Phytologist, 200, 304–321. https://doi.org/10.1111/nph.12465

McDowell, N. G. (2011). Mechanisms Linking Drought, Hydraulics, Carbon Metabolism, and Vegetation Mortality. Plant Physiology, 155(3), 1051–1059. https://doi.org/10.1104/pp.110.170704

McDowell, N. G., Beerling, D. J., Breshears, D. D., Fisher, R. A., Raffa, K. F., & Stitt, M. (2011). The interdependence of mechanisms underlying climate-driven vegetation mortality. Trends in Ecology and Evolution, 26(10), 523–532. https://doi.org/10.1016/j.tree.2011.06.003

McDowell, N. G., & Sevanto, S. (2010). The mechanisms of carbon starvation: how, when, or does it even occur at all? New Phytologist, 186(2), 264–266. https://doi.org/https://doi.org/10.1111/j.1469-8137.2010.03232.x

McDowell, N. G., Williams, A. P., Xu, C., Pockman, W. T., Dickman, L. T., Sevanto, S., Pangle, R., Limousin, J., Plaut, J., Mackay, D. S., Ogee, J., Domec, J. C., Allen, C. D., Fisher, R. A., Jiang, X., Muss, J. D., Breshears, D. D., Rauscher, S. A., & Koven, C. (2016). Multi-scale predictions of massive conifer mortality due to chronic temperature rise. Nature Climate Change, 6(3), 295–300. https://doi.org/10.1038/nclimate2873

McDowell, N., Pockman, W. T., Allen, C. D., David, D., Cobb, N., Kolb, T., Plaut, J., Sperry, J., West, A., Williams, D. G., & Yepez, E. A. (2008). Mechanisms of plant survival and mortality during drought: why do some plants survive while others succumb to drought? New Phytologist, 178(4), 719–739. https://doi.org/10.1111/j.1469-8137.2008.02436.x

Mencuccini, M., Minunno, F., Salmon, Y., Martínez-Vilalta, J., & Hölttä, T. (2015). Coordination of physiological traits involved in drought-induced mortality of woody plants. New Phytologist, 208(2), 396–409. https://doi.org/10.1111/nph.13461

Michaelian, M., Hogg, E. H., Hall, R. J., & Arsenault, E. (2011). Massive mortality of aspen following severe drought along the southern edge of the Canadian boreal forest. Global Change Biology, 17(6), 2084–2094. https://doi.org/10.1111/j.1365-2486.2010.02357.x

Mitchell, P. J., O'Grady, A. P., Pinkard, E. A., Brodribb, T. J., Arndt, S. K., Blackman, C. J., Duursma, R. A., Fensham, R. J., Hilbert, D. W., Nitschke, C. R., Norris, J., Roxburgh, S. H., Ruthrof, K. X., & Tissue, D. T. (2016). An ecoclimatic framework for evaluating the resilience of vegetation to water deficit. Global Change Biology, 22(5), 1677–1689. https://doi.org/10.1111/gcb.13177

Mitchell, P. J., O'Grady, A. P., Tissue, D. T., Worledge, D., & Pinkard, E. A. (2014). Co-ordination of growth, gas exchange and hydraulics define the carbon safety margin in tree species with contrasting drought strategies. Tree Physiology, 34(5), 443–458. https://doi.org/10.1093/treephys/tpu014

Moorcroft, P. R. (2006). How close are we to a predictive science of the biosphere? Trends in Ecology and Evolution, 21(7), 400–407. https://doi.org/10.1016/j.tree.2006.04.009

Moré, J. J. (1978). The Levenberg-Marquardt algorithm: implementation and theory. Numerical Analysis, 105–116.

Muller, B., Pantin, F., Génard, M., Turc, O., Freixes, S., Piques, M., & Gibon, Y. (2011). Water deficits uncouple growth from photosynthesis, increase C content, and modify the relationships between C and growth in sink organs. Journal of Experimental Botany, 62(6), 1715–1729. https://doi.org/10.1093/jxb/erq438

Neufeld, H. S., Grantz, D. A., Meinzer, F. C., Goldstein, G., Crisosto, G. M., & Crisosto, C. (1992). Genotypic variability in vulnerability of leaf xylem to cavitation in water-stressed and well-irrigated sugarcane. Plant Physiology, 100(2), 1020–1028. https://doi.org/https://doi.org/10.1104/pp.100.2.1020

O'Brien, M. J., Leuzinger, S., Philipson, C. D., Tay, J., & Hector, A. (2014). Drought survival of tropical tree seedlings enhanced by non-structural carbohydrate levels. Nature Climate Change, 4(8), 710–714. https://doi.org/10.1038/nclimate2281

O'sullivan, O. S., Heskel, M. A., Reich, P. B., Tjoelker, M. G., Weerasinghe, L. K., Penillard, A., Zhu, L., Egerton, J. J. G., Bloomfield, K. J., Creek, D., Bahar, N. H. A., Griffin, K. L., Hurry, V., Meir, P., Turnbull, M. H., & Atkin, O. K. (2017). Thermal limits of leaf metabolism across biomes. Global Change Biology, 23(1), 209–223. https://doi.org/10.1111/gcb.13477

Ogée, J., Brunet, Y., Loustau, D., Berbigier, P., & Delzon, S. (2003). MuSICA, a CO2, water and energy multilayer, multileaf pine forest model: Evaluation from hourly to yearly time scales and sensitivity analysis. Global Change Biology, 9(5), 697–717. https://doi.org/10.1046/j.1365-2486.2003.00628.x

Oleson, K. W., Lawrence, D. M., Bonan, G. B., Flanner, M. G., Kluzek, E., Lawrence, P. J., Levis,

S., Swenson, S. C., & Thornton, P. E. (2010). Technical description of version 4.0 of the Community Land Model (CLM). papers2://publication/uuid/6858EE7A-C77E-4439-832D-CEC2791FBEBA

Oliva, J., Stenlid, J., & Martínez-Vilalta, J. (2014). The effect of fungal pathogens on the water and carbon economy of trees: Implications for drought-induced mortality. New Phytologist, 203(4), 1028–1035. https://doi.org/10.1111/nph.12857

Olson, M. E., Soriano, D., Rosell, J. A., Anfodillo, T., Donoghue, M. J., Edwards, E. J., León-Gómez, C., Dawson, T., Julio Camarero Martínez, J., Castorena, M., Echeverría, A., Espinosa, C. I., Fajardo, A., Gazol, A., Isnard, S., Lima, R. S., Marcati, C. R., & Méndez-Alonzo, R. (2018). Plant height and hydraulic vulnerability to drought and cold. Proceedings of the National Academy of Sciences, 115(29), 7551–7556. https://doi.org/10.1073/pnas.1721728115

Oogathoo, S., Houle, D., Duchesne, L., & Kneeshaw, D. (2020). Vapour pressure deficit and solar radiation are the major drivers of transpiration of balsam fir and black spruce tree species in humid boreal regions, even during a short-term drought. Agricultural and Forest Meteorology, 291(2019), 108063. https://doi.org/10.1016/j.agrformet.2020.108063

Pammenter, N., & Van der Willigen, C. (1998). A mathematical and statistical analysis of the curves illustrating vulnerability of xylem to cavitation. Tree Physiology, 18, 589–593. https://doi.org/https://doi.org/10.1093/treephys/18.8-9.589

Pan, Y., Birdsey, R. A., Fang, J., Houghton, R., Kauppi, P. E., Kurz, W. A., Phillips, O. L., Shvidenko, A., Lewis, S. L., Canadell, J. G., Ciais, P., Jackson, R. B., Pacala, S. W., McGuire, A. D., Piao, S., Rautiainen, A., Sitch, S., & Hayes, D. (2011). A large and persistent carbon sink in the world's forests. Science. https://doi.org/10.1126/science.1201609

Pan, Y., Birdsey, R. A., Fang, J., Houghton, R., Kauppi, P. E., Kurz, W. A., Phillips, O. L., Shvidenko, A., Lewis, S. L., Canadell, J. G., Ciais, P., Jackson, R. B., Pacala, S. W., McGuire, A. D., Piao, S., Rautiainen, A., Sitch, S., & Hayes, D. (2014). Impacts of droughts on carbon sequestration by China's terrestrial ecosystems from 2000 to 2011. Biogeosciences, 11(10), 2583–2599. https://doi.org/10.5194/bg-11-2583-2014

Parton, W. ., Scurlock, J. ., Ojima, D. ., Gilmanov, T. ., Scholes, R. ., & Schimel, D. . (1993). Observations and modeling of biomass and soil organic matter dynamics for the grassland biome worldwide. Global Biogeochemical Cycles, 7, 785–809. https://doi.org/https://doi.org/10.1029/93GB02042

Parton, W. J., Schimel, D. S., Cole, C. V., & Ojima, D. S. (1987). Analysis of Factors Controlling Soil Organic Matter Levels in Great Plains Grasslands. Soil Science Society of America

Journal, 51(5), 1173–1179. https://doi.org/10.2136/sssaj1987.03615995005100050015x

Parton, W. J., Scurlock, J. M. O., Ojima, D. S., Scholes, R. J., Kirchner, T., Seastedt, T., & Garcia, E. (1993). Modeling Grassland Biomes and soil organic matter dynamics for the grassland biome worldwide. Global Biogeochemical Cycles, 7(4), 785–809. http://www.agu.org/journals/ABS/1993/93GB02042.shtml

Peng, C., Liu, J., Dang, Q., Apps, M. J., & Jiang, H. (2002). TRIPLEX: A generic hybrid model for predicting forest growth and carbon and nitrogen dynamics. Ecological Modelling, 153(1–2), 109–130. https://doi.org/10.1016/S0304-3800(01)00505-1

Peng, C., Ma, Z., Lei, X., Zhu, Q., Chen, H., Wang, W., Liu, S., Li, W., Fang, X., & Zhou, X. (2011). A drought-induced pervasive increase in tree mortality across Canada's boreal forests. Nature Climate Change, 1(9), 467–471. https://doi.org/10.1038/nclimate1293

Piper, F. I., & Fajardo, A. (2016). Carbon dynamics of Acer pseudoplatanus seedlings under drought and complete darkness. Tree Physiology, 36(11), 1–9. https://doi.org/10.1093/treephys/tpw063

Plaut, J. A., Yepez, E. A., Hill, J., Pangle, R., Sperry, J. S., Pockman, W. T., & Mcdowell, N. G. (2012). Hydraulic limits preceding mortality in a piñon-juniper woodland under experimental drought. Plant, Cell and Environment, 35(9), 1601–1617. https://doi.org/10.1111/j.1365-3040.2012.02512.x

Powell, T. L., Galbraith, D. R., Christoffersen, B. O., Harper, A., Imbuzeiro, H. M. A., Rowland, L., Almeida, S., Brando, P. M., da Costa, A. C. L., Costa, M. H., Levine, N. M., Malhi, Y., Saleska, S. R., Sotta, E., Williams, M., Meir, P., & Moorcroft, P. R. (2013). Confronting model predictions of carbon fluxes with measurements of Amazon forests subjected to experimental drought. New Phytologist, 200(2), 350–365. https://doi.org/10.1111/nph.12390

Purves, D., & Pacala, S. (2008). Predictive Models of Forest Dynamics. Science, 320, 1452–1453. https://doi.org/10.1126/science.342.6160.776-d

Quirk, J., McDowell, N. G., Leake, J. R., Hudson, P. J., & Beerling, D. J. (2013). Increased susceptibility to drought-induced mortality in Sequoia sempervirens (Cupressaceae) trees under Cenozoic atmospheric carbon dioxide starvation. American Journal of Botany, 100(3), 582–591. https://doi.org/10.3732/ajb.1200435

Régnière, J. (1996). Generalized approach to landscape-wide seasonal forecasting with temperature-driven simulation models. Environmental Entomology, 25(5), 869–881. https://doi.org/10.1093/ee/25.5.869

Reichstein, M., Ciais, P., Papale, D., Valentini, R., Running, S., Viovy, N., Cramer, W., Granier,

A., Ogée, J., Allard, V., Aubinet, M., Bernhofer, C., Buchmann, N., Carrara, A., Grünwald, T., Heimann, M., Heinesch, B., Knohl, A., Kutsch, W., … Zhao, M. (2007). Reduction of ecosystem productivity and respiration during the European summer 2003 climate anomaly: A joint flux tower, remote sensing and modelling analysis. Global Change Biology, 13(3), 634–651. https://doi.org/10.1111/j.1365-2486.2006.01224.x

Rosner, S., Heinze, B., Savi, T., & Dalla-Salda, G. (2019). Prediction of hydraulic conductivity loss from relative water loss: new insights into water storage of tree stems and branches. Physiologia Plantarum, 165(4), 843–854. https://doi.org/10.1111/ppl.12790

Sala, A., Piper, F., & Hoch, G. (2010). Physiological mechanisms of drought-induced tree mortality are far from being resolved. New Phytologist, 274–281. https://doi.org/10.1111/nph.12154

Sevanto, S., Mcdowell, N. G., Dickman, L. T., Pangle, R., & Pockman, W. T. (2014). How do trees die? A test of the hydraulic failure and carbon starvation hypotheses. Plant, Cell and Environment, 37(1), 153–161. https://doi.org/10.1111/pce.12141

Sitch, S., Smith, B., Prentice, I. C., Arneth, A., Bondeau, A., Cramer, W., Kaplan, J. O., Levis, S., Lucht, W., Sykes, M. T., Thonicke, K., & Venevsky, S. (2003). Evaluation of ecosystem dynamics, plant geography and terrestrial carbon cycling in the LPJ dynamic global vegetation model. Global Change Biology, 9(2), 161–185. https://doi.org/10.1046/j.1365-2486.2003.00569.x

Sperry, J. S., Adler, F. R., Campbell, G. S., & Comstock, J. S. (1998). Limitation of plant water use by rhizosphere and xylem conductance: results from a model. Plant Cell And Environment, 21, 347–359. https://doi.org/https://doi.org/10.1046/j.1365-3040.1998.00287.x

Sperry, J. S., & Tyree, M. T. (1988). Mechanism of Water Stress-Induced. Plant Physiology, 88(3), 581–587. https://doi.org/10.1104/pp.88.3.581

Stovall, A. E. L., Shugart, H., & Yang, X. (2019). Tree height explains mortality risk during an intense drought. Nature Communications, 10(1), 1–6. https://doi.org/10.1038/s41467-019-12380-6

Suarez, M. L., & Kitzberger, T. (2008). Recruitment patterns following a severe drought: Long-term compositional shifts in Patagonian forests. Canadian Journal of Forest Research, 38(12), 3002–3010. https://doi.org/10.1139/X08-149

Sun, J., Peng, C., McCaughey, H., Zhou, X., Thomas, V., Berninger, F., St-Onge, B., & Hua, D. (2008). Simulating carbon exchange of Canadian boreal forests. II. Comparing the carbon budgets of a boreal mixedwood stand to a black spruce forest stand. Ecological Modelling, 219(3–4), 276–286. https://doi.org/10.1016/j.ecolmodel.2008.03.031

Tague, C. L., McDowell, N. G., & Allen, C. D. (2013). An integrated model of environmental effects on growth, carbohydrate balance, and mortality of Pinus ponderosa forests in the southern Rocky Mountains. PLoS ONE, 8(11), e80286. https://doi.org/10.1371/journal.pone.0080286

Tarnocai, C., & Lacelle, B. (1996). Soil organic carbon of Canada map.

Trenberth, K. E., Dai, A., Van Der Schrier, G., Jones, P. D., Barichivich, J., Briffa, K. R., & Sheffield, J. (2014). Global warming and changes in drought. Nature Climate Change, 4(1), 17–22. https://doi.org/10.1038/nclimate2067

Urli, M., Porté, A. J., Cochard, H., Guengant, Y., Burlett, R., & Delzon, S. (2013). Xylem embolism threshold for catastrophic hydraulic failure in angiosperm trees. Tree Physiology, 33(7), 672–683. https://doi.org/10.1093/treephys/tpt030

Vilagrosa, A., Bellot, J., Vallejo, V. R., & Gil-Pelegrín, E. (2003). Cavitation, stomatal conductance, and leaf dieback in seedlings of two co-occurring Mediterranean shrubs during an intense drought. Journal of Experimental Botany, 54(390), 2015–2024. https://doi.org/10.1093/jxb/erg221

Wang, W., Peng, C., Kneeshaw, D. D., Larocque, G. R., & Luo, Z. (2012). Drought-induced tree mortality: ecological consequences, causes, and modeling. Environmental Reviews, 20(2), 109–121. https://doi.org/10.1139/a2012-004

Wang, W., Peng, C., Kneeshaw, D. D., Larocque, G. R., Song, X., & Zhou, X. (2012). Quantifying the effects of climate change and harvesting on carbon dynamics of boreal aspen and jack pine forests using the TRIPLEX-Management model. Forest Ecology and Management, 281, 152–162. https://doi.org/10.1016/j.foreco.2012.06.028

Wang, W., Peng, C., Zhang, S. Y., Zhou, X., Larocque, G. R., Kneeshaw, D. D., & Lei, X. (2011). Development of TRIPLEX-Management model for simulating the response of forest growth to pre-commercial thinning. Ecological Modelling, 222(14), 2249–2261. https://doi.org/10.1016/j.ecolmodel.2010.09.019

Williams, A. P., Allen, C. D., Macalady, A. K., Griffin, D., Woodhouse, C. A., Meko, D. M., Swetnam, T. W., Rauscher, S. A., Seager, R., Grissino-Mayer, H. D., Dean, J. S., Cook, E. R., Gangodagamage, C., Cai, M., & Mcdowell, N. G. (2013). Temperature as a potent driver of regional forest drought stress and tree mortality. Nature Climate Change, 3(3), 292–297. https://doi.org/10.1038/nclimate1693

Willmott, C. J. (1981). On the validation of models. Physical Geography, 2(2), 184–194. https://doi.org/10.1080/02723646.1981.10642213

Xu, C., Fisher, R., Wullschleger, S. D., Wilson, C. J., Cai, M., & McDowell, N. G. (2012). Toward a mechanistic modeling of nitrogen limitation on vegetation dynamics. PLoS ONE, 7(5), 1–11. https://doi.org/10.1371/journal.pone.0037914

Xu, C., Mcdowell, N. G., Sevanto, S., & Fisher, R. A. (2013). Our limited ability to predict vegetation dynamics under water stress. New Phytologist, 200(2), 298–300. https://doi.org/10.1111/nph.12450

Zhou, X., Peng, C., & Dang, Q. (2004). Assessing the generality and accuracy of the TRIPLEX model using in situ data of boreal forests in central Canada. Environmental Modelling and Software, 19(1), 35–46. https://doi.org/10.1016/S1364-8152(03)00108-7

Zhou, X., Peng, C., & Dang, Q. L. (2006). Formulating and parameterizing the allocation of net primary productivity for modeling overmature stands in boreal forest ecosystems. Ecological Modelling, 195(3–4), 264–272. https://doi.org/10.1016/j.ecolmodel.2005.11.022

Zhou, X., Peng, C., Dang, Q. L., Chen, J., & Parton, S. (2005). Predicting forest growth and yield in northeastern Ontario using the process-based model of TRIPLEX1.0. Canadian Journal of Forest Research, 35(9), 2268–2280. https://doi.org/10.1139/x05-149

CHAPTER III

DROUGHT-INDUCED INCREASE IN TREE MORTALITY AND CORRESPONDING DECREASE IN THE CARBON SINK CAPACITY OF CANADA'S BOREAL FORESTS FROM 1970 TO 2020

Qiuyu Liu, Changhui Peng, Robert Schneider, Dominic Cyr, Nate G. McDowell, Daniel Kneeshawe

The article has been under review in *Global Change Biology*. 2022

3.1. Resume

Les forêts boréales du Canada, qui occupent environ 30 % des forêts boréales du monde, jouent un rôle important dans le bilan global du carbone. Cependant, peu d'information est disponible sur les changements spatio-temporels de la mortalité des arbres induite par la sécheresse et leurs impacts sur la dynamique du carbone de la biomasse dans les forêts boréales du Canada. Dans cette étude, nous développons des estimations spatio-temporelles explicites de la mortalité et des changements de capacité de puits de carbone de la biomasse de la forêt boréale du Canada de 1970 à 2020. Nous démontrons qu'il y a une tendance à la hausse de la mortalité des arbres causée par la sécheresse de 1970 à 2020 avec une accélération depuis 2002. Environ 43 % des forêts boréales du Canada ont connu une tendance significative à l'augmentation de la mortalité des arbres. Cette augmentation a entraîné une importante perte de carbone à un taux approximatif de 1.51 ± 0.29 MgC ha^{-1} an^{-1} avec une perte totale approximative de 0.46 ± 0.09 PgC par an. Il s'agit d'un énorme flux de carbone qui équivaut à environ 210 % des émissions annuelles totales de carbone du Canada. Avec l'augmentation prévue de la sécheresse au cours de ce siècle, les forêts boréales du Canada pourraient ne plus remplir leur rôle d'important puits de carbone.

3.2. Abstract

Canada's boreal forests, which occupy about 30% of the boreal forests worldwide, play an important role in the global carbon budget. However, there is little information available on spatiotemporal changes in drought-induced tree mortality and associated impacts on biomass carbon dynamics in Canada's boreal forests. Here, we develop spatiotemporally explicit estimates of mortality and biomass carbon sink capacity changes of Canada's boreal forest from 1970 to 2020. We show that there is an increasing trend in drought-induced tree mortality from 1970 to 2020 with an acceleration since 2002. Approximately 43% of Canada's boreal forests experienced a significant trend of increasing tree mortality. This increase in tree mortality has resulted in a significant carbon loss at an approximate rate of 1.51 ± 0.29 MgC ha^{-1} $year^{-1}$ with an approximate total loss of 0.46 ± 0.09 PgC per year. This is a huge carbon flux which is equivalent to approximately 210% of Canada's total annual carbon emissions. Under this century's predicted drought increase, Canada's boreal forests may forego their role as strong carbon sinks.

3.3. Introduction

Globally, forest-based carbon (C) uptake has removed approximately one-third of annual anthropogenically-derived C emissions from the atmosphere since 1990 (Pan et al., 2011). Compared to all terrestrial biomes, boreal forests have the second-highest C storage rates, estimated at 367.3–1715.8 Pg C (Bradshaw & Warkentin, 2015; Pan et al., 2011). The land area of Canada's boreal forests (which includes other wooded land types) covers 309 Mha (Brandt et al., 2013), nearly 30% of the boreal forested area globally (Brandt, 2009), thus playing a critical role in Earth's surface albedo effect (Bonan, 2008) and global carbon budget (Kurz et al., 2008).

However, evidence suggests that boreal forests are especially vulnerable to global-change-type drought (Brodrick & Asner, 2017; Hogg et al., 2008; Michaelian et al., 2011; Peng et al., 2011; Sulla-Menashe et al., 2018). Global-change-type droughts are droughts under high temperatures (Breshears et al., 2005), that have caused widespread tree mortality events across boreal biomes (Allen et al., 2010). They have a significant influence on boreal forest C dynamics (Ma et al., 2012; Van der Molen et al., 2011; Wang et al., 2012), ultimately impacting the global C cycle. Forest inventory plots have revealed that drought-induced mortality in Western Canada has resulted in aboveground biomass loss of 2.6 t ha^{-1} $year^{-1}$ (corresponding to 1.3 MgC ha^{-1} $year^{-1}$) (Michaelian et al., 2011). However, considerable uncertainty can result when extrapolating data from plot-scale inventories to the entire Canadian boreal forest region. This is due to variability in forest composition and climatic and soil conditions that control forest structure, function, and resilience to drought stress (Huntingford et al., 2013). Given that recent projections (Trenberth et al., 2014) indicate global warming may cause longer and more intense drought events (Xu et al., 2019), the failure to account for the impacts of drought-induced tree mortality on C cycling could result in C sink overestimations and consequently the potential of forests to offset anthropogenically-derived carbon dioxide (CO_2) emissions (Kurz et al., 2008). Therefore, accurately quantifying tree mortality and its impact on forest C source dynamics at a large scale is critical (Choat et al., 2018).

In this study, a state-of-the-art tree mortality model (TRIPLEX-Mortality model), which has been successfully validated against long-term forest permanent sampling plots across the Canadian boreal forests (Liu et al., 2021), was used to estimate drought-induced tree mortality and further quantify their impact on Canadian boreal forest C stocks and dynamics between 1970 and 2020.

For a more robust representation of modelling results, we also used the climate moisture index (CMI) calculated from Canada's weather station network from 1970 to 2020, and long-term remotely sensed NDVI (1984-2020) to evaluate their relationships with the simulated mortality rates. We investigate spatiotemporal changes in drought-induced tree mortality rate trends and biomass C loss rate trends throughout Canada's boreal forests using a linear least squares regression approach in which trends change at each point in space. Additionally, we used a piecewise linear regression algorithm to detect the potential turning points of changing trends. Finally, we quantify the drought-induced forest C sink loss of the entire Canadian boreal forest bio-region throughout the study period (1970–2020).

3.4. Materials and Methods

3.4.1. Climate data

Canada's boreal forest covers approximately 310 Mha (Brandt et al., 2013). TRIPLEX-Mortality model simulations run at a monthly time step, on a 5x5 km spatial resolution grid. Throughout the study area (i.e., over $2x10^6$ grids), we obtained 100 years (1920–2020) of monthly temperature (°C), precipitation (sum, mm), and relative humidity (%) data for each simulated grid using the BioSIM interpolation model (see the Materials and Methods section in Supplementary information) (Régnière, 1996) based on daily climate data from the Canadian network of weather stations (National Climate Data and Information Archive, under the authority of Environment Canada [2020], available from *climate.weather.gc.ca/*, which we accessed on November 11, 2021). Monthly potential evapotranspiration (PET, mm) was estimated based on Hamon parameterization (Hamon PET) (Hamon, 1961).

The drought index can provide a comprehensive picture of drought events, which makes drought characteristics such as duration, severity, and intensity measurable. More importantly, the drought index allows direct comparisons between regions under different climatic conditions. CMI has been widely used in the evaluation of drought impacts on boreal forest ecosystems (i.e., Berner et al., 2017; D'Orangeville et al., 2018; Hogg et al., 2013; Ma et al., 2012; Peng et al., 2011). In this study, CMI was selected to evaluate drought conditions. This index is calculated as the difference between precipitation and PET over period *i* in water (mm):

$$CMI_i = Precipitation_i - PET_i \quad (3.\ 1).$$

3.4.2. Forest stands and soil information

For each simulation grid, required data for TRIPLEX-Mortality model initialization includes forest stand type, tree age and tree species, tree height, soil texture, and soil C content. Forest stand information used in this study (i.e., stand age, tree species, and tree height) derived from the published remote sensing dataset (Beaudoin et al., 2014) (see Fig 3. S1). Soil information used in this study (i.e., soil texture and soil C content) was obtained from the published datasets (Batjes, 2012; Tarnocai & Lacelle, 1996) (see Fig 3. S2). Collected forest stand and soil information were extracted or resampled to a 5x5 km scale to match each simulation grid (see the Materials and Methods section in Supplementary information).

3.4.3. Remotely sensed NDVI data

Given that model simulations cover a 50-year period (i.e., 1970–2020), we selected Landsat 5–8 satellite series data at a 30 m spatial resolution, which covers a relatively long period (1984–2020), to assess vegetation dynamics. Additionally, NDVI was generated from the near-infrared and red bands of each scene as (NIR - Red) / (NIR + Red). Between 1984–2020, annual NDVI extrapolated from all Landsat 5–8 images started on the first and ended on the last day of each year. All annual NDVI composites used in this study were made from orthorectified scenes, using computed top-of-atmosphere (TOA) reflectance (Chander et al., 2009). Drought legacy effects have been reported to be common in boreal and temperate forests globally (Anderegg et al., 2015), and these effects can last for 3 years or more (Itter et al., 2019; Peltier et al., 2016; Yang et al., 2018). To better evaluate correlations between tree mortality and NDVI, a three-year moving average treatment and the linear least squares regression method in conjunction with a t-test were used for annual average NDVI to detect changes.

3.4.4. TRIPLEX-Mortality model

The TRIPLEX-Mortality model was developed from the original TRIPLEX model (Peng et al., 2002), which has been widely used to simulate forest growth, C, and nitrogen (N) dynamics in boreal forests (Sun et al., 2008; Wang et al., 2012; Zhou et al., 2008). The physiological process-

based TRIPLEX-Mortality model has been successfully validated against observations from permanent sample plots across Canada's boreal forests, offering good reliability in estimating drought-induced tree mortality and associated biomass C dynamics (Liu et al., 2021). Two key physiological mechanisms (hydraulic failure and carbon starvation) (McDowell et al., 2008; McDowell, 2011) of drought-induced mortality were considered and incorporated into the model. Hydraulic failure was assessed by the percentage loss of hydraulic conductivity (PLC, Eq. 3. 2), whereas carbon starvation was quantified by dynamics of non-structural carbohydrate (NSC, Eq. 3) concentrations in the TRIPLEX-Mortality model (Liu et al., 2021).

$$PLC = 100\left(1 - e^{\left(\frac{--swp}{b}\right)^{c}}\right) \quad (3.\ 2)$$

where b is the critical SWP that results in a 63% reduction in conductivity, and c is a shape parameter.

$$NSC = NPP * \alpha - C_m - C_s \quad (3.\ 3)$$

where C_m represents the carbohydrate consumption from NSC to support basic metabolic processes, and C_s is the carbohydrate consumption from NSC that is transferred to structural carbon.

More detailed information on model structure, function, and development can be found in Supplementary Information (TRIPLEX-Mortality model section) and publications (Liu et al., 2021; Peng et al., 2002).

3.4.5. Piecewise regression model

To identify abnormal trends in the annual tree mortality rate, the biomass loss rate, the CMI, and the remotely sensed NDVI trend, we used the piecewise regression model to quantitatively identify turning points between 1970–2020. The model was applied using the following formula (Piao et al., 2011; Toms & Lesperance, 2003; Wang et al., 2011; Zhang et al., 2013):

$$Y = \begin{cases} \beta_0 + \beta_1 x + \varepsilon x \leq \alpha \\ \beta_0 + \beta_1 x + \beta_2 (x - \alpha) + \varepsilon x > \alpha \end{cases} \quad (3.\ 4)$$

where x is the year; Y represents each variable (i.e., tree mortality rate, biomass loss rate, CMI, NDVI); α is the estimated turning point of the variable change rate, which was determined by the least square error method. β_1 and $\beta_1 + \beta_2$ are the change rates before and after the turning point, respectively. ε is the residual error. A t-test was used to test the significance in single and piecewise regressions, while a P value < 0.05 was considered significant.

3.5. Results

3.5.1. Spatiotemporal patterns in tree mortality

We simulated the average annual tree mortality rate in Canada's boreal forests between 1970–2020 as 2.7% using TRIPLEX-Mortality (see Methods) (see Fig. 3.1A and B). The forests experienced an increase in their average annual mortality rates (slope = 0.03%, $P < 0.05$, $R^2 = 0.55$) (see Fig. 3. S3). However, further analysis on annual tree mortality trends in Canada's boreal forests showed that trends in annual average tree mortality were not temporally homogeneous throughout the study period (1970–2020). A piecewise linear regression and a *t*-test (see the Methods section) showed a significant ($P < 0.05$) increase in annual average tree mortality rates after 2002, with an acceleration in annual average mortality rates through 2020 (Fig. 3. 1B). Specifically, after 2002, increasing trends in annual average mortality rates were greater by a factor of 5 compared to before 2002 (see Fig. 3. 1B). The areas that experienced significant changes ($P < 0.05$) in mortality trends in periods before (1970-2001) and after (2002-2020) 2002 were counted, respectively. Although the percentage of areas that experienced decreased trend in mortality rate (trend < 0, $P < 0.05$) after turning point year (2002-2020) was slightly higher (approximately 0.8% higher; Fig. 3. 1C) than that before turning point year (1970-2001), the percentage of areas that experienced an increased trend in mortality rate (trend > 0, $P < 0.05$) area after turning point year (2002-2020; 79%) was much higher (Fig. 3. 1C) than that before turning point year (1970-2001; 71%). Similarly, the percentage of areas that experienced a relatively remarkable decreased trend (trend < -0.05; $P < 0.05$) in tree mortality after the turning point year was slightly higher (around 2.1% higher; Fig. 1C) than that before the turning point year, while approximately 30% of Canadian

boreal forests experienced relatively remarkable increased trend (trend > 0.05, $P < 0.05$; Fig. 3. 1C) after the turning point year. In comparison, before the turning point, only 1.5% of the Canadian boreal forests experienced a remarkably increased trend (trend > 0.05, $P < 0.05$; Fig. 3. 1C) in tree mortality.

Analysis of mortality rate trends based on linear least squares regression in conjunction with a *t*-test indicated that trends in mortality rates were not spatially homogeneous throughout 1970–2020. Approximately 47% of Canada's boreal forested area experienced significant changes ($P < 0.05$) in drought-induced tree mortality rates (Fig. 3. 1D and Fig. 3. S4); approximately 43% of Canada's boreal forested area experienced increasing trends in mortality rates; approximately 4% of Canada's boreal forested area experienced slightly decreasing trends throughout 1970–2020 (see Fig. 3. 1D, E). Specifically, most areas that experienced increasing mortality rates (approximately 71%) occurred in the western region of the country (i.e., the Yukon, the Northwest Territories, British Columbia, Alberta, Saskatchewan, and Manitoba) while most areas that experienced decreasing mortality rates (approximately 59%) occurred in the eastern region of the county (i.e., Ontario, Quebec, New Brunswick, Newfoundland and Labrador, Prince Edward Island, and Nova Scotia) (see Fig. 3. 1E). Additionally, the average annual mortality rate in the western region (3.5%) was much higher than the eastern region of the country (1.1%) (see Fig. 3. 1A).

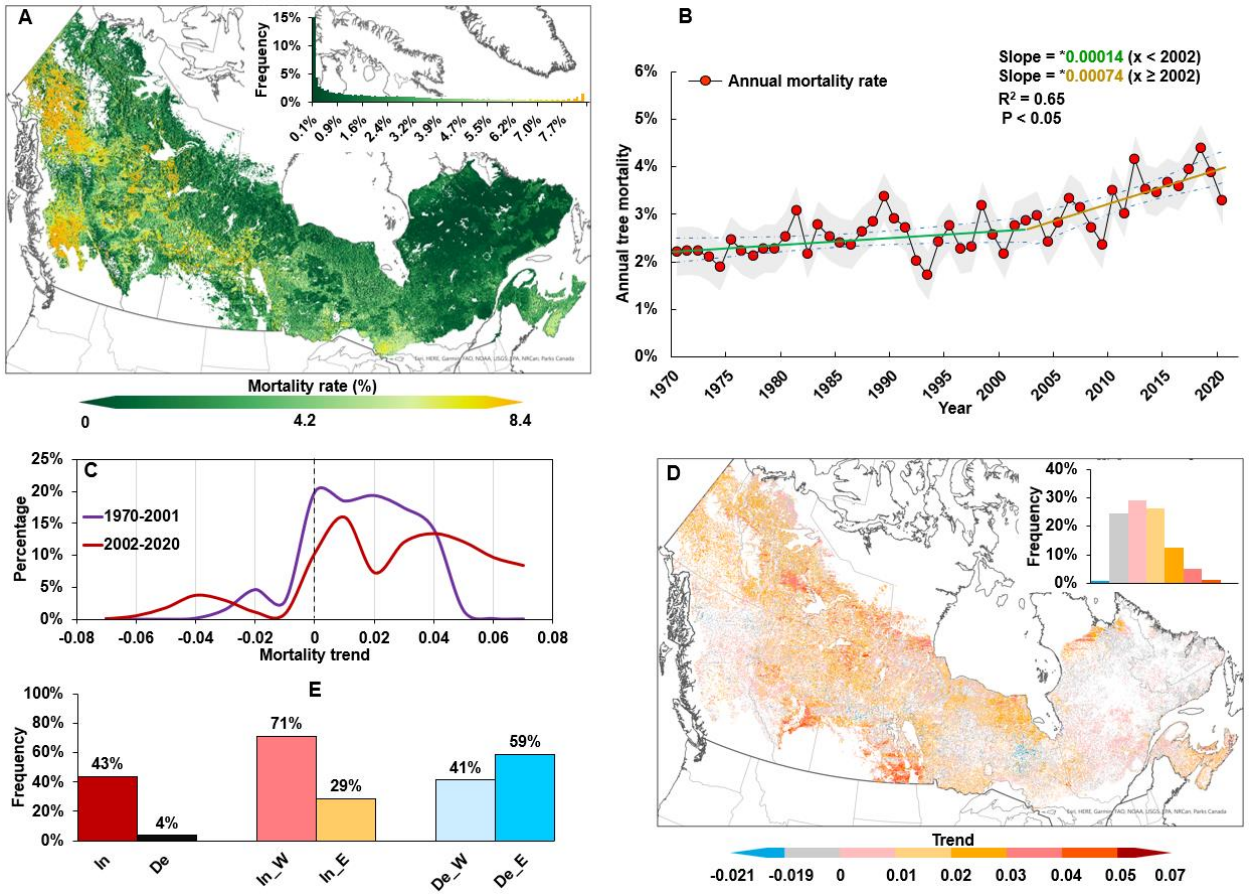

Figure 3. 1. **Average annual tree mortality distribution and annual mortality trends in Canada's boreal forested area between 1970–2020.** (A) Spatial patterns of average annual tree mortality between 1970–2020. (B) Annual average tree mortality time series. The gray shaded area indicates ± 1 standard deviation. Green and brown dashed lines show linear fitted data before (1970–2002) and after (2002–2020) the turning point, respectively, using a piecewise linear regression model. Dashed lines in (B) represent 95% confidence intervals of the piecewise regression. * Indicates significant changes at a significance level of $P < 0.05$. (C) The probability density function of mortality trends ($P < 0.05$) before and after the turning point (i.e., 2002). (D) Annual mortality trends ($P < 0.05$) in Canada's boreal forests between 1970–2020. (E) Frequency of tree mortality trends between 1970–2020. In and De represent increasing and decreasing trends, respectively. In_W and In_E refer to the frequency of an increasing trend in the western region, an increasing trend in the eastern region. De_W, and De_E represent and a decreasing trend in the western region and the eastern region of the county, respectively.

3.5.2. Relationship between simulated tree mortality and observed drought conditions

We used the Climate Moisture Index (CMI), which we estimated based on observational data from Canada's weather station network, to analyze long-term (1970–2020) drought trends throughout Canada's boreal forests. Statistical analysis using the linear least squares regression method in conjunction with a *t*-test, showed that Canada's boreal forested area experienced overall increasing trends in drought events, where most occurred in the western region of the country (Fig. 3. 2A, B, and Fig. 3. S3). However, anomalies in this drought related index showed that drought trends in Canada's boreal forests were temporally and spatially heterogeneous throughout the study period (1970–2020) (Fig. 3. 2A, B, and C). For the time series, although an overall decreased trend (trend = -0.17, $P < 0.05$, Fig. 3. S3) was detected in annual average CMI over the past 50 years, the trend in average CMI of Canada's boreal forest between 1970–2001 (before the turning point year) and between 2002-2020 (after the turning point year) showed differences. Analysis results of changing CMI values showed that annual average CMI values in Canada's boreal forests significantly decreased (trend = -0.19, $P < 0.05$) during the period before the turning point year (1970-2001). Although a decreasing trend (trend = -0.11) in CMI values was detected for the period after the turning point (2002–2020), this trend was not significant ($P = 0.25$). Particularly, accounting for there is a sharp increase in CMI values from 2018 onwards (Fig. 3. 2C). Therefore, changes in CMI values were detected between 2002–2018 showing a significant decreasing trend for the CMI (trend = -0.22, $P < 0.05$). Spatially, we found more severe and intensive drought events in the western region (CMI = 2.1) than the eastern region of the country (CMI = 38.4) between 1970–2020 (Fig. 3. 2A). Between 1970 and 2020, trend analysis throughout the study area showed that most of Canada's boreal forested area experienced increasing trends in drought events, where most occurred in the western region of the country (see the Results section in Supplementary Information and Fig. 3. S4). Nonlinear mixed-effects models (see the Results section in Supplementary Information and Eq. 3. S8) were used to quantify the relationships between tree mortality rates and CMI index. Regression analysis results indicated a significant negative relationship ($P < 0.05$) between CMI and mortality rates (see Fig. 3. 2D, the Results section in Supplementary information and Table. 3. S1) indicating higher mortality rates tended to occur at lower CMI values when drought was more severe.

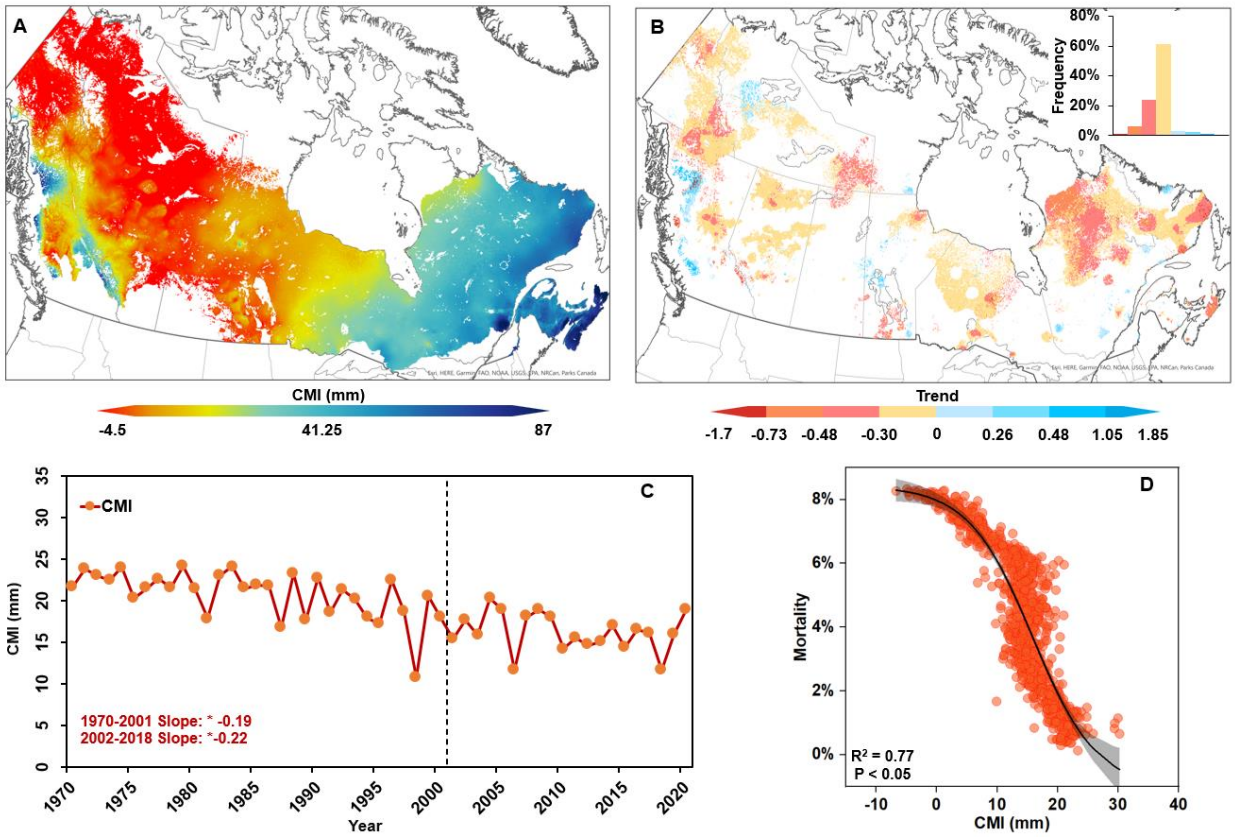

Figure 3. 2. **Distribution maps of CMI, annual CMI trends and comparisons of CMI and mortality rate.** (A) the distribution of average annual CMI across Canada's boreal forests between 1970–2020. (B) the distribution of areas that experienced the significant change ($P < 0.05$) in CMI trend across Canada's boreal forests between 1970–2020. (C) Time series of annual CMI values between 1970–2020. (D) The relationship between averaged annual CMI values and averaged annual mortality. Gray shaded areas in (D) represent 95% confidence intervals of nonlinear regressions.

3.5.3. The comparison of simulated tree mortality with remotely sensing NDVI

In this study, we used remotely sensed normalized difference vegetation index (NDVI) data from all of Canada's boreal forests between 1984–2020 (see the Methods section) to assess vegetation status and then compared it with simulated tree mortality trends. From 1984 to 2020, the annual average NDVI exhibited a decreasing trend (trend = -0.001, $P < 0.05$, Fig. 3. 3A). Spatially, there were no significant changes were detected in NDVI trends in the eastern region (Fig. 3. S5A). While a significant change ($P < 0.05$) was detected in the western region of the country, showing

a decreasing trend (trend = -0.001, $P < 0.05$) throughout the period of 1984-2020 (Fig. 3. S6A). These results show that Canada's western region exhibited a more significant decreasing NDVI trend than in the eastern region of the country. Statistical analysis results based on annual average tree mortality rates and NDVI showed a significant negative relationship ($R^2 = 0.3$, $P < 0.05$, Fig. 3. 3B) between NDVI and mortality rates. However, the relationship between NDVI and mortality was different in the eastern and western regions of the country. In western regions, NDVI was significantly negatively correlated with the mortality rate (Fig. 3. S6B), while the relationship between NDVI and mortality was not significant in the eastern regions (Fig. 3. S5B).

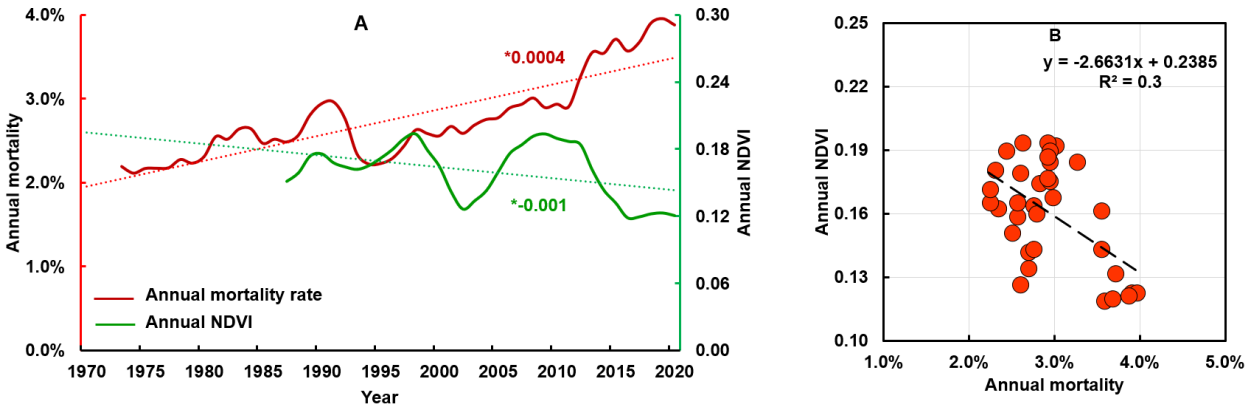

Figure 3. 3. **Comparisons of NDVI trend and mortality trend over the Canada's boreal forest from 1984 to 2020.** (A)Three-year moving averages representing annual tree mortality (red line) and remotely sensed NDVI (green line). (B)The relationship between tree mortality and NDVI. * Indicates significant changes at a significance level of $P < 0.05$.

3.5.4. Changes in biomass carbon sinks caused by drought-induced tree mortality

The estimated change rate in average annual biomass over 1970–2020 to be approximately -2.7% per year (Fig. 3. 4A). A decreasing trend in the change rates of annual average biomass was detected (trend = -0.03%, $P < 0.05$, $R^2 = 0.54$, Fig. 3. S7), which indicated progressively more biomass loss throughout the study period. Piecewise linear regression and *t*-test analysis results (see the Methods section below) on change trends in annual biomass of Canada's boreal forests indicated, however, that it was not temporally homogeneous throughout the study period (1970–2020). Specifically, 2002 was determined to be the turning point year in the biomass change rate time series. After 2002, a significant ($P < 0.05$) change was observed in annual average biomass

change rate trends, showing an acceleration in annual average biomass change rates (Fig. 3. 4B). This acceleration implied that drought-induced biomass loss increased after 2002.

Spatial heterogeneity was observed in linear least squares regression and *t*-test results as they relate to trends in changing biomass rates between 1970–2020 throughout Canada's boreal forests (Fig. 3. 4C). Approximately 48% of Canada's boreal forested area underwent significant alteration ($P < 0.05$) in biomass change rates over the past 50 years. An increasing trend in biomass loss rates was observed in nearly 44% of these areas, while only approximately 4% of these areas experienced decreasing trends (Fig. 3. 4C and D). For the difference in the trend between eastern and western regions, most areas experiencing decreasing trends in biomass loss rate (i.e., approximately 59%) were in the eastern region and most areas experiencing increasing trends (approximately 71%) in biomass loss rate were in the western region of the country (Fig. 3. 4C and D).

Biomass reduction from 1970-2020 was estimated at 3.01 ± 0.58 Mg ha^{-1} $year^{-1}$ (95% confidence interval) with a total biomass loss throughout all boreal forested areas in Canada of approximately 0.93 ± 0.18 Pg, of which 83% was aboveground biomass and 17% was belowground biomass (see Fig. 3. 4E). This decrease in biomass is equivalent to a net decrease in the carbon sink of 1.51 ± 0.29 MgC ha^{-1} $year^{-1}$. Multiplying this by the area of the Canadian boreal forest (310 Mha), the reduction of the carbon sink throughout Canada's boreal forest is equal to 0.46 ± 0.09 PgC $year^{-1}$. There was a significant difference between annual carbon loss in the western region and the eastern region of the country, which indicated considerably higher carbon loss in the former (0.36 ± 0.05 Pg) compared to the latter (0.10 ± 0.03 Pg).

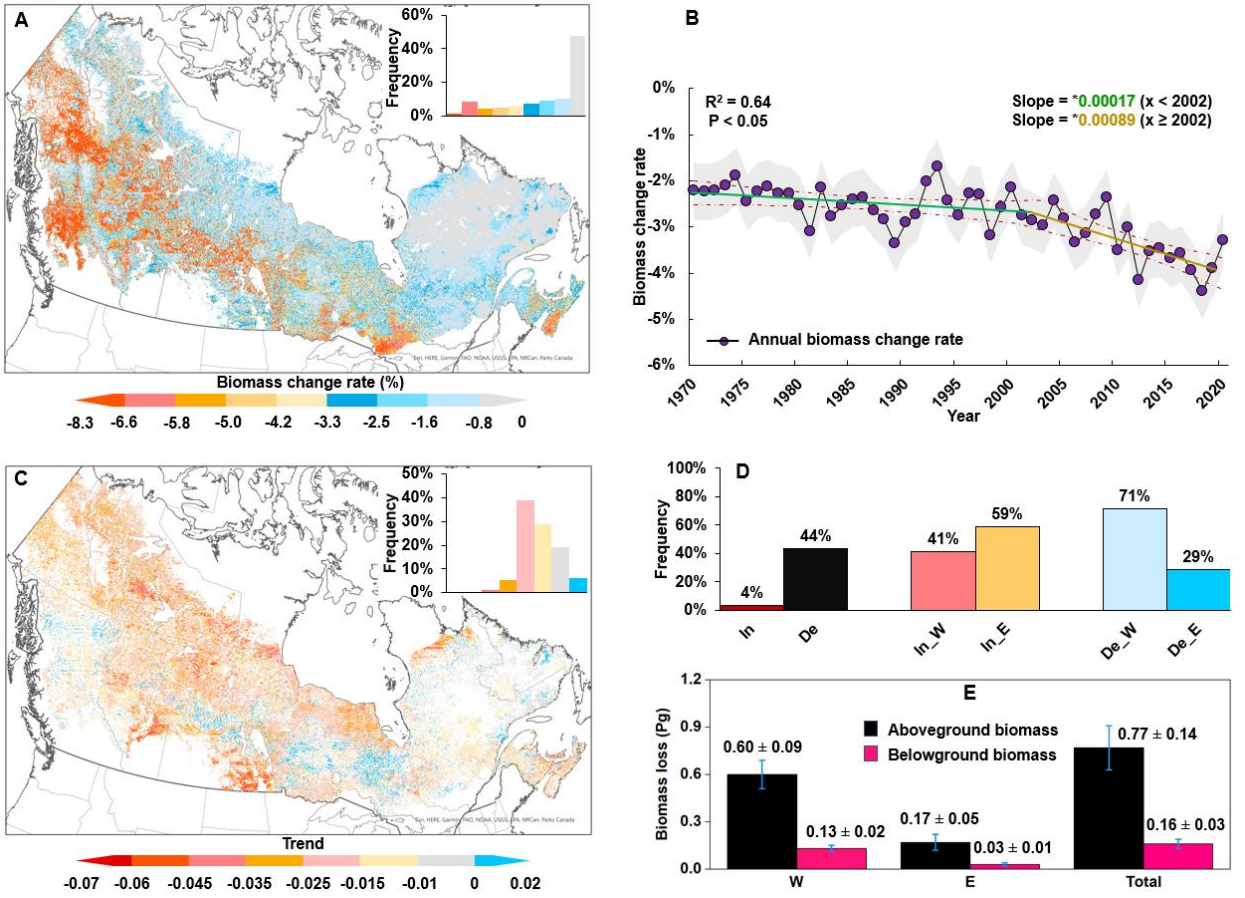

Figure 3. 4. **Distribution of average annual biomass change rate and time series of annual average biomass change rate across Canada's boreal forests between 1970–2020.** (A) Spatial patterns of average annual biomass change rates (%) between 1970–2020. (B) Time series of annual biomass change rate. The gray shaded area indicates ± 1 standard deviation. Using a piecewise linear regression model, green and brown dashed lines show the linear fitted data between 1970–2002 (i.e., before the 2002 turning point) and between 2002–2020 (i.e., after the 2002 turning point), respectively. The dash lines represent 95% confidence intervals of the piecewise linear regression model. (C) The trend ($P < 0.05$) in the annual average biomass change rates across Canada's boreal forests between 1970–2020. (D) Frequency of biomass change rates between 1970–2020. In and De represent increasing and decreasing trends, respectively. In_W and In_E refer to the frequency of an increasing trend in the western region, an increasing trend in the eastern region. De_W, and De_E represent and a decreasing trend in the western region and the eastern region of the Canada's boreal forests, respectively. (E) Drought-induced annual biomass loss estimations in Canada's boreal forests between 1970–2020. W, E, and Total represent the western, the eastern, and the entire Canadian boreal forested region, respectively.

3.6. Discussion

This study provides the evidence at the national scale that boreal forests throughout Canada have undergone an increase in drought-induced tree mortality, which has caused a significant loss in the biomass C sink between 1970–2020. Results showed that forest mortality and C loss rates in the western region were greater by an approximate factor of 3 compared to the eastern region of the country (see Fig. 3. 1A and Fig. 3. 4A). Time series results showed that 2002 was the turning point, wherein annual mortality and biomass C loss rate trends accelerated (Fig. 3. 1B and Fig. 3. 4B).

Parts of the finding in this study (i.e., increase in drought-induced tree mortality and biomass C loss) can be well supported by previous studies (i.e., (Ma et al., 2012; Peng et al., 2011a) based on plot observation at a plot-to-regional scale. This study is an update to these previous reports since the quantified information of entire Canada's boreal forests is provided. Spatiotemporal variations in drought-induced tree mortality rates were closely related to changes in drought intensity (see Fig. 3. 2D). Observed CMI showed that Canada's boreal forest experienced increased drought conditions with trends becoming more pronounced since 2002 (Fig. 3. 2C) and western Canada experienced more severe and extensive drought compared to Eastern Canada (see Fig. 3. 2A and B). This heterogeneous temporal and spatial variation in drought conditions throughout Canada's boreal forests can be well supported by previous studies (Wang et al., 2014). Additionally, previous studies have shown that Canada's boreal forests experienced one of the worst and most widespread drought events in 2001–2002, where the hardest-hit areas were located in the western region of the country following two to three consecutive years of below-average precipitation (Bonsai & Wheaton, 2005; Wang et al., 2014). Furthermore, observations from meteorological stations showed that atmospheric warming and an increase in the amount and frequency of precipitation over the last several decades have had no significant effect on the severity of summer drought in the eastern region of the country (Girardin et al., 2004). These previous findings not only support the spatiotemporal variations detected by this study in drought condition but also can be the potential reasons for spatiotemporal variations in mortality and biomass C loss trends in Canada's boreal forests, throughout the study period. We compared the trends of remotely sensed NDVI with the trends of simulated tree mortality. Although a decrease in remotely sensed NDVI is a comprehensive result that can be caused by many disturbances (e.g., fire, insect, wind, and drought damage), an increase in drought-induced tree mortality is a primary driver of changes in vegetation

indices throughout North American (Allen et al., 2010; Bonsai & Wheaton, 2005; Girardin et al., 2004; Y. Wang et al., 2014). Therefore, the observed spatiotemporal variation in NDVI patterns (i.e., decreased trend in NDVI across study area over the study period and more significant decreased trend in western regions NDVI) and the significant negative relationship between remotely sensed NDVI and simulated mortality rates (Fig. 3. 3) can provide additional evidence that supports our simulation results.

Estimations of biomass C loss from this study were consistent with those from previous studies in Canada's boreal forests at regional scales and in tropical forests of the Amazon basin. Our modeling estimation of aboveground biomass loss (3.01 ± 0.58 Mg ha^{-1} $year^{-1}$) across 309 M ha of Canadian boreal forested area is approximately 20% higher than that reported by Michaelian et al. (2.5 Mg ha^{-1} $year^{-1}$) (Michaelian et al., 2011), which was estimated based on a combination of ground-based and remote sensing observations and interpolation model results from a drought event across 11.5 M ha in western Canada between 2001–2002 (causing approximately 0.03 Pg of aboveground biomass loss). This difference can potentially be explained by a continued increase in drought intensification and in drought-induced tree mortality rates over the past few decades, especially since the turning point year (2002, see Fig. 3. 1D). Additionally, the aboveground biomass C loss estimated in our study (i.e., approximately 1.51 ± 0.29 MgC ha^{-1} $year^{-1}$) is consistent with recent findings on extensive biomass C loss caused by widespread drought in Amazon forests, for which Yang et al. (Yang et al., 2018) used LiDAR to estimate the average drought-induced aboveground biomass C loss (i.e., approximately 2.35 ± 1.8 MgC ha^{-1} $year^{-1}$). Differences in quantified results may be attributed to the resilience of different forest ecosystems to drought (Gazol et al., 2018) (Schwalm et al., 2017) as well as the higher C density of tropical forests compared to boreal forests (Malhi et al., 1999) (Dixon et al., 1994). The estimated decrease in total annual biomass loss (approximately 0.93 ± 0.18 Pg [Fig. 3. 3E]) throughout the entire Canadian boreal forest region (309 M ha) resulted in a large reduction in its C sink capacity (0.46 ± 0.09 PgC $year^{-1}$), which is equivalent to approximately 210% of Canada's total annual C emissions (*Environment Canada (2019) National Inventory Report: Greenhouse Gas Sources and Sinks in Canada 1990–2019 (Government of Canada, Gatineau, QC).*, n.d.). This result provides new estimations to support previous studies (Angert et al., 2005; Piao et al., 2008; Stephens et al., 2007) that predicted weaker C uptake at higher latitudes in the Northern Hemisphere, and

challenges the conventional view that Northern Hemisphere forests will continue to dominate as a sink for C emissions.

Despite significant progress, uncertainties remain. The annual drought-induced tree mortality rate estimated in this study may be slightly overestimated compared to observational extrapolations (see Fig. 3. S8) (Peng et al., 2011a). Biases in modeling results may be due to a lack of a clear understanding of the interdependency of mechanisms related to drought-induced tree mortality (e.g., hydraulic failure and carbon starvation) that have not been well integrated into model simulations (McDowell et al., 2011). In addition, processes such as vegetation regeneration, which have yet to be integrated into the model, may also offset mortality to some extent, leading to drought-induced tree mortality overestimations. Some additional mechanisms involved in tree mortality (e.g., the lag effect) (Kannenberg et al., 2020) are not well understood and therefore need to be integrated into the TRIPLEX-Mortality model in the future. Drought-induced water stress not only affects ecosystem functions during drought events, but it can also cause a lag effect in vegetation that can last for years (Kannenberg et al., 2020). This phenomenon, commonly referred to as the "drought legacy effect," has yet to be fully captured by the model, resulting in uncertainties in simulated mortality. Such uncertainties in drought-induced tree mortality rates may also cause uncertainties in simulated biomass C loss.

3.7. Conclusions

Results from this study demonstrate that since 1970, droughts have triggered a widespread increase in tree mortality rates across Canada's boreal forests, which accelerated after 2002, and indicate that this increase in tree mortality is a dominant contributing factor to the large biomass C losses across Canada's boreal forests. Previous studies that did not account for impacts related to drought-induced tree mortality likely overestimated the biomass C sink capacity of Canada's boreal forests. The projected ongoing increase in drought events could potentially have a considerable negative impact on vegetation productivity and health, while also resulting in a reduction in the boreal forest C sink potential globally, which will result in accelerated positive feedback that will affect both regional and global climate conditions.

3.8. Supplementary Information Text

3.8.1. Materials and Methods

3.8.1.1. Climate data

The land area of Canada's boreal forests (which include other wooded land types) covers approximately 310 Mha, nearly 30% of the boreal forested area globally (Brandt et al., 2013). The entire study area was latched to 22209 grids (5x5 km) for model simulation. In each simulation grid, monthly temperature (°C), precipitation (sum; mm), and relative humidity (%) data between 1920–2020 were generated by the average or sum of daily data using the BioSIM interpolation model (Régnière, 1996). The BioSIM interpolation model has been widely applied in studies on climate impacts on forest ecosystems (D'Orangeville et al., 2018; Girardin et al., 2016; Liu et al., 2021; Luo & Chen, 1957; Puchi et al., 2019). Specifically, monthly values were interpolated from the eight closest weather stations, and adjusted for differences in latitude, longitude, and elevation between data sources and study site locations, and then averaged using a $1/d^2$ weight, where d represents distance. For this procedure, the number of matched weather stations used to generate weather data was kept constant through time. More detailed information on the BioSIM interpolation model can be found in the study by Régnière (Régnière, 1996).

3.8.1.2. Forest stands and soil information

Original forest stand and soil information obtained from published datasets (Batjes, 2012; Beaudoin et al., 2014; Tarnocai & Lacelle., 1996) used different spatial resolutions. To match the simulation grid (5x5 km), we counted the percentage of each species and soil texture in each grid, and the highest percentage of species (Fig. 3. S9A) and soil texture types (Fig. 3. S10) were used as the dominant species and the dominant soil texture in the simulation grid. In each simulation grid, we counted the average value of stand age (Fig. 3. S9B), height (Fig. 3. S9C), and soil carbon (C) content (Fig. 3. S9D), and these averaged values were then used in the simulated grid. Although the distribution of vegetation species, soil texture, and soil C content have changed slightly over time, we assumed that these attributes remained constant due to a lack of continuous data.

3.8.2. TRIPLEX-Mortality model

The TRIPLEX-Mortality model was developed from the original TRIPLEX model (Peng et al., 2002). The TRIPLEX-Mortality model intergrated key physiological mechanisms (hydraulic failure and carbon starvation) (McDowell et al., 2008; McDowell, 2011) of drought-induced mortality.

3.8.2.1. Hydraulic failure (HF)

The soil water pools simulated in TRIPLEX-Mortality model account for monthly water loss through transpiration and evaporation, soil water content and snow water content. When monthly mean air temperature is less than 0°C, total monthly precipitation is designated as snow (Parton et al., 1987, 1993). The water balance (L_w) is calculated as a function of water inputs and outputs as follows (Peng et al., 2002):

$$\Delta L_w = R - T - E - L \quad (3.1)$$

R is rainfall (cm), and T, E and L represent transpiration (cm), evaporation (cm) and leached water (cm), respectively.

The physiological HF mechanism represents the complete loss of water transport to the canopy resulting from xylem embolism. During drought events, as transpiration persists, the soil water potential (SWP, in MPa) dramatically declines below the air entry pressure. The hydraulic connection between roots and soil is consequently severed, and HF subsequently takes place (Plaut et al., 2012). Based on soil water conditions, SWP is calculated using the reference soil water potential of saturated soil ($swps$, in MPa), the volumetric saturation (*vs*) in soil pores and the soil attribution parameter (λ) as follows (Oleson et al., 2010):

$$SWP = swps * vs^{-\lambda} \quad (3.\ 2)$$

Based on the Community Land Model (CLM) (Oleson et al., 2010), Eq. 3. 3 is used to calculate vs, where t is the thickness of the topsoil layer; s (mm^3) is the saturated volumetric water content of the topsoil layer; P_{liq} is the density of liquid water; and W_{liq} is the mass of liquid water of the topsoil layer.

$$vs = \frac{1}{ts}\left[\frac{W_{liq}}{P_{liq}}\right] \quad (3.3)$$

The $swps$ is correlated to the soil organic matter fraction (f), the saturated organic matter matric potential (swp_{om}) and the saturated mineral soil matric potential (swp_{sat}) as follows:

$$swps = (1-f)swp_{sat} + f swp_{om} \quad (3.4)$$

The loss of xylem conductivity along with a decrease in the xylem water potential is represented by the PLC index, which is plotted against pressure and fitted to a Weibull function to generate a vulnerability curve (Neufeld et al., 1992; Rosner et al., 2019). Based on the research by (Plaut et al., 2012), the root water potential is assumed to be equal to the SWP.

$$PLC = 100\left(1 - e^{\left(-\frac{-swp}{b}\right)^c}\right) \quad (3.5)$$

where b is the critical SWP that results in a 63% reduction in conductivity, and c is a shape parameter (Neufeld et al., 1992; Pammenter & Van der Willigen, 1998; Sperry & Tyree, 1988).

3.8.2.2 Carbon starvation (CS)

Plants must regulate multiple demands on stomatal control during drought events where a decrease in water availability will promote HF. And a decrease in stomatal conductance (G_s) will reduce the risk of HF but subsequently limit CO_2 assimilation into leaves increasing the risk of CS (Damour et al., 2010; Plaut et al., 2012). The response of G_s to drought varies across the isohydric-anisohydric continuum of hydraulic strategies (Martínez-Vilalta et al., 2014). For this hydraulic strategy continuum, the canopy scale (G_s) simulation has been adapted based on models developed by (Buckley et al., 2003) and (Gao et al., 2002) as follows:

$$G_s = (1 - PLC)/(VPD * p)(SWP - \Psi_l) \quad (3.6)$$

where Ψ_l (MPa) is the leaf water potential (LWP), VPD (mb) is the vapor pressure deficit of the canopy and p is a coefficient. Eq. 6 indicates that mortality may increase when drought causes a

sustained decrease in the soil water potential, while an increase in VPD can potentially be considered the greatest threat to survival because increasing global temperatures are driving a chronic increase in the VPD despite concurrent increases in specific humidity (Williams et al., 2013).

We adapted the original nonstructual carbon content (NSC) submodel from the RHESSys process-based model ((Tague et al., 2013) and then integrated this model into the TRIPLEX-Mortality model to estimate dynamic NSC pools. The NSC pool maintains a net balance between carbohydrate allocation and consumption. Under normal conditions, it is assumed that a portion of carbohydrates (α, see Table 3. S1) is allocated to the NSC pool until the total NSC reaches a threshold ($P_{threshold}$, see Table 3. S1) percentage of the total aboveground biomass (Fisher et al., 2010; Genet et al., 2009; Gruber et al., 2012). The remaining carbohydrate is then transferred to the structural carbon pool. During drought events, in conjunction with a rapid decline in productivity, if the ratio of leaves to aboveground carbon falls below 0.05, a value that derives from (Callaway et al., 1994) and (Tague et al., 2013) or if the climate moisture index is less than -20, trees will access the NSC pool to maintain respiration requirements and restore their hydraulic function and leaf biomass.

$$NSC = NPP * \alpha - C_m - C_s \quad (3.\ 7)$$

where C_m represents the carbohydrate consumption from NSC to support basic metabolism, and C_s is the carbohydrate consumption from NSC that is transferred to structural carbon.

3.8.3. Results

3.8.3.1. Relationship between tree mortality and drought conditions

The rate of tree mortality was regressed as a function of drought indices (i.e., CMI) to test for significant trends. We used the following nonlinear mixed-effects model:

$$y = A1 + \frac{A2-A1}{1+10^{(LOGx0-x)p}} \quad (3.\ 8)$$

where y is tree mortality rate, and x represents the CMI values. $A1$, $A2$, $LOGx0$, and p are model parameters. The fixed parameters of the mixed model can be found in Table 3. S1.

Table 3. S1. Fixed effects of the linear mixed models (Eq. S3. 8) that describe the relationships between the rate of tree mortality and drought indices

$A1$	$A2$	$LOGx0$	p	P value	R^2
-0.010	0.0842	15.867	-0.082	< 0.05	0.77

Statistical analysis results showed that approximately 32% of Canada's boreal forested area underwent significant changes in CMI ($P < 0.05$) between 1970–2020. Among these areas, approximately 93% of them exhibited a decreasing CMI trend, and most of these areas (approximately 51%) were in the western region of the country (Fig. 3. S4). By comparison, only 7% of these areas underwent increased CMI trends, and most of these areas were in the eastern region of the country (Fig. 3. S4).

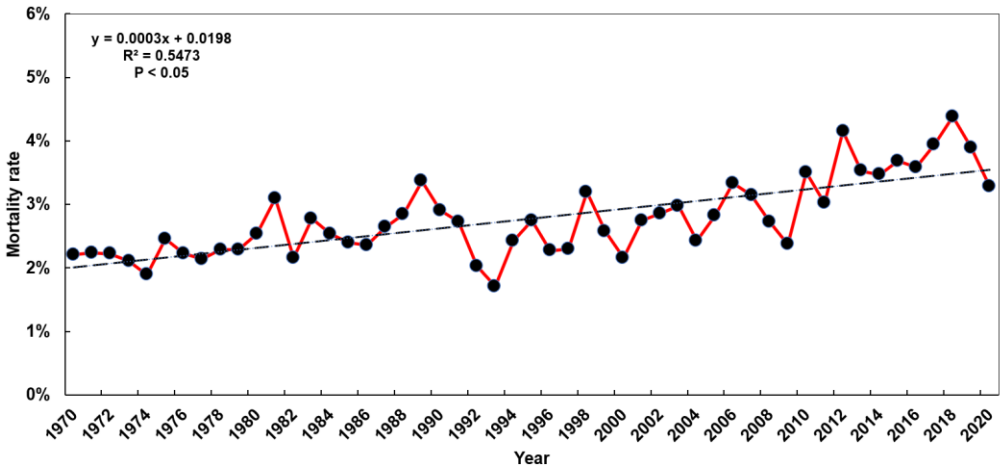

Figure 3. S1. The annual average drought-induced tree mortality rate in Canada's boreal forests between 1970–2020.

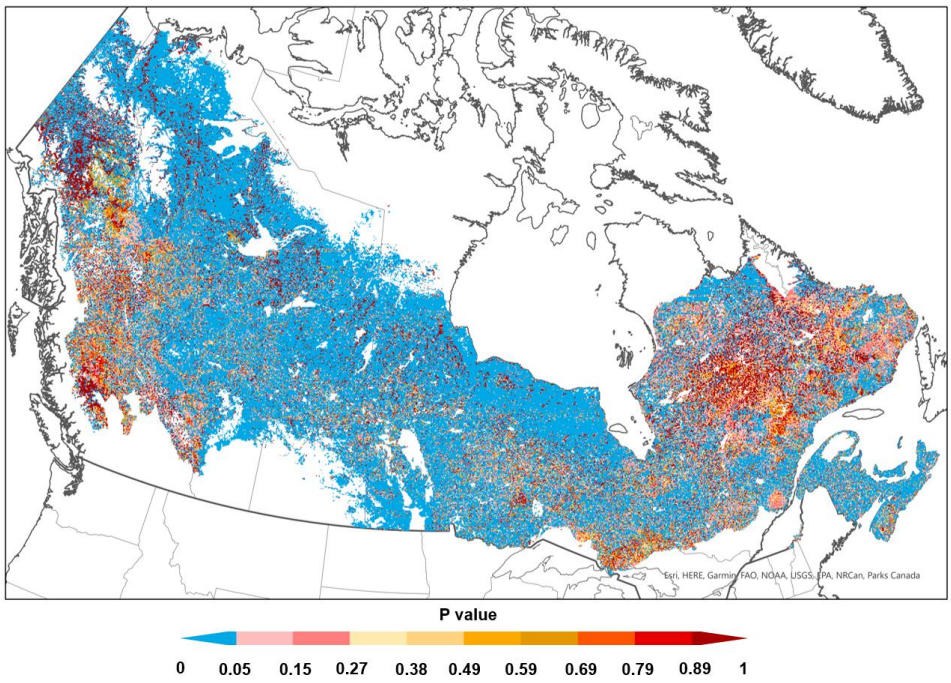

Figure 3. S2. P-value distribution of the drought-induced tree mortality rate trend based on the linear least squares regression method in conjunction with a t-test between 1970–2020.

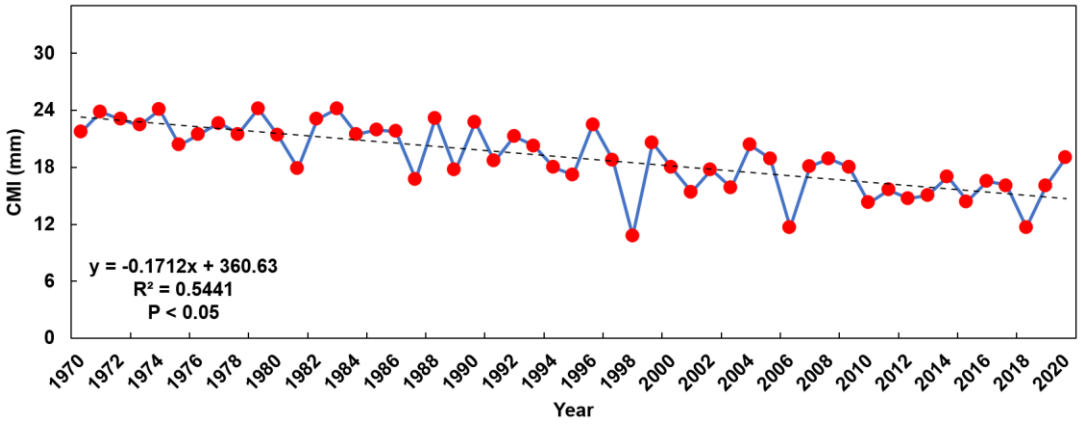

Figure 3. S3. Time series of annual average CMI in Canada's boreal forests between 1970–2020.

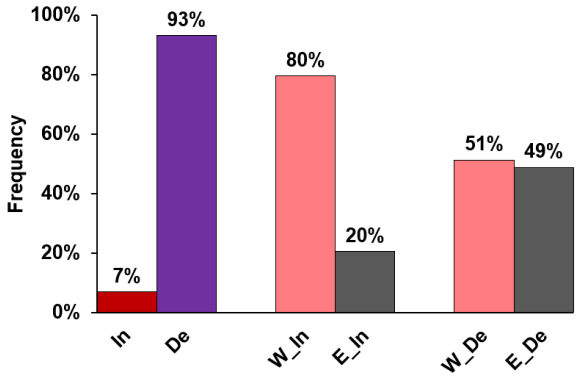

Figure 3. S4. Frequency of CMI trends between 1970–2020. In and De represent increasing and decreasing trends, respectively. In_W, In_E, De_W, and De_E represent an increasing trend in the western region, an increasing trend in the eastern region, and a decreasing trend in the western region and in the eastern region, respectively.

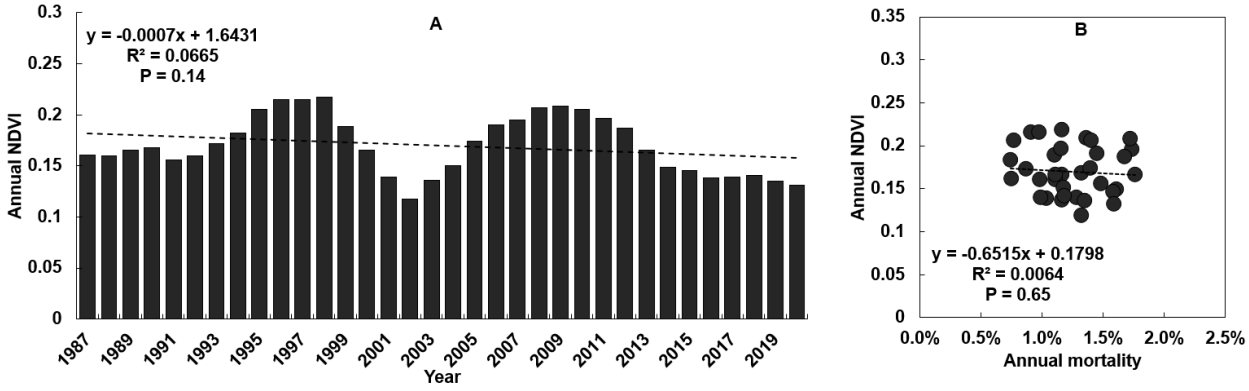

Figure 3. S5. Time series of NDVI in the eastern region of the country (A) and a comparison between annual tree mortality and NDVI in the eastern region of the country (B).

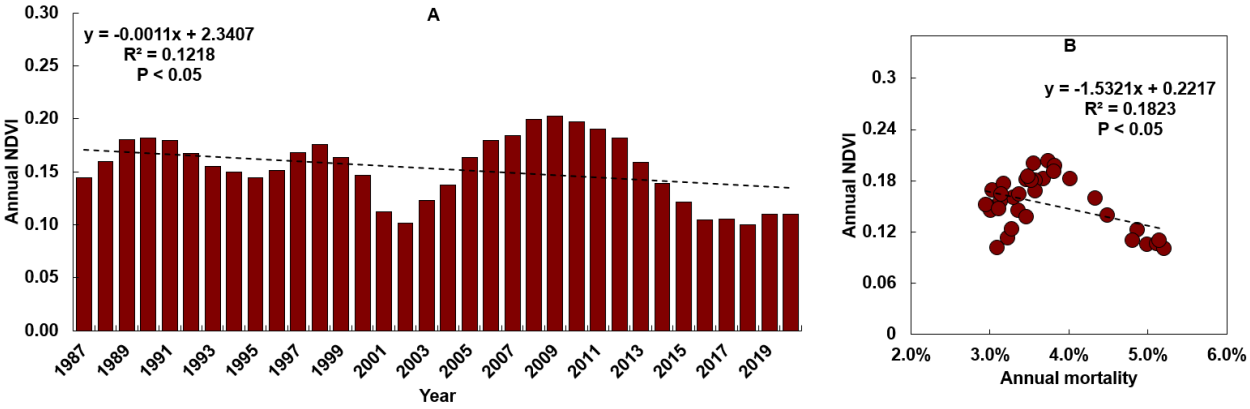

Figure 3. S6. Time series of NDVI in the western region of the country (A) and a comparison between annual tree mortality and NDVI in the western region of the country (B).

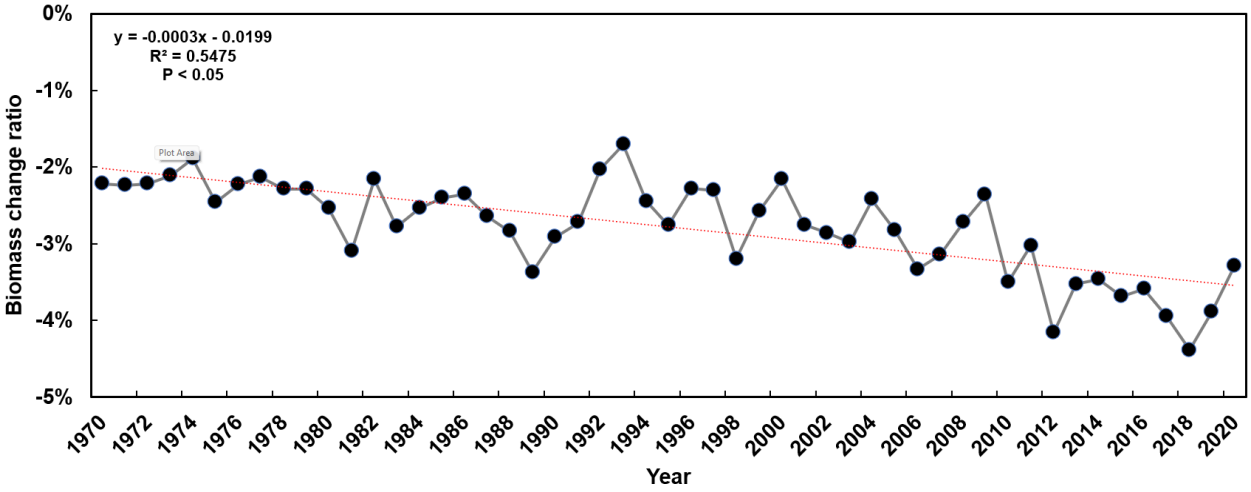

Figure 3. S7. Time series of annual average biomass change rates in Canada's boreal forests between 1970–2020.

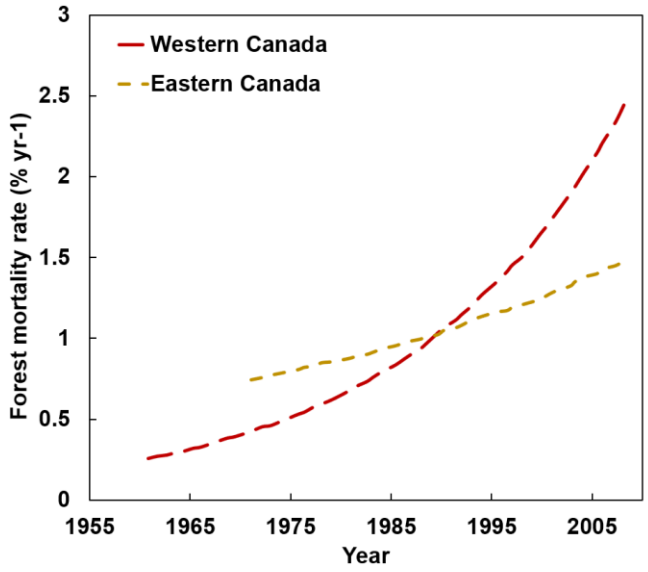

Figure 3. S8. Studies on tree mortality (Peng et al., 2011a; McDowell et al., 2016) have been increasing throughout Canada's boreal forests, across a mean annual precipitation range from 202–3928 mm yr^{-1} and a mean annual temperature range from -5.7–12.0°C.

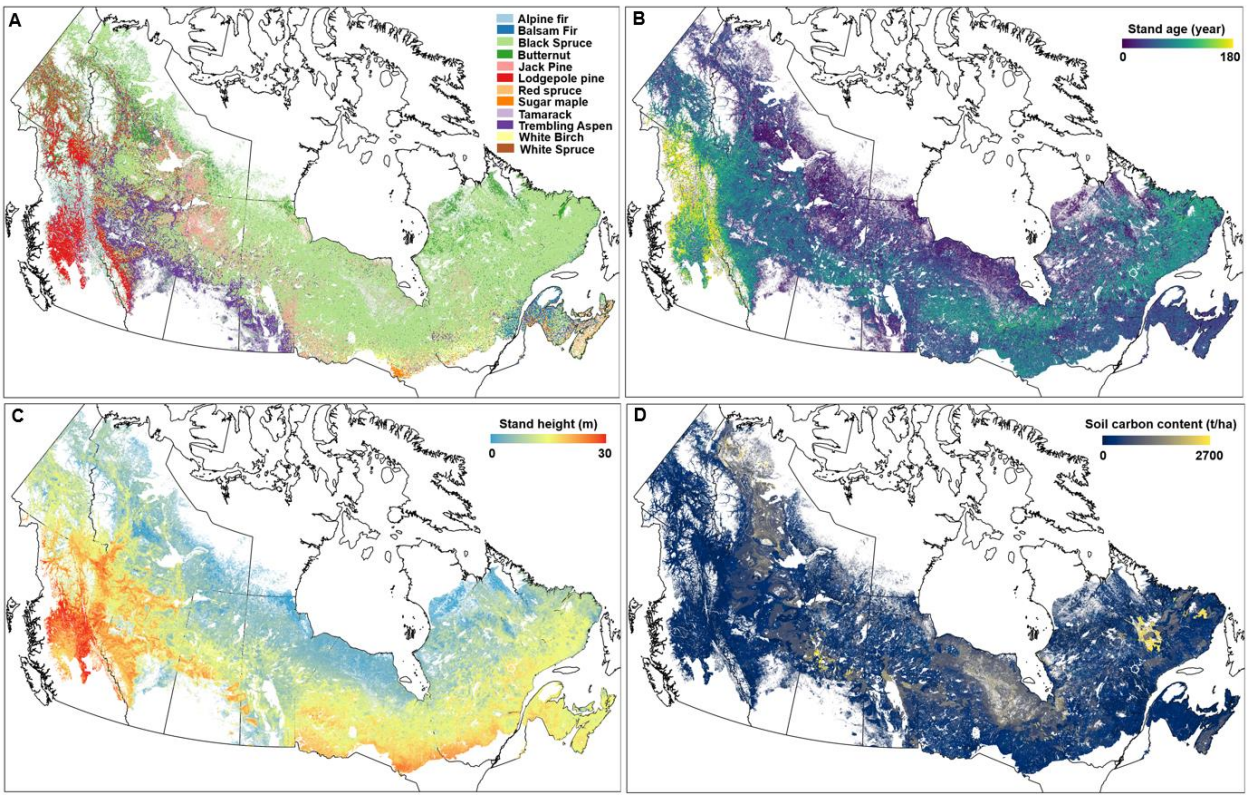

Figure 3. S9. The dominate tree species in each simulation grid (A). Forest stand age of the study

area in each simulation grid (B). Forest stand height of the study area in each simulation grid (C). Soil carbon content of the study area (D).

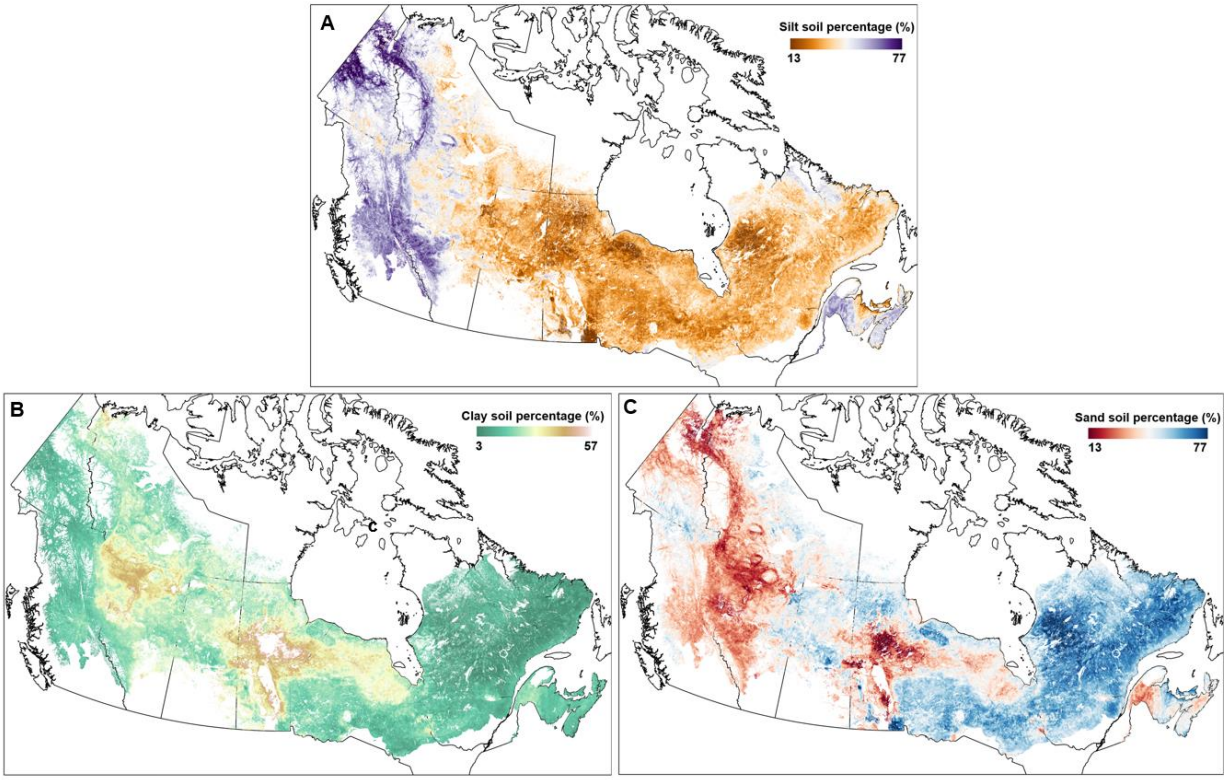

Figure 3. S10. Soil texture map of the study area. Silt soil percentage (A). Clay soil percentage (B). Sand soil percentage (C).

3.9. References

Allen, C. D., Macalady, A. K., Chenchouni, H., Bachelet, D., McDowell, N., Vennetier, M., Kitzberger, T., Rigling, A., Breshears, D. D., Hogg, E. H. (Ted., Gonzalez, P., Fensham, R., Zhang, Z., Castro, J., Demidova, N., Lim, J. H., Allard, G., Running, S. W., Semerci, A., & Cobb, N. (2010). A global overview of drought and heat-induced tree mortality reveals emerging climate change risks for forests. Forest Ecology and Management, 259(4), 660–684. https://doi.org/10.1016/j.foreco.2009.09.001

Anderegg, W. R. L., Schwalm, C., Biondi, F., Camarero, J. J., Koch, G., Litvak, M., Ogle, K., Shaw, J. D., Shevliakova, E., Williams, A. P., Wolf, A., Ziaco, E., & Pacala, S. (2015). Pervasive drought legacies in forest ecosystems and their implications for carbon cycle models. Science, 349(6247), 528–532. https://doi.org/10.1126/science.aab1833

Angert, A., Biraud, S., Bonfils, C., Henning, C. C., Buermann, W., Pinzon, J., Tucker, C. J., & Fung, I. (2005). Drier summers cancel out the CO2 uptake enhancement induced by warmer springs. Proceedings of the National Academy of Sciences of the United States of America, 102(31), 10823–10827. https://doi.org/10.1073/pnas.0501647102

Batjes, N. H. (2012). ISRIC-WISE derived soil properties on a 5 by 5 arc-minutes global grid (ver. 1.2). ISRIC-World Soil Information.

Beaudoin, A., Bernier, P. Y., Guindon, L., Villemaire, P., Guo, X. J., Stinson, G., Bergeron, T., Magnussen, S., & Hall, R. J. (2014). Mapping attributes of Canada's forests at moderate resolution through kNN and MODIS imagery. Canadian Journal of Forest Research, 44(5), 521–532. https://doi.org/10.1139/cjfr-2013-0401

Berner, L. T., Law, B. E., & Hudiburg, T. W. (2017). Water availability limits tree productivity, carbon stocks, and carbon residence time in mature forests across the western US. Biogeosciences, 14(2), 365–378. https://doi.org/10.5194/bg-14-365-2017

Bonan, G. B. (2008). Forests and Climate Change: Forcings, Feedbacks, and the Climate Benefits of Forests. Science, 320(5882), 1444–1449. https://doi.org/10.1126/science.1155121

Bonsai, B. R., & Wheaton, E. E. (2005). Atmospheric circulation comparisons between the 2001 and 2002 and the 1961 and 1988 canadian prairie droughts. Atmosphere - Ocean, 43(2), 163–172. https://doi.org/10.3137/ao.430204

Bradshaw, C. J. A., & Warkentin, I. G. (2015). Global estimates of boreal forest carbon stocks and flux. Global and Planetary Change, 128, 24–30. https://doi.org/10.1016/j.gloplacha.2015.02.004

Brandt, J. P. (2009). The extent of the North American boreal zone. Environmental Reviews, 17, 101–161. https://doi.org/10.1139/A09-004

Brandt, J. P., Flannigan, M. D., Maynard, D. G., Thompson, I. D., & Volney, W. J. A. (2013). An introduction to Canada's boreal zone: Ecosystem processes, health, sustainability, and environmental issues. Environmental Reviews, 21(4), 207–226. https://doi.org/10.1139/er-2013-0040

Breshears, D. D., Cobb, N. S., Rich, P. M., Price, K. P., Allen, C. D., Balice, R. G., Romme, W. H., Kastens, J. H., Floyd, M. L., Belnap, J., Andersonc, J., Myers, O. B., & Meyer, C. W. (2005). Regional vegetation die-off in response to global-change-type drought. Proceedings of the National Academy of Sciences, 102(42), 15144–15148. https://doi.org/10.1890/080016

Brodrick, P. G., & Asner, G. P. (2017). Remotely sensed predictors of conifer tree mortality during severe drought. Environmental Research Letters, 12(11). https://doi.org/10.1088/1748-

9326/aa8f55

Buckley, T. N., Mott, K. A., & Farquhar, G. D. (2003). A hydromechanical and biochemical model of stomatal conductance. Plant, Cell and Environment, 26(10), 1767–1785. https://doi.org/10.1046/j.1365-3040.2003.01094.x

Callaway, R. M., DeLucia, E. H., & Schlesinger, W. H. (1994). Biomass allocation of montane and desert ponderosa pine: An analog for response to climate change. Ecology, 75(5), 1474–1481. https://doi.org/10.2307/1937470

Chander, G., Markham, B. L., & Helder, D. L. (2009). Summary of current radiometric calibration coefficients for Landsat MSS, TM, ETM+, and EO-1 ALI sensors. Remote Sensing of Environment, 113(5), 893–903. https://doi.org/10.1016/j.rse.2009.01.007

Choat, B., Brodribb, T. J., Brodersen, C. R., Duursma, R. A., López, R., & Medlyn, B. E. (2018). Triggers of tree mortality under drought. Nature, 558(7711), 531–539. https://doi.org/10.1038/s41586-018-0240-x

D'Orangeville, L., Houle, D., Duchesne, L., Phillips, R. P., Bergeron, Y., & Kneeshaw, D. (2018). Beneficial effects of climate warming on boreal tree growth may be transitory. Nature Communications, 9(1), 1–10. https://doi.org/10.1038/s41467-018-05705-4

Damour, G., Simonneau, T., Cochard, H., & Urban, L. (2010). An overview of models of stomatal conductance at the leaf level. Plant, Cell and Environment, 33(9), 1419–1438. https://doi.org/10.1111/j.1365-3040.2010.02181.x

Dixon, R. K. ., Brown, S. ., Houghton, R. A. ., Solomon, A. M. ., Trexler, M. C. ., & Wisniewski, J. (1994). Carbon pools and flux of global forest ecosystems. Science, 263(5144), 185–190. https://doi.org/Carbon pools and flux of global forest ecosystems

Fisher, J. B., Sitch, S., Malhi, Y., Fisher, R. A., Huntingford, C., & Tan, S.-Y. (2010). Carbon cost of plant nitrogen acquisition: A mechanistic, globally applicable model of plant nitrogen uptake, retranslocation, and fixation. Global Biogeochemical Cycles, 24(1). https://doi.org/10.1029/2009gb003621

Gao, Q., Zhao, P., Zeng, X., Cai, X., & Shen, W. (2002). A model of stomatal conductance to quantify the relationship between leaf transpiration, microclimate and soil water stress. Plant, Cell and Environment, 25(11), 1373–1381. https://doi.org/10.1046/j.1365-3040.2002.00926.x

Gazol, A., Camarero, J. J., Vicente-Serrano, S. M., Sánchez-Salguero, R., Gutiérrez, E., de Luis, M., Sangüesa-Barreda, G., Novak, K., Rozas, V., Tíscar, P. A., Linares, J. C., Martín-Hernández, N., Martínez del Castillo, E., Ribas, M., García-González, I., Silla, F., Camisón,

A., Génova, M., Olano, J. M., … Galván, J. D. (2018). Forest resilience to drought varies across biomes. Global Change Biology, 24(5), 2143–2158. https://doi.org/10.1111/gcb.14082

Genet, H., Bréda, N., & Dufrêne, E. (2009). Age-related variation in carbon allocation at tree and stand scales in beech (Fagus sylvatica L.) and sessile oak (Quercus petraea (Matt.) Liebl.) using a chronosequence approach. Tree Physiology, 30(2), 177–192. https://doi.org/10.1093/treephys/tpp105

Girardin, M. P., Bouriaud, O., Hogg, E. H., Kurz, W., Zimmermann, N. E., Metsaranta, J. M., De Jong, R., Frank, D. C., Esper, J., Büntgen, U., Guo, X. J., & Bhatti, J. (2016). No growth stimulation of Canada's boreal forest under half-century of combined warming and CO2 fertilization. Proceedings of the National Academy of Sciences of the United States of America, 113(52), E8406–E8414. https://doi.org/10.1073/pnas.1610156113

Girardin, M. P., Tardif, J., Flannigan, M. D., Wotton, B. M., & Bergeron, Y. (2004). Trends and periodicities in the Canadian Drought Code and their relationships with atmospheric circulation for the southern Canadian boreal forest. Canadian Journal of Forest Research, 34(1), 103–119. https://doi.org/10.1139/x03-195

Gruber, A., Pirkebner, D., Florian, C., & Oberhuber, W. (2012). No evidence for depletion of carbohydrate pools in Scots pine (Pinus sylvestris L.) under drought stress. Plant Biology, 14(1), 142–148. https://doi.org/10.1111/j.1438-8677.2011.00467.x

Hamon, W. R. (1961). Estimating potential evapotranspiration. Journal of the Hydraulics Division, 87(3), 107–120. https://doi.org/https://doi.org/10.1061/JYCEAJ.0000599

Hogg, E. H., Barr, A. G., & Black, T. A. (2013). A simple soil moisture index for representing multi-year drought impacts on aspen productivity in the western Canadian interior. Agricultural and Forest Meteorology, 178–179, 173–182. https://doi.org/10.1016/j.agrformet.2013.04.025

Hogg, E. H., Brandt, J. P., & Michaelian, M. (2008). Impacts of a regional drought on the productivity, dieback, and biomass of western Canadian aspen forests. Canadian Journal of Forest Research, 38(6), 1373–1384. https://doi.org/10.1139/X08-001

Huntingford, C., Zelazowski, P., Galbraith, D., Mercado, L. M., Sitch, S., Fisher, R., Lomas, M., Walker, A. P., Jones, C. D., Booth, B. B. B., Malhi, Y., Hemming, D., Kay, G., Good, P., Lewis, S. L., Phillips, O. L., Atkin, O. K., Lloyd, J., Gloor, E., … Cox, P. M. (2013). Simulated resilience of tropical rainforests to CO2 -induced climate change. Nature Geoscience, 6(4), 268–273. https://doi.org/10.1038/ngeo1741

Itter, M. S., D'Orangeville, L., Dawson, A., Kneeshaw, D., Duchesne, L., & Finley, A. O. (2019).

Boreal tree growth exhibits decadal-scale ecological memory to drought and insect defoliation, but no negative response to their interaction. Journal of Ecology, 107(3), 1288–1301. https://doi.org/10.1111/1365-2745.13087

Kannenberg, S. A., Schwalm, C. R., & Anderegg, W. R. L. (2020). Ghosts of the past: how drought legacy effects shape forest functioning and carbon cycling. Ecology Letters, 23(5), 891–901. https://doi.org/10.1111/ele.13485

Kurz, W. A., Dymond, C. C., Stinson, G., Rampley, G. J., Neilson, E. T., Carroll, A. L., Ebata, T., & Safranyik, L. (2008). Mountain pine beetle and forest carbon feedback to climate change. Nature, 452(7190), 987–990. https://doi.org/10.1038/nature06777

Liu, Q., Peng, C., Schneider, R., Cyr, D., Liu, Z., Zhou, X., & Kneeshaw, D. (2021). TRIPLEX-Mortality model for simulating drought-induced tree mortality in boreal forests: Model development and evaluation. Ecological Modelling, 455. https://doi.org/10.1016/j.ecolmodel.2021.109652

Luo, Y., & Chen, H. Y. H. (1957). Observations from old forests underestimate climate change effects on tree mortality[Supplementary figures]. Svenska Lakartidningen, 54(22), 1859–1861. http://www.ncbi.nlm.nih.gov/pubmed/13455520

Ma, Z., Peng, C., Zhu, Q., Chen, H., Yu, G., Li, W., Zhou, X., Wang, W., & Zhang, W. (2012). Regional drought-induced reduction in the biomass carbon sink of Canada's boreal forests. Proceedings of the National Academy of Sciences of the United States of America, 109(7), 2423–2427. https://doi.org/10.1073/pnas.1111576109

Malhi, Y., Baldocchi, D. D., & Jarvis, P. G. (1999). The carbon balance of tropical, temperate and boreal forests. Plant, Cell and Environment, 22(6), 715–740. https://doi.org/10.1046/j.1365-3040.1999.00453.x

Martínez-Vilalta, J., Poyatos, R., Aguadé, D., Retana, J., & Mencuccini, M. (2014). A new look at water transport regulation in plants. New Phytologist, 204(1), 105–115. https://doi.org/10.1111/nph.12912

McDowell, N. G. (2011). Mechanisms Linking Drought, Hydraulics, Carbon Metabolism, and Vegetation Mortality. Plant Physiology, 155(3), 1051–1059. https://doi.org/10.1104/pp.110.170704

McDowell, N. G., Beerling, D. J., Breshears, D. D., Fisher, R. A., Raffa, K. F., & Stitt, M. (2011). The interdependence of mechanisms underlying climate-driven vegetation mortality. Trends in Ecology and Evolution, 26(10), 523–532. https://doi.org/10.1016/j.tree.2011.06.003

McDowell, N. G., Williams, A. P., Xu, C., Pockman, W. T., Dickman, L. T., Sevanto, S., Pangle,

R., Limousin, J., Plaut, J., Mackay, D. S., Ogee, J., Domec, J. C., Allen, C. D., Fisher, R. A., Jiang, X., Muss, J. D., Breshears, D. D., Rauscher, S. A., & Koven, C. (2016). Multi-scale predictions of massive conifer mortality due to chronic temperature rise. Nature Climate Change, 6(3), 295–300. https://doi.org/10.1038/nclimate2873

McDowell, N., Pockman, W. T., Allen, C. D., David, D., Cobb, N., Kolb, T., Plaut, J., Sperry, J., West, A., Williams, D. G., & Yepez, E. A. (2008). Mechanisms of plant survival and mortality during drought: why do some plants survive while others succumb to drought? New Phytologist, 178(4), 719–739. https://doi.org/10.1111/j.1469-8137.2008.02436.x

Michaelian, M., Hogg, E. H., Hall, R. J., & Arsenault, E. (2011). Massive mortality of aspen following severe drought along the southern edge of the Canadian boreal forest. Global Change Biology, 17(6), 2084–2094. https://doi.org/10.1111/j.1365-2486.2010.02357.x

Neufeld, H. S., Grantz, D. A., Meinzer, F. C., Goldstein, G., Crisosto, G. M., & Crisosto, C. (1992). Genotypic variability in vulnerability of leaf xylem to cavitation in water-stressed and well-irrigated sugarcane. Plant Physiology, 100(2), 1020–1028. https://doi.org/https://doi.org/10.1104/pp.100.2.1020

Oleson, K. W., Lawrence, D. M., Bonan, G. B., Flanner, M. G., Kluzek, E., Lawrence, P. J., Levis, S., Swenson, S. C., & Thornton, P. E. (2010). Technical description of version 4.0 of the Community Land Model (CLM). papers2://publication/uuid/6858EE7A-C77E-4439-832D-CEC2791FBEBA

Pammenter, N., & Van der Willigen, C. (1998). A mathematical and statistical analysis of the curves illustrating vulnerability of xylem to cavitation. Tree Physiology, 18, 589–593. https://doi.org/https://doi.org/10.1093/treephys/18.8-9.589

Pan, Y., Birdsey, R. A., Fang, J., Houghton, R., Kauppi, P. E., Kurz, W. A., Phillips, O. L., Shvidenko, A., Lewis, S. L., Canadell, J. G., Ciais, P., Jackson, R. B., Pacala, S. W., McGuire, A. D., Piao, S., Rautiainen, A., Sitch, S., & Hayes, D. (2011). A large and persistent carbon sink in the world's forests. Science. https://doi.org/10.1126/science.1201609

Parton, W. ., Scurlock, J. ., Ojima, D. ., Gilmanov, T. ., Scholes, R. ., & Schimel, D. . (1993). Observations and modeling of biomass and soil organic matter dynamics for the grassland biome worldwide. Global Biogeochemical Cycles, 7, 785–809. https://doi.org/https://doi.org/10.1029/93GB02042

Parton, W. J., Schimel, D. S., Cole, C. V., & Ojima, D. S. (1987). Analysis of Factors Controlling Soil Organic Matter Levels in Great Plains Grasslands. Soil Science Society of America Journal, 51(5), 1173–1179. https://doi.org/10.2136/sssaj1987.03615995005100050015x

Peltier, D. M. P., Fell, M., & Ogle, K. (2016). Legacy effects of drought in the southwestern United States: A multi-species synthesis. Ecological Monographs, 86(3), 312–326. https://doi.org/10.1002/ecm.1219

Peng, C., Liu, J., Dang, Q., Apps, M. J., & Jiang, H. (2002). TRIPLEX: A generic hybrid model for predicting forest growth and carbon and nitrogen dynamics. Ecological Modelling, 153(1–2), 109–130. https://doi.org/10.1016/S0304-3800(01)00505-1

Peng, C., Ma, Z., Lei, X., Zhu, Q., Chen, H., Wang, W., Liu, S., Li, W., Fang, X., & Zhou, X. (2011). A drought-induced pervasive increase in tree mortality across Canada's boreal forests. Nature Climate Change, 1(9), 467–471. https://doi.org/10.1038/nclimate1293

Piao, S., Ciais, P., Friedlingstein, P., Peylin, P., Reichstein, M., Luyssaert, S., Margolis, H., Fang, J., Barr, A., Chen, A., Grelle, A., Hollinger, D. Y., Laurila, T., Lindroth, A., Richardson, A. D., & Vesala, T. (2008). Net carbon dioxide losses of northern ecosystems in response to autumn warming. Nature, 451, 49–52. https://doi.org/10.1038/nature06444

Piao, S., Wang, X., Ciais, P., Zhu, B., Wang, T., & Liu, J. (2011). Changes in satellite-derived vegetation growth trend in temperate and boreal Eurasia from 1982 to 2006. Global Change Biology, 17(10), 3228–3239. https://doi.org/10.1111/j.1365-2486.2011.02419.x

Plaut, J. A., Yepez, E. A., Hill, J., Pangle, R., Sperry, J. S., Pockman, W. T., & Mcdowell, N. G. (2012). Hydraulic limits preceding mortality in a piñon-juniper woodland under experimental drought. Plant, Cell and Environment, 35(9), 1601–1617. https://doi.org/10.1111/j.1365-3040.2012.02512.x

Puchi, P. F., Castagneri, D., Rossi, S., & Carrer, M. (2019). Wood anatomical traits in black spruce reveal latent water constraints on the boreal forest. In Global Change Biology. https://doi.org/10.1111/gcb.14906

Régnière, J. (1996). Generalized approach to landscape-wide seasonal forecasting with temperature-driven simulation models. Environmental Entomology, 25(5), 869–881. https://doi.org/10.1093/ee/25.5.869

Rosner, S., Johnson, D. M., Voggeneder, K., & Domec, J.-C. (2019). The conifer-curve: fast prediction of hydraulic conductivity loss and vulnerability to cavitation. Annals of Forest Science, 76(3), 1–15. https://doi.org/10.1007/s13595-019-0868-1

Schwalm, C. R., Anderegg, W. R. L., Michalak, A. M., Fisher, J. B., Biondi, F., Koch, G., Litvak, M., Ogle, K., Shaw, J. D., Wolf, A., Huntzinger, D. N., Schaefer, K., Cook, R., Wei, Y., Fang, Y., Hayes, D., Huang, M., Jain, A., & Tian, H. (2017). Global patterns of drought recovery. Nature, 548(7666), 202–205. https://doi.org/10.1038/nature23021

Sperry, J. S., & Tyree, M. T. (1988). Mechanism of Water Stress-Induced. Plant Physiology, 88(3), 581–587. https://doi.org/10.1104/pp.88.3.581

Stephens, B. B., Gurney, K. R., Tans, P. P., Sweeney, C., Peters, W., Bruhwiler, L., Ciais, P., Ramonet, M., Bousquet, P., Nakazawa, T., Aoki, S., Machida, T., Inoue, G., Vinnichenko, N., Lloyd, J., Jordan, A., Heimann, M., Shibistova, O., Langenfelds, R. L., … Denning, A. S. (2007). Weak northern and strong tropical land carbon uptake from vertical profiles of atmospheric CO2. Science, 316(5832), 1732–1735. https://doi.org/10.1126/science.1137004

Sulla-Menashe, D., Woodcock, C. E., & Friedl, M. A. (2018). Canadian boreal forest greening and browning trends: An analysis of biogeographic patterns and the relative roles of disturbance versus climate drivers. Environmental Research Letters, 13(1). https://doi.org/10.1088/1748-9326/aa9b88

Sun, J., Peng, C., McCaughey, H., Zhou, X., Thomas, V., Berninger, F., St-Onge, B., & Hua, D. (2008). Simulating carbon exchange of Canadian boreal forests. II. Comparing the carbon budgets of a boreal mixedwood stand to a black spruce forest stand. Ecological Modelling, 219(3–4), 276–286. https://doi.org/10.1016/j.ecolmodel.2008.03.031

Tague, C. L., McDowell, N. G., & Allen, C. D. (2013). An integrated model of environmental effects on growth, carbohydrate balance, and mortality of Pinus ponderosa forests in the southern Rocky Mountains. PLoS ONE, 8(11), e80286. https://doi.org/10.1371/journal.pone.0080286

Tarnocai, C., & Lacelle, B. (1996). Soil organic carbon of Canada map.

Toms, J. D., & Lesperance, M. . (2003). Piecewise regression: a tool for identifying ecological thresholds. Ecology, 84(8), 2034–2041. https://doi.org/https://doi.org/10.1890/02-0472

Trenberth, K. E., Dai, A., Schrier, G. Van Der, Jones, P. D., Barichivich, J., Briffa, K. R., & Sheffield, J. (2014). Global warming and changes in drought. Nature Climate Change, 4(1), 17–22. https://doi.org/10.1038/NCLIMATE2067

Van der Molen, M. K., Dolman, A. J., Ciais, P., Eglin, T., Gobron, N., Law, B. E., Meir, P., Peters, W., Phillips, O. L., Reichstein, M., Chen, T., Dekker, S. C., Doubková, M., Friedl, M. A., Jung, M., van den Hurk, B. J. J. M., de Jeu, R. A. M., Kruijt, B., Ohta, T., … Wang, G. (2011). Drought and ecosystem carbon cycling. Agricultural and Forest Meteorology, 151(7), 765–773. https://doi.org/10.1016/j.agrformet.2011.01.018

Wang, W., Peng, C., Kneeshaw, D. D., Larocque, G. R., & Luo, Z. (2012). Drought-induced tree mortality: ecological consequences, causes, and modeling. Environmental Reviews, 20(2), 109–121. https://doi.org/10.1139/a2012-004

Wang, W., Peng, C., Kneeshaw, D. D., Larocque, G. R., Song, X., & Zhou, X. (2012). Quantifying the effects of climate change and harvesting on carbon dynamics of boreal aspen and jack pine forests using the TRIPLEX-Management model. Forest Ecology and Management, 281, 152–162. https://doi.org/10.1016/j.foreco.2012.06.028

Wang, X., Piao, S., Ciais, P., Li, J., Friedlingstein, P., Koven, C., & Chen, A. (2011). Spring temperature change and its implication in the change of vegetation growth in North America from 1982 to 2006. Proceedings of the National Academy of Sciences of the United States of America, 108(4), 1240–1245. https://doi.org/10.1073/pnas.1014425108

Wang, Y., Hogg, E. H., Price, D. T., Edwards, J., & Williamson, T. (2014). Past and projected future changes in moisture conditions in the Canadian boreal forest. Forestry Chronicle, 90(5), 678–691. https://doi.org/10.5558/tfc2014-134

Williams, A. P., Allen, C. D., Alison K. Macalady, Daniel Griffi, Connie A.Woodhouse, & David M. Meko. (2012). Temperature as a potent driver of regional forest drought stress and tree mortality. Nature Climate Change, 3(3), 292–297. https://doi.org/10.1038/nclimate1693

Xu, C., McDowell, N. G., Fisher, R. A., Wei, L., Sevanto, S., Christoffersen, B. O., Weng, E., & Middleton, R. S. (2019). Increasing impacts of extreme droughts on vegetation productivity under climate change. Nature Climate Change, 9(12), 948–953. https://doi.org/10.1038/s41558-019-0630-6

Yang, Y., Saatchi, S. S., Xu, L., Yu, Y., Choi, S., Phillips, N., Kennedy, R., Keller, M., Knyazikhin, Y., & Myneni, R. B. (2018). Post-drought decline of the Amazon carbon sink. Nature Communications, 9(1). https://doi.org/10.1038/s41467-018-05668-6

Zhang, G., Zhang, Y., Dong, J., & Xiao, X. (2013). Green-up dates in the Tibetan Plateau have continuously advanced from 1982 to 2011. Proceedings of the National Academy of Sciences of the United States of America, 110(11), 4309–4314. https://doi.org/10.1073/pnas.1210423110

Zhou, X., Peng, C., Dang, Q. L., Sun, J., Wu, H., & Hua, D. (2008). Simulating carbon exchange in Canadian Boreal forests. I. Model structure, validation, and sensitivity analysis. Ecological Modelling, 219(3–4), 287–299. https://doi.org/10.1016/j.ecolmodel.2008.07.011

CHAPTER IV

FORECASTING DROUGHT-INDUCED TREE MORTALITY AND ITS IMPACT ON THE BIOMASS CARBON SINK OF CANADA'S BOREAL FOREST BY THE END OF THE TWENTY-FIRST CENTURY

Qiuyu Liu, Changhui Peng, Robert Schneider, Dominic Cyr, Nate G. McDowell, Daniel Kneeshawe

The article will be submitted to the journal of *Nature Climate Change*. 2022

4.1. Resume

Les événements généralisés de mortalité des arbres induits par la sécheresse menacent le cycle global du carbone. La forêt boréale canadienne, qui occupe environ 30% des forêts boréales du monde, joue un rôle essentiel dans le bilan global du carbone. Il existe peu d'information sur la mortalité des arbres induite par la sécheresse et son impact sur la dynamique du carbone de la forêt boréale du Canada dans le cadre des futurs changements climatiques. En utilisant un modèle de mortalité des arbres basé sur des processus de pointe ainsi que des scénarios de changement climatique dérivées des projections de la phase six du projet d'intercomparaison de modèles couplés (CMIP6), nous prévoyons la mortalité des arbres induite par la sécheresse et ses impacts sur la capacité de capture de carbone provenant de la biomasse dans la forêt boréale du Canada d'ici la fin du 21e siècle. Nous avons constaté qu'avec une augmentation du forçage radiatif pour les scénarios climatiques, la mortalité des arbres induite par la sécheresse continue d'augmenter et ce, avec une diminution associée de la capacité de puits de carbone. Nous avons estimé la mortalité annuelle moyenne des arbres à 4.2 % ± 0.4 % ~ 7.2 % ± 0.4 %, ce qui entraîne par conséquent une perte de carbone de la biomasse de 0.7 ± 0.06 Pg C an^{-1} ~ 1.29 ± 0.05 Pg C an^{-1} pendant la période 2050-2100. Si les futurs changements climatiques suivent la trajectoire climatique pessemiste, la forêt boréale du Canada risque fortement de perdre son rôle de puits de carbone.

4.2. Abstract

Widespread drought-induced tree mortality events threaten the global carbon cycle. The Canadian boreal forest, which occupies about 30% of the boreal forests worldwide, plays a critical role in the global carbon budget. There is little information on drought-induced tree mortality and its impact on the carbon dynamics of Canada’s boreal forest under future climate change. Here, using a state-of-the-art process-based tree mortality model in conjunction with climate change scenarios derived from projections of Phase Six of the Coupled Model Intercomparison Project (CMIP6), we forecast the drought-induced tree mortality and its impacts on biomass carbon sink capacity in Canada’s boreal forest by the end of the 21st century. We found that with an increase in the radiative forcing for the climate scenarios, drought-induced tree mortality continues to increase with an associated decline in the carbon sink capacity. We estimated average annual tree mortality at 4.2% ± 0.4%~7.2% ± 0.4%, which accordingly leads to 0.7 ± 0.06 Pg C $year^{-1}$ ~1.29 ± 0.05 Pg

C $year^{-1}$ biomass carbon loss during 2050-2100. If future climate change follows the high-end climate pathway, Canada's boreal forest is at significant risk to lose its role as a carbon sink.

4.3. Introduction

Hydroclimatic change, especially drought, is one of the most important regional consequences of climate change on ecosystems (Breshears et al., 2018; Humphrey et al., 2018; Vicente-Serrano et al., 2020). The most concerning effect of drought on forest ecosystems is widespread tree mortality and subsequent carbon loss (Choat et al., 2018). An increasing number of studies have reported sudden and widespread drought-induced tree mortality across all major biomes, suggesting an increase in tree mortality with climate warming (Allen et al., 2010; Phillips et al., 2009; Van Mantgem et al., 2009). Forests are a large carbon sink, taking up around 8.8 Pg CO_2 equivalents $year^{-1}$ (over 2000-2007; Pan et al., 2011; Pugh et al., 2019). Threats to the forest carbon sink as a result of drought-induced tree mortality have been documented in previous studies (Michaelian et al., 2011; Phillips et al., 2009; Van Mantgem et al., 2009). Given that future climate warming will result in continued alterations to the hydroclimate (Trenberth et al., 2014), forecasting drought-induced tree mortality and its impacts on forest carbon dynamics under future climate change is of paramount importance.

To date, most attempts to predict drought-induced tree mortality have used empirical relationships between climate extremes and observed tree mortality rates (Gustafson & Sturtevant, 2013; Mitchell et al., 2016; Peng et al., 2011; Williams et al., 2013). These empirical relationships, while providing insights into the drivers of tree mortality and spatiotemporal information on historical tree mortality rates, may not work well in the future if plant sensitivity changes over time or new climatic conditions occur in the future. For instance, plant responses to drought can be altered by elevated CO_2 concentrations (Cruz et al., 2016; McDowell et al., 2022) and rising temperatures (O'sullivan et al., 2017). In addition, empirical relationships used to model and predict tree mortality may also fail in areas with long-term shifts to new, drier climates (O'sullivan et al., 2017). Process-based models focus on simulating detailed physical or biological processes that explicitly describe the behavior of a system (Korzukhin et al., 1996) and can be more comprehensive and explicitly integrated with mechanisms (Adams et al., 2013). Therefore, process-based models can include new or non-simulated responses that may occur under future conditions (Williams &

Jackson, 2007). Using process-based models that incorporate sound physiological mechanisms holds high promise for predicting drought-induced tree mortality and its impacts on carbon dynamics of forests under future climate change (Choat et al., 2018). However, existing predictions of future forest mortality are still very limited. A recent use of a process-based model to forecast tree mortality predicted widespread conifer mortality throughout the southwestern United States using a multiple-scale model (McDowell et al., 2016). Also, De Kauwe et al., (2020) identified the area at risk of drought-induced tree mortality across South-Eastern Australia. These studies point to threats of future tree mortality, highlighting the importance of making accurate tree mortality predictions under future climate change. The failure to account for the impacts of tree mortality in carbon cycle modeling may have resulted in an overestimation of carbon sinks in previous research on the potential for forests to offset or sequester anthropogenic CO_2 (Kurz, Stinson, et al., 2008). Canada's boreal forest land area covers 309 Mha, 21%~27% of the global boreal forests and 8% of the world's forests (Brandt et al., 2013), and thus plays a critical role in the global carbon cycle (Kurz, Stinson, et al., 2008). Recent progress has been made in investigating severe drought impacts on tree mortality (Hogg et al., 2008; Luo & Chen, 2015, 2013; Michaelian et al., 2011; Peng et al., 2011) and biomass carbon sink capacity (Ma et al., 2012; Michaelian et al., 2011) in Canada's boreal forests; suggesting that these forests may be vulnerable to rapid increases in tree mortality due to warmer temperatures and more severe droughts, affecting its carbon sink capacity. Quantifying and predicting drought-induced tree mortality and its impact on the carbon dynamics of Canada's boreal forests is imperative and an ongoing challenge that has not yet been conducted.

Here, we used the state-of-the-art process-based tree mortality model (TRIPLEX-Mortality model), which has been successfully validated against long-term forest permanent sampling plots across the Canadian boreal forests (Liu et al., 2021), to forecast drought-induced tree mortality and further quantify its impact on the capacity of the Canadian boreal forest biomass to sequester carbon under future climate (2050-2100). To attain these objectives, the climate data derived from climate simulations from the latest, state-of-the-art climate models participating in Phase Six of the Coupled Model Intercomparison Project (CMIP6) were used to drive the TRIPLEX-Mortality model. Specifically, we forecast changes in drought-induced tree mortality and corresponding changes in biomass carbon sink capacity across a range of radiative forcing scenarios (shared socioeconomic pathways; SSPs) developed for ScenarioMIP (O'Neill et al., 2016).

4.4. Methods and Data

4.4.1. TRIPLEX-Mortality model

The physiological process-based TRIPLEX-Mortality model was developed from the original TRIPLEX model (Peng et al., 2002). To date, the TRIPLEX model has been widely used to simulate and predict forest growth, carbon, and nitrogen dynamics of forests (Peng et al., 2002, 2009; Sun et al., 2008; Wang et al., 2012; Zhang et al., 2008; Zhou et al., 2005, 2008). To model drought-induced tree mortality and corresponding impacts on forest carbon dynamics, the advanced drought-induced physiological mortality mechanisms (i.e., hydraulic failure and carbon starvation) (Hartmann, 2015; McDowell et al., 2011, 2022; McDowell & Sevanto, 2010), has been successfully integrated into the TRIPLEX-Mortality model (Liu et al., 2021). To date, the TRIPLEX-Mortality model has been successfully validated against observations from permanent sample plots across Canada's boreal forests (Liu et al., 2021), offering good reliability in predicting drought-induced tree mortality and associated biomass carbon dynamics under both past and future climate change conditions. Some major processes (i.e., hydraulic failure and carbon starvation) of TRIPLEX-Mortality can be found in supplementary materials. More detailed information on model structure, function, and development can be found in Liu et al., (2021) and Peng et al., (2002) .

4.4.2. Forest stand, soil information and climate data used to initialize and drive the model

Required data for TRIPLEX-Mortality model initialization is as follows: forest stand type, forest stand age and tree species, average tree height, soil texture, and soil carbon content. Forest stand information used in this study (i.e., stand age and tree species) was derived from the remote sensing dataset generated by Beaudoin et al., (2014) (see Figure 4. S2). Soil information used in this study (i.e., soil texture and soil carbon content) was obtained from the datasets generated by Tarnocai & Lacelle, (1996) and Batjes, (2012) (see Figure 4. S3).

As a driving force, climate variables in the TRIPLEX-Mortality model primarily include mean monthly temperature, monthly precipitation, monthly mean relative humidity, and potential evapotranspiration (PET). Based on the data usability of the corresponding variables, we obtained the values for these variables from the mean values of 8 specific climate models (see Table 4.1)

outputs in the CMIP6 database (https://esgf-node.llnl.gov/search/cmip6/), using four SSPs (2015–2100) from ScenarioMIP (O'Neill et al., 2016). The SSP represents a range of future greenhouse gas emissions and land-use change scenarios estimated by comprehensive assessment models and based on various assumptions about economic growth, climate mitigation efforts, and global governance. The SSPs are used to generate different radiative forcing paths, and associated warming, up to the end of the 21st century. To consider a range of possible future climates, we use simulations from four SSPS from Tier 1 of ScenarioMIP: SSP1-2.6 (+2.6 Wm^{-2} unbalanced; low forced sustainability path), SSP2-4.5 (+4.5 Wm^{-2}; medium forced intermediate path), SSP3-7.0 (+7.0 Wm^{-2}; Mid-high forced path) and SSP5-8.5 (+8.5 Wm^{-2}; High-end forced path).

Table 4. 1. List of models from CMIP6 used to generate climate data in this study, along with each model's Equilibrium Climate Sensitivity (ECS; K/2xCO2) and reference for submission to CMIP6.

Model	ECS	References
BCC-CSM2-MR	3.1	(Wu et al., 2018)
CESM2	5.2	(Danabasoglu et al., 2019)
CESM2-WACCM	4.7	(Danabasoglu et al., 2019)
GFDL-ESM4	2.7	(Krasting et al., 2018)
MRI-ESM2-0	3.2	(Yukimoto et al., 2019)
CMCC-CM2-SR5	NA	(Lovato & Peano, 2020)
TaiESM1	4.4	(Lee & Liang, 2020)
FGOALS-f3-L	3.0	(Yu, 2019)

Note. ECS values are taken from (Pendergrass, 2019) and https://www.carbonbrief.org/cmip6-the-next-generation -of-climate-models-explained.

4.4.3. Analyses

For most analyses, we calculate anomalies and changes occurring by the end of the 21st century, 2050–2100, relative to a baseline drought-induced tree mortality of 1970-2020, which was simulated by Liu et al., 2022. Under review). This baseline allows us to evaluate the changes in tree mortality and the corresponding change in biomass carbon from climate change. To facilitate comparisons between model results and baseline tree mortality, all models are linearly interpolated to a new uniform 5 km spatial resolution. In addition, it is difficult to calculate the change ratio

between future tree mortality and baseline tree mortality because many areas used in calculating the baseline have no tree mortality. Therefore, in this study, we directly calculated the difference in absolute value between baseline and future tree mortality (i.e., SSPs tree mortality minus baseline tree mortality) to evaluate the difference between them. Given that many previous studies have shown differences in climatic conditions between the western region (i.e., the Yukon, the Northwest Territories, British Columbia, Alberta, Saskatchewan, and Manitoba) and the eastern region (i.e., Ontario, Quebec, New Brunswick, Newfoundland and Labrador, Prince Edward Island, and Nova Scotia) of Canada (Hogg et al., 2008; Wang et al., 2014) and these two regions have been widely used to compare the difference in tree mortality and related biomass changes (i.e., Ma et al., 2012; Peng et al., 2011). Similarly, in this study, we divided Canada's boreal forest into western and eastern regions. Moreover, to better examine the trend of drought-induced tree mortality with climate change, we also calculated drought-induced tree mortality between 2030 and 2100.

To identify trends in the annual tree mortality rate, and the biomass loss rate, we used a piecewise regression model to quantitatively identify turning points observed during the study period. The model was applied using the following formula (Piao et al., 2011; Toms & Lesperance, 2003; Wang et al., 2011; Zhang et al., 2013):

$$Y = \begin{cases} \beta_0 + \beta_1 x + \varepsilon x \leq \alpha \\ \beta_0 + \beta_1 x + \beta_2 (x - \alpha) + \varepsilon x > \alpha \end{cases} \quad (1)$$

Where x is the year; Y represents each variable (i.e., tree mortality rate, biomass loss rate); α is the estimated turning point of the variable change rate, which was determined by the least square error method. β_1 and $\beta_1 + \beta_2$ are the change rates before and after the turning point, respectively. ε is the residual error. A *t*-test was used to test the significance in single and piecewise regressions, while a P value < 0.05 was considered significant. Least squares linear regression was used to detect the trend of tree mortality. Similarly, a *t*-test was used to test the significance in these linear regressions, while a P value < 0.05 was considered significant.

The climate moisture index (CMI) has been widely used in the study of drought impacts on Canada's boreal ecosystem (Berner et al., 2017; D'Orangeville et al., 2018; Hogg et al., 2013; Ma

et al., 2012; Peng et al., 2011). The CMI was calculated as the balance of PET and precipitation over a period (CMI = precipitation - PET). In this study, the CMI index was used to evaluate drought conditions in the study area over the study period. A nonlinear mixed-effects model (see Eq. S9) was used to fit the relationship between mortality rate and CMI index.

4.5. Results

4.5.1. Mortality rates across the SSP scenarios

All four SSP scenarios show an increased drought-induced tree mortality rate by the end of the twenty-first century (Figure 4. 1a). Due to emissions beginning to slow or plateau in the more aggressive mitigation scenarios, SSP1-2.6 and SSP2-4.5, tree mortality trajectories across SSP scenarios vary most after 2050. For the period 2050-2100, annual average tree mortality for each SSP scenario is as follows: 4.2% ± 0.4% (SSP1-2.6); 4.8% ± 0.4% (SSP2-4.5), 5.7% ± 0.5% (SSP3-7.0), and 7.2% ± 0.4% (SSP5-8.5) (See Figure 4. 1b). In the SSP1-2.6 and SSP-4.5 scenarios, the increase in mortality rate is subtle, especially for SSP1-2.6, whereas in the SSP3-7.0 and SSP-8.5 scenarios, the increase in mortality is much more pronounced. In particular, the tree mortality of SSP5-8.5 not only increased significantly but also was higher than that of other scenarios. Overall, with the increase in radiative forcing for the different SSP scenarios (i.e., from SSP1-2.6 to SSP5-8.5), there was an increase in the tree mortality rate (Figure 4. 1b).

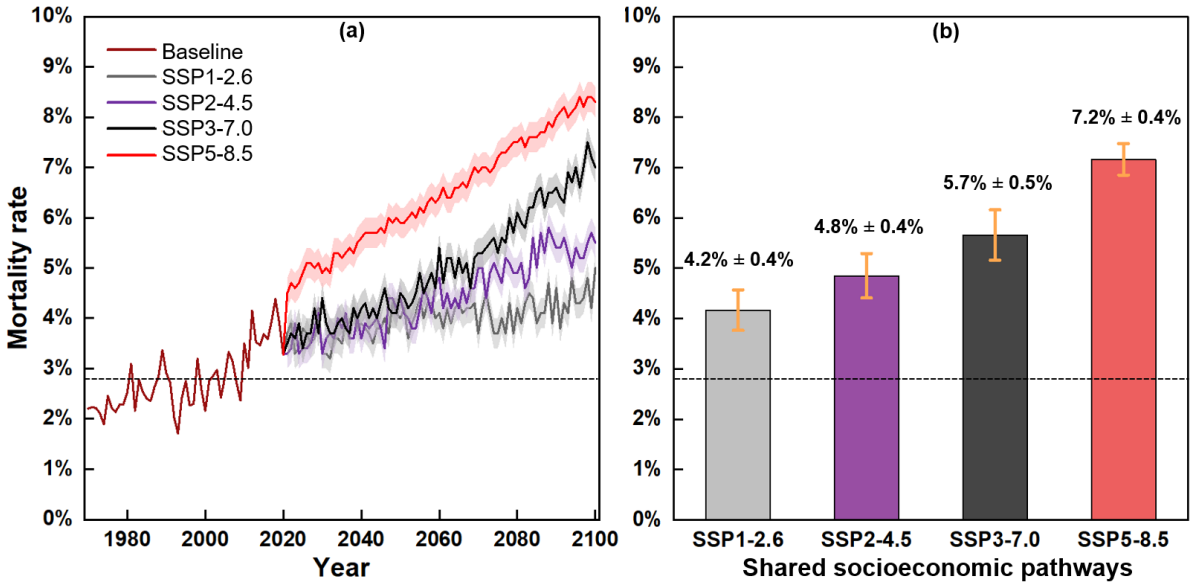

Figure 4. 1. Time series, showing annual average drought-induced tree mortality of Canada's boreal forest for the four SSP scenarios in the CMIP6 ensemble (a). The black dotted lines show the average tree mortality of the baseline (1970-2020). (b) shows the average drought-induced tree mortality over the period 2050-2100 for the four SSP scenarios, respectively. The color shade areas in (a) and error bars in (b) represent 95% confidence intervals.

4.5.2. Future tree mortality vs baseline mortality

We compared tree mortality in all SSP scenarios (2050-2100) with baseline tree mortality (1970-2020) spatially. Overall, a greater number of areas show higher tree mortality than baseline mortality with the increase in radiative forcing for the different SSP scenarios (i.e., from SSP1-2.6 to SSP5-8.5; see Figure 4. 2). For example, compared with the baseline, even under the most moderate climate change scenario (SSP1-2.6), the areas with increases in mortality (50%) are much greater than the areas with mortality decreases (12.4%; see Figures 4. 2a and 2b). Among these, the average tree mortality rate of over 32.2% area increased by more than 5.0% in the absolute value of tree mortality (i.e., SSPs tree mortality minus baseline tree mortality, see 2.3. Analyses), while only 3.8% of the area declined by more than 5.0%. Around 37.5% of areas show no changes in tree mortality between SSP1-2.6 and baseline tree mortality (Figure 4. 2a). In addition, we estimated the average changes in tree mortality absolute value between SSP1-2.6 tree mortality and baseline tree mortality in all western region areas as well as in all eastern region areas, respectively. The increase in tree mortality in the western region (2.25% on average) is much higher than that in the eastern region (0.12% on average).

The increase in tree mortality from the baseline was higher in the SSP2-4.5 scenario than in the SSP1-2.6 scenario (Figure 4. 2b). For example, under the SSP2-4.5 scenario, there are around 58.1% of areas show an increase in tree mortality, while only 9.1% of areas show a decrease in tree mortality (Figure 4. 2b). Among these areas, around 39.7% of areas increase by more than 5% in absolute value. In contrast, only 2.7% of areas decline by more than 5% in tree mortality. Additionally, under the SSP2-4.5 scenario, the areas that have no changes in tree mortality decrease (from 37.5% to 32.8%) compared with the SSP1-2.6 scenario. Similar to the SSP1-2.6 scenario, the increase in tree mortality absolute value in the western region area (2.91%) is much higher than in the eastern region (0.75%).

Compared with the SSP1-2.6 and SSP2-4.5 scenario, the difference between tree mortality and the baseline is further increased in SSP3-7.0, indicating that the risk of tree mortality increases. Under the SSP3-7.0 scenario, the areas (67.8%) that have an increase in tree mortality rate are much larger than the areas (5.7%) that have a decrease in tree mortality rate (Figure 2c). Among these, 48% of areas had absolute tree mortality that increased by over 5.0%, while only there was a decrease of only 0.9% of areas with absolute tree mortality over 5.0%. Notably, from the SSp3-7.0 scenario, no areas show a decrease that is more than 7.5% in the tree mortality rate for SSP3-7.0. In addition, the areas that show no change in tree mortality decreased compared to the SSP1-2.6 and SSP2-4.5 scenario. In this mid-to-high end forcing scenario (SSP3-7.0), both the magnitude of the increase in mortality and the increase in the area where it occurred is significant. In terms of mortality change in the western and eastern region, the increases in absolute tree mortality for both the western and eastern regions under the SSP3-7.0 scenario are much higher (3.71% for the west and 1.52% for the east) compared with SSP1-2.6 and SSP2-4.5 scenarios.

Compared with the SSP1-2.6, SSP2-4.5, and SSP3-7.0 scenarios, there are many more areas that show an increase in tree mortality rate compared to baseline tree mortality under the SSP5-8.5 scenario, indicating that the most significant increase in tree mortality occurs under this high-end forcing scenario (SSP5-8.5) (Figure 4. 2d). Specifically, only 2.3% of areas show a decrease in tree mortality, while nearly 82.8% of areas show an increase in tree mortality. There is almost no area that shows a decrease of at least 5.0% in absolute tree mortality, while around 66.2% of the area shows an increase of more than 5.0% in absolute mortality compared to the baseline tree mortality. Under the SSP5-8.5 scenario, only a small number of areas (15.1%) showed no change in tree mortality compared with the baseline. Although the increase in absolute tree mortality for the western region of the SSP5-8.5 scenario (3.79%) is almost equal to the SSP3-7.0 scenario, the increase in the eastern region (4.61%) is much higher than the SSP3-7.0 scenario (1.52%).

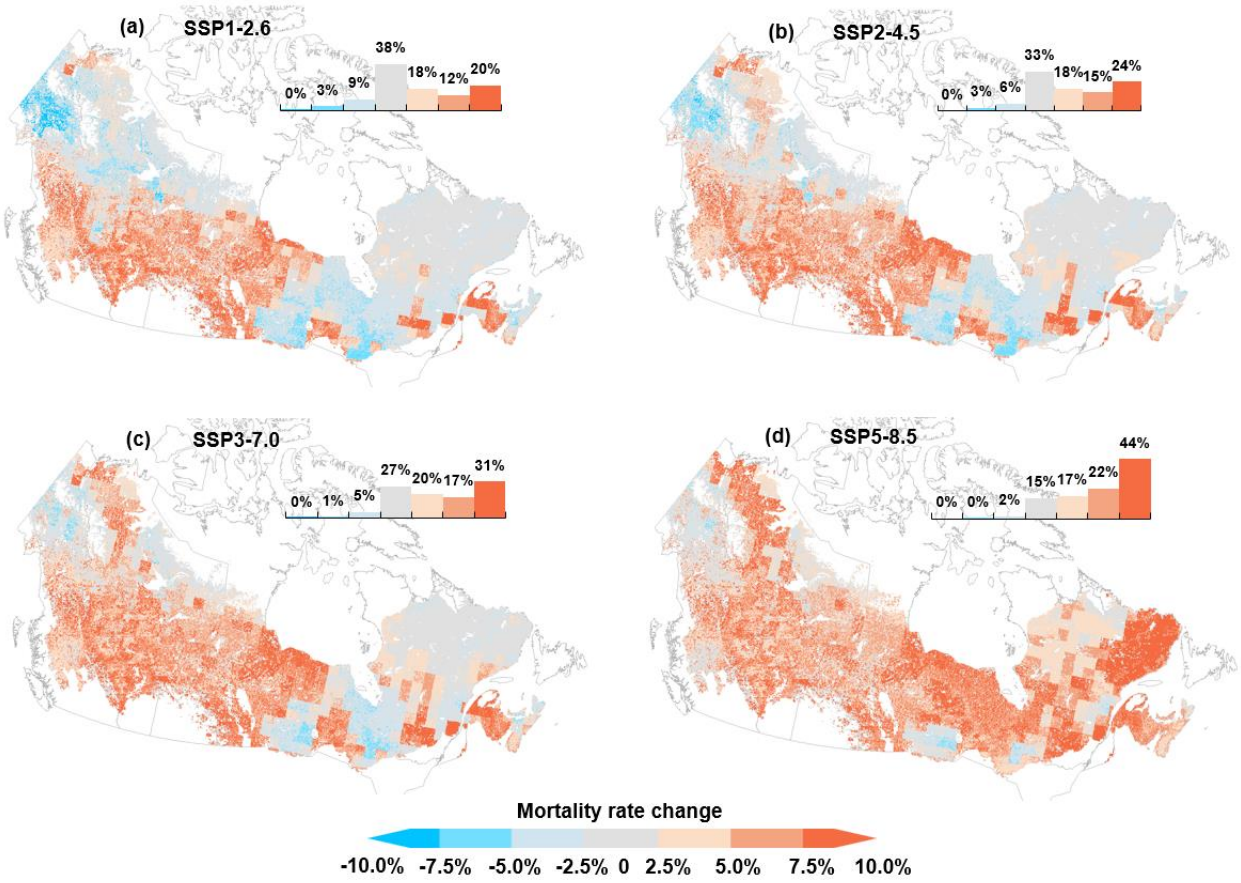

Figure 4. 2. The spatial distribution of changes in tree mortality for four SSP climate change scenarios (average mortality for the period 2050-2100 minus baseline mortality) compared with baseline mortality (1970-2020) (a for SSP1-2.6; b for SSP2-4.5; c for SSP3-7.0 and d for SSP5-8.5), respectively.

4.5.3. Mortality change trend across each scenario

Drought-induced tree mortality showed an overall increasing trend for all SSP scenarios (Figure 4. 1a). However, further analysis by using piecewise linear regression and a t-test on annual average tree mortality trends shows that trends in annual average tree mortality in each SSP scenario are not temporally homogeneous throughout the period (2030-2100, see Figure 4. 3). Specifically, the piecewise linear regression model detected different turning points for each SSP scenarios, due to variations in tree mortality trends in each scenario (Figure 4. 3). Among the different SSP scenarios, only SSP1-2.6 had a smaller slope for tree mortality after the turning point year than before. In each of the other SSP scenarios, the slope of the trend in tree mortality after the turning point year

is higher than before, indicating an acceleration in tree mortality after the turning point year. Although the slope of the annual tree mortality trend after the turning point year is only slightly higher than in the period before the turning point year under SSP5-8.5, the overall slope (i.e., the average of before and after the turning point year) of the annual tree mortality trend is the highest among all SSP scenarios (Figure 4. 3d). In general, tree mortality increases more rapidly as climate change intensifies.

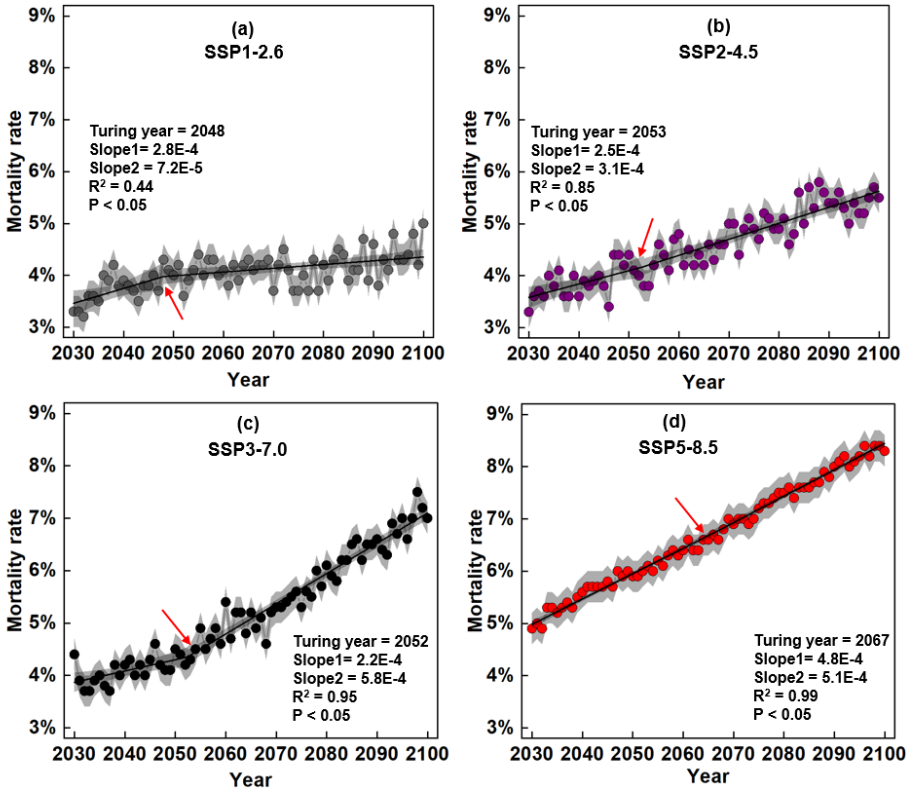

Figure 4. 3. Annual tree mortality under the four SSP scenarios. The gray and color shaded areas indicate 95% confidence intervals. Black solid lines show linear fitted data before and after the turning point (red arrows), using a piecewise linear regression model, respectively. Slope1 represents the trend slope over the period before the turning point year and slope2 represents the trend slope over the period after the turning point year.

Analysis of tree mortality rate trends based on linear least squares regression in conjunction with a t-test indicates that change trends in tree mortality rates were not spatially homogeneous and the areas with a significant increased trend ($P < 0.05$) in tree mortality increase across SSP1-2.6 to SSp5-8.5 scenario throughout 2050-2100 (Figure 4. 4). Under the SSP1-2.6 scenario, areas with a

significant increased trend (18.7%) are much higher than areas with significant decreased trend (5.2%; see Figure 4. 4a and b). Spatially, most areas (78.1%) that have an increased trend in tree mortality are located in the western region, while only 21.9% of areas with an increased trend in mortality are located in the eastern region (see Table 4. 2). Compared with the SSP1-2.6 scenario, there are more areas with a significant increased trend in tree mortality (from 18.7% to 33.1%), and there are fewer areas with a significant decreased trend (from 5.2% to 2.4%) under the SSP2-4.5 scenario. Spatially, similar to the SSP1-2.6 scenario, most areas that showed an increasing trend in tree mortality are located in the western region (68.85%) under the SSP2-4.5 scenario. However, compared to the SSP1-2.6 scenario, there are more areas with a significant increased trend in the eastern region (31.15%; see Table 4. 2). For the SSP3-7.0 scenario, 52.6% of areas show a significant increased trend in tree mortality and only 1.8% of areas show a significantly decreased trend in tree mortality. Specifically, the area (10.1%) that has a remarkably significant increased trend (the trend is over 2.4E-3; see Figure 4. 4) in tree mortality is around 10 times higher than the SSP1-2.6 scenario (0.9%) and over 3 times higher than the SSP2-4.5 scenario (2.9%). Although most of the areas with an increased trend in tree mortality are still in the western region (59.38%, see Table 4. S2), the areas with a significant increased trend in the eastern region have doubled compared with the SSP1-2.6 scenario and are also higher than the SPP2-4.5 scenario under the SSP3-7.0 scenario. Although the area with a significant increased rate of tree mortality under the SSP5-8.5 scenario is slightly less than the SSP3-7.0 scenario, the SSP5-8.5 scenario has the highest percentage of the area (10.6%) with a remarkably significant increased trend (the trend is over 2.4E-3; see Figure 4. 4) for increased tree mortality. For the SSP5-8.5, the percentage of areas with an increased trend in tree mortality in the western and eastern regions is almost equal (50.13% for the west and 49.87% for the east, see Table 4. S2). Among all SSP scenarios, the eastern region has the highest proportion of regions with a significant increased trend in tree mortality under the SSP5-8.5 scenario (see Table 4. S2).

Table 4. 2. The percentage of areas that have increased or decreased the trend in mortality and their locations.

SSP scenarios	Region	The percentage of area that has an increased trend in mortality	The percentage of area that has a decreased trend in mortality
SSP1-2.6	West	78.08%	56.96%

	East	21.92%	39.24%
SSP2-4.5	West	68.85%	60.00%
	East	31.15%	40.00%
SSP3-7.0	West	59.38%	21.43%
	East	40.63%	78.57%
SSP5-8.5	West	50.13%	80.00%
	East	49.87%	20.00%

Note: The percentages shown here are the ratio of areas with significant trends to the east and west, respectively

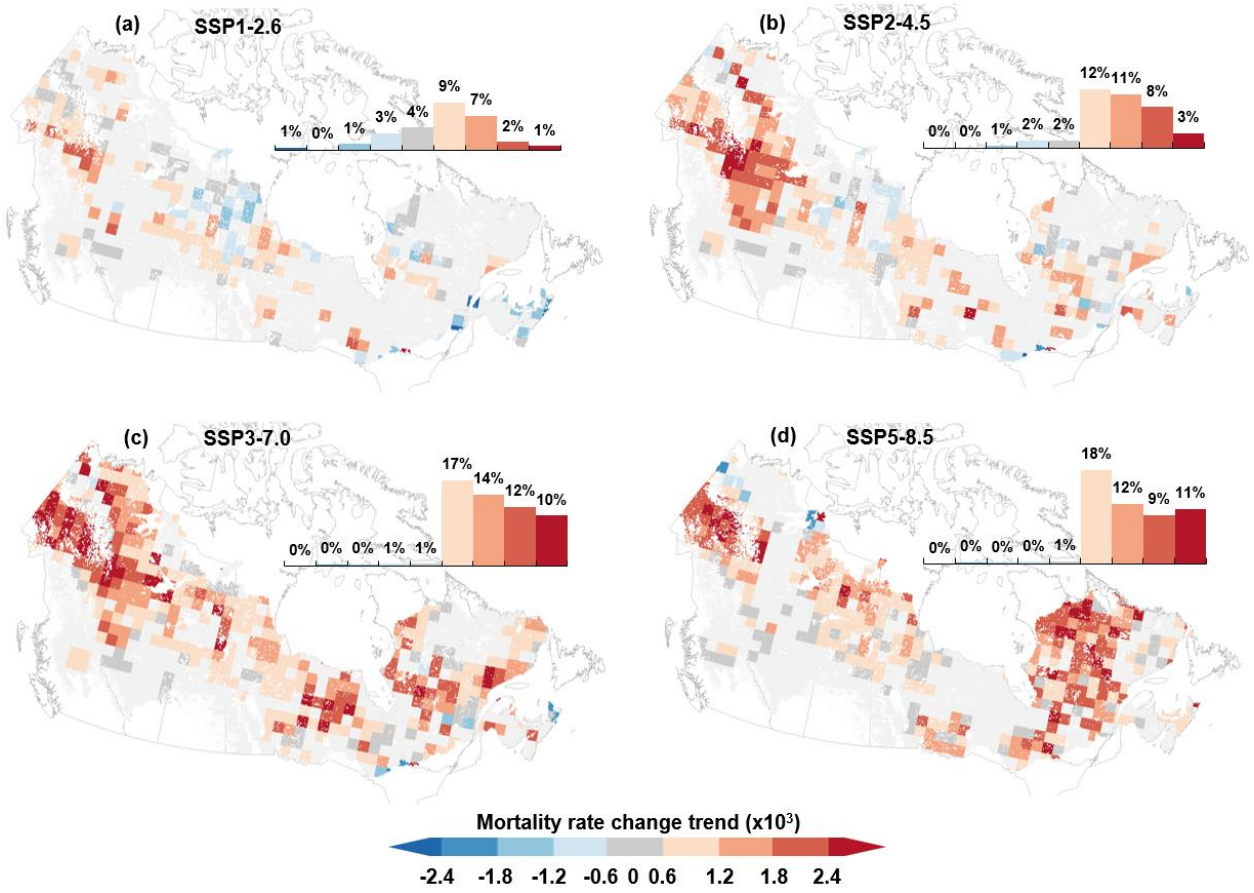

Figure 4. 4. The spatial distribution of tree mortality changes trend/slope ($P < 0.05$) from 2050 to 2100 by using linear least squares regression in conjunction with a t-test under the four SSP scenarios (a for SSP1-2.6; b for SSP2-4.5; c for SSP3-7.0 and d for SSP5-8.5), respectively.

4.5.4. Drought condition and its relationship with mortality across each SSP scenario

To evaluate drought conditions, we used CMI, which was calculated based on independent precipitation and PET data from SSP scenarios, to analyze the drought trends (2030-2100) of Canada's boreal forests. Statistical analysis using the linear least squares regression method in conjunction with a *t*-test, shows that Canada's boreal forested area experienced overall increasing trends in drought events for all SSP scenarios (Figure 4. 5a). And drought conditions increased with the increase in radiative forcing for the different SSP scenarios (i.e., from SSP1-2.6 to SSP5-8.5). We calculated the average CMI of the period before and after the turning point year for each SSP scenario. For SSP1-2.6, the average CMI for the period after and before the turning point year shows a slight difference(see Table 4. 3). However, for SSP2-4.5. SSP3-7.0 and SSP5-8.5 scenario, the CMI of the period after the turning point year is much higher than in the period before the turning point year (see Table 4. 3), showing more severe drought conditions for the period after the turning point year. These changes and trends in drought conditions, to some extent, are similar to changes and trends in tree mortality. Subsequently, a nonlinear mixed-effects model (see Supplementary Information and Eq. S9) was used to quantify the relationships between tree mortality rates and the CMI index for each SSP scenario. A significant negative relationship ($P < 0.05$) between CMI and tree mortality rates (see Fig. 4. 5b, c, d, e) was detected for all SSP scenarios. This negative relationship indicates higher tree mortality rates tended to occur at lower CMI values when drought was more severe.

Table 4. 3. Drought conditions (CMI index) before and after the turning point year for each SSP scenario, respectively.

Climate change senarios	SSP1-2.6		SSP2-4.5		SSP3-7.0		SSP5-8.5	
Time period	2030-2048	2048-2100	2030-2053	2053-2100	2030-2052	2052-2100	2030-2067	2067-2100
Average CMI (mm)	18.87	17.75	17.91	14.79	16.51	10.93	-154.82	-245.04

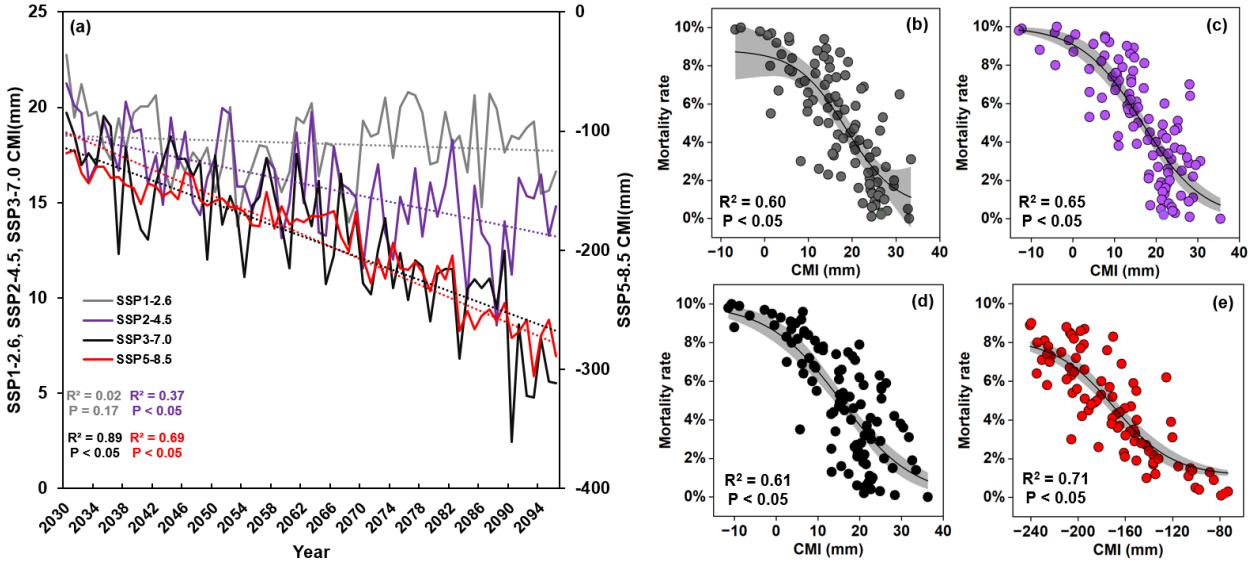

Figure 4. 5. Time series of annual average CMI for each SSP scenario (a). And the relationship between annual average CMI values and annual averaged tree mortality for the four SSP scenarios (b for SSP1-2.6; c for SSP2-4.5; d for SSP3-7.0 and e for SSP5-8.5), respectively. Gray shaded areas in (d) represent 95% confidence intervals of nonlinear regressions.

4.5.5. Reductions in biomass carbon sink caused by tree mortality under 4 SSP scenarios

Compared with baseline biomass carbon loss (0.46 ± 0.09 PgC year^{-1}), the biomass carbon loss for SSP1-2.6 is higher than the baseline by 61.2% and the SSP2-4.5 scenario is higher by 88.1%. For the SSP3-7.0 scenario, biomass carbon loss is more than twice as high as the baseline biomass carbon loss. For the most extreme warming scenario (SSP5-8.5), the biomass carbon loss (1.29 ± 0.05 Pg C year^{-1}) is nearly three times as high as the baseline biomass carbon loss. The increased drought-induced tree mortality of each SSP scenario results in a corresponding reduction in the biomass carbon sink (Figure 4. 6). With the increase in radiative forcing for SSP scenarios (i.e., from SSP1-2.6 to SSP5-8.5), there is an increase in biomass carbon sink reduction (Figure 4. 6). Specifically, for the SSP1-2.6 scenario, biomass reduction from 2050-2100 was estimated to be 4.83 ± 0.35 Mg ha^{-1} year^{-1}. This reduction multiplied by the area of Canada's boreal forests (310 Mha), results in a total biomass loss of approximately 1.50 ± 0.11 Pg year^{-1} throughout all boreal forest areas in Canada (see Figure 4. 6). This reduction in biomass is equivalent to a net decrease in the carbon sink of 2.41 ± 0.17 Mg C ha^{-1} year^{-1} (with a total of 0.7 ± 0.06 Pg C year^{-1}). The biomass reduction for the SSP2-4.5 scenario is higher by 24% than the SSP1-2.6 scenario (Figure

4. 6). Compared with the SSP1-2.6 and SSP2-4.5 scenario, the biomass reduction for the SSP3-7.0 scenario increased by 45% and 17%, respectively. Among all SSP scenarios, the SSP5-8.5 underwent the highest biomass loss. The biomass carbon sink loss (4.16 ± 0.15 Mg C ha^{-1} $year^{-1}$ with a total carbon loss of 1.29 ± 0.05 Pg C $year^{-1}$) under the SSP5-8.5 scenario, is the highest among all SSP scenarios. Spatially, although the biomass carbon loss in both western and eastern regions showed an overall increased trend following the increase in radiative forcing for SSP scenarios, the biomass carbon loss in the western region is still higher than that in the eastern region across all SSP scenarios (Figure 4. 6). Nevertheless, under the SSP5-8.5 scenario, the biomass carbon loss in the eastern region is the highest among all scenarios, and it is very close to the biomass carbon loss in the western region, indicating the eastern region is likely to experience a risk of carbon loss similar to the western region under this high-end forcing scenario.

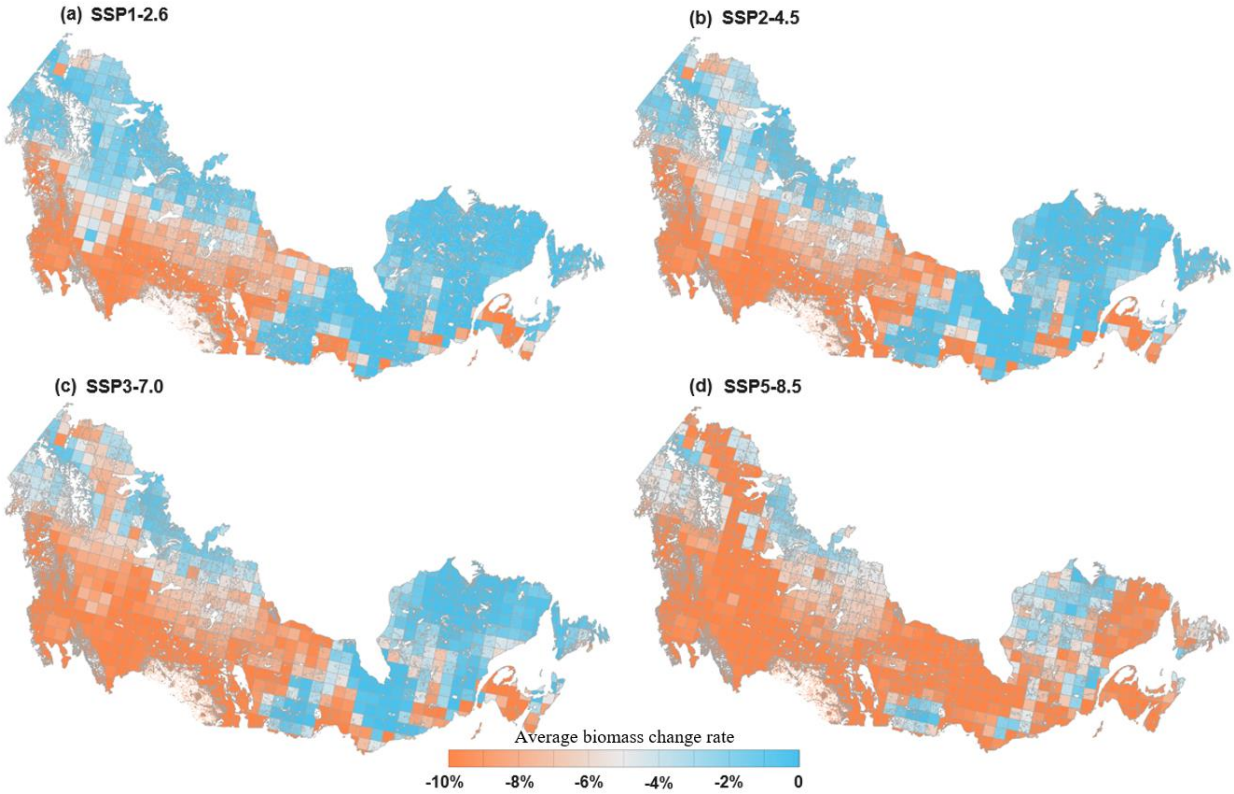

Figure 4. 6. Spatial distribution of annual biomass loss of Canada's boreal forest due to tree mortality over the period 2050-2100 under the four SSP scenarios, respectively.

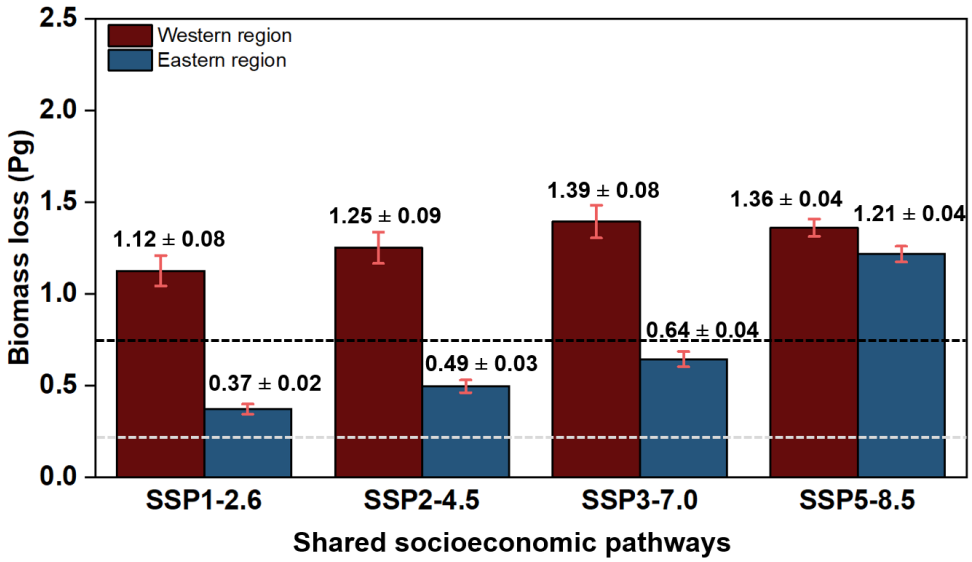

Figure 4. 3. The annual biomass loss of Canada's boreal forest due to tree mortality over the period 2050-2100 under the four SSP scenarios, respectively.

4.6. Discussion

4.6.1. Changes in tree mortality

Understanding how drought-induced tree mortality and its associated impacts on forest carbon sink dynamics will change in a warming world is an area of active research. This study, for the first time, provides a quantification of drought-induced tree mortality and its impacts on the carbon sink capacity in Canada's boreal forests by the end of the twenty-first century. The tree mortality trend increases following the increase in radiative forcing for the SSP scenarios (Figure 4. 1). With an increase in radiative forcing for SSP scenarios, the difference between predicted tree mortality and baseline tree mortality increased. As expected, this difference in SSP5-8.5 is the largest, followed by SSP3-7.0. With the increase in radiative forcing for SSP scenarios (across SSP1-2.6, SSP2-4.5, and SSP3-7.0 scenarios), the increase in tree mortality in the western region remains higher than the increase in the eastern region (see Figure 4. 2). In addition, with the increase in radiative forcing for SSP scenarios, the areas that have significant increased trends ($P < 0.05$) in tree mortality during the period 2050-2100 expand, while the areas that have significantly decreased trends ($P < 0.05$) in tree mortality decline. Especially those areas with a significant and rapid increased trend ($P < 0.05$, Trend > 2.4E-3) expanded following the increase in radiative forcing for SSP scenarios. These findings potentially confirm earlier studies that western Canada's boreal forest seems to be more sensitive to drought than eastern Canada's boreal forest (Peng et al., 2011). However, for the SSP5-8.5 scenario (High-end forced path), the increase in tree mortality in the eastern region attains the highest level of all SSP scenarios and is higher than in the western region. Therefore, if future change clime follows the most extreme pathway (SSP5-8.5), not only western Canada's boreal forests will be affected by climate change, but eastern Canada's boreal forests will be as well.

We detected turning point years (2048 for SSP1-2.6, 2053 for SSP2-4.5, 2052 for SSP3-70, and 2067 for SSP5-8.5) in time series of tree mortality rates for all SSP scenarios by using the piecewise linear regression model (Figure 4. 3). For the SSP1-2.6 scenario, after the turning point year, the increased trend in tree mortality slowed down, while for the SSP2-4.5, SSP3-7.0, and SSP5-8.5 scenario, the tree mortality trend after the turning point year is higher than that in the period before the turning point year. The results of variation in tree mortality change trend across

SSP scenarios demonstrate the clear benefits of greenhouse gas mitigation for reducing climate change forced increases in drought stress on the health of Canada's boreal forest ecosystem.

We used a CMI index that was calculated from independent climate data to evaluate drought conditions during the study period across the Canada boreal forest. Detected anomalies and changes in drought conditions are well supported by previous studies (i.e., Cook et al., 2020; Trenberth et al., 2014). In parallel, these anomalies and changes in drought conditions could potentially explain changes in tree mortality across SSP scenarios for several reasons. First, we detected an increase in drought conditions across SPP1-2.6 to SPP5-8.5 scenarios and an acceleration in drought conditions under all scenarios, which is consistent with the increase and accelerations detected in tree mortality rate (Figure 4. 5a and Table 4. 3). Second and most importantly, a significantly negative relationship between the CMI index and mortality was detected across all scenarios (Figure 4. 5b, c, d, e)

4.6.2. Changes in biomass carbon sink capacity

Increased tree mortality results in corresponding biomass loss. Similar to tree mortality, biomass loss increased following the increase in radiative forcing for SSP scenarios (Figure 4. 6). All SSP scenarios show a higher amount of biomass loss than the baseline amount of biomass loss and the SPP5-8.5 scenario shows the biggest difference from baseline (higher by around 170%). This large biomass loss throughout the entire Canadian boreal forest region can result in a significant reduction in its carbon sink capacity. If future climate change follows the high-end forcing pathway (SSP5-8.5 scenario), Canada's boreal forest carbon sink could be severely diminished over the next century, causing positive feedback on global warming. Previous studies indicated that western Canada's boreal forests may have a higher risk than the eastern region to become net carbon sources due to accelerated drought under future climate change (Ma et al., 2012). This study potentially confirms these previous implications, as the results showed that the carbon loss in the western region is higher than that in the eastern region for the SSP1-2.6, SSP2-4.5 and SSP3-7.0 scenarios (Figure 4. 6b). However, for the SSP5-8.5 scenario, the biomass carbon loss in the eastern region increased significantly. If future climate change follows the high-end forcing pathway (SSP5-8.5 scenario), eastern Canada's boreal forests also face the loss of significant carbon sinks.

4.6.3. Limitations and uncertainties

Process-based models provide a useful tool for understanding and forecasting the impact of changing environments on tree mortality. To date, numerous empirical measurements and mechanistic explorations make it possible to model the coupling between carbon and water states of trees during drought on both short and long-time scales, allowing mechanistically constrained parameterization and large scaling potential (De Kauwe et al., 2020; McDowell et al., 2022). Nevertheless, some modeling challenges remain for those processes that are represented, partly due to the poor understanding of the interactive mechanisms of drought-induced tree mortality (Choat et al., 2018; McDowell et al., 2013). Furthermore, some processes (i.e., legacy effect) that might be critical to quantifying tree mortality and its impacts on carbon dynamics are not yet well understood (Kannenberg et al., 2020). Therefore, although the TRIPLEX-Mortality model has been validated across Canada's boreal forest by using long-term forest permanent sampling plots (Liu et al., 2021), modeling results may have uncertainties for making future predictions due to the failure to fully capture these interdependent and critical processes. Another source of uncertainty is the absence of acclimation in our model. This is mainly due to the lack of knowledge of what parameters acclimate and at what rate under future climate change (McDowell et al., 2022). In model prediction, the values of key parameters are based on historical empirical values, which may cause uncertainty to model simulation results under a changing future climate. Finally, numerous studies indicated that drought can promote the effects of many other forest disturbances, such as insect outbreaks and wildfires (i.e., Seidl & Rammer, 2017). These disturbances, however, can also affect the carbon sequestration capacity of boreal forests (Kurz, Dymond, et al., 2008; Liu et al., 2019, 2020). Therefore, the contribution of drought to other disturbances should also be taken into account when quantifying the impact of drought on the forest carbon sink, otherwise, the quantification of drought impact will be underestimated.

4.7. Conclusion

This study used the state-of-the-art process-based tree mortality model, and the latest climate model projections of CMIP6, combined with other soil and forest information, to forecast the likelihood of drought-induced tree mortality and its impacts on Canada's boreal biomass carbon sinks by the end of the twenty-first century. We estimate average annual tree mortality to range

from 4.2% ± 0.4% to 7.2% ± 0.4% during 2050-2100. There is an increase trend in this increased drought-induced tree mortality following the increase in radiative forcing for SSP scenarios and peaked at the SSP5-8.5 scenario. The spatial extent of increased drought-induced tree mortality increases under the higher forcing and warming scenarios, especially for the western region of Canada. This increased tree mortality can result in a huge reduction (0.7 ± 0.06 Pg C year^{-1} ~1.29 ± 0.05 Pg C year^{-1}) in the biomass carbon sink capacity of Canada's boreal forest. Similar to tree mortality, the spatial extent of reduction in biomass loss increases under the higher forcing and warming scenarios, especially for the western region of Canada. If future climate change follows the high-end forcing pathway (SSP5-8.5 scenario), there is, however, a great reduction in biomass carbon sink in the eastern region. Overall, Canada's boreal forest has a significant risk to lose its role as a robust carbon sink under future climate change. This requires adaptation measures to reduce the risk and increased severity of drought forced by climate change to ensure the future fate of forest ecosystems.

4.8. Supplementary Information for

4.8.1. TRIPLEX-Mortality model

4.8.1.1. Hydraulic failure (HF)

The TRIPLEX-Mortality model is designed to simulate soil water pools that account for monthly water loss through transpiration and evaporation, soil water content and snow water content. When monthly mean air temperature is less than 0°C, total monthly precipitation is designated as snow (Parton et al., 1993; Parton et al., 1987). The water balance (L_w) is calculated as a function of water inputs and outputs as follows (Peng et al., 2002):

$$\Delta L_w = R - T - E - L \quad (4.\ 1)$$

R is rainfall (cm), and T, E and L represent transpiration (cm), evaporation (cm) and leached water (cm), respectively.

The physiological HF mechanism represents the complete loss of water transport to the canopy resulting from xylem embolism. During drought events, as transpiration persists, the soil water

potential (SWP, in MPa) dramatically declines below the air entry pressure. The hydraulic connection between roots and soil is consequently severed, and HF subsequently takes place (Plaut et al., 2012). Based on soil water conditions, SWP is calculated using the reference soil water potential of saturated soil ($swps$, in MPa), the volumetric saturation (vs) in soil pores and the soil attribution parameter (λ) as follows (Oleson et al., 2010):

$$SWP = swps * vs^{-\lambda} \quad (4.\ 2)$$

Based on the Community Land Model (CLM) (Oleson et al., 2010), Eq. 4. 3 is used to calculate vs, where t is the thickness of the topsoil layer; s (mm^3) is the saturated volumetric water content of the topsoil layer; P_{liq} is the density of liquid water; and W_{liq} is the mass of liquid water of the topsoil layer.

$$vs = \frac{1}{ts}\left[\frac{W_{liq}}{P_{liq}}\right] \quad (4.\ 3)$$

The $swps$ is correlated to the soil organic matter fraction (f), the saturated organic matter matric potential (swp_{om}) and the saturated mineral soil matric potential (swp_{sat}) as follows:

$$swps = (1-f)swp_{sat} + f swp_{om} \quad (4.\ 4)$$

The loss of xylem conductivity along with a decrease in the xylem water potential is represented by the PLC index, which is plotted against pressure and fitted to a Weibull function to generate a vulnerability curve (Neufeld et al., 1992; Rosner et al., 2019). Based on the research by (Plaut et al., 2012), the root water potential is assumed to be equal to the SWP.

$$PLC = 100\left(1 - e^{\left(-\frac{-swp}{b}\right)^c}\right) \quad (4.\ 5)$$

where b is the critical SWP that results in a 63% reduction in conductivity, and c is a shape parameter (Neufeld et al., 1992; Pammenter & Van der Willigen, 1998; Sperry & Tyree, 1988).

4.8.1.2. Carbon starvation (CS)

Plants must regulate multiple demands on stomatal control during drought events where a decrease in water availability will promote HF. And a decrease in stomatal conductance (G_s) will reduce the risk of HF but subsequently limit CO_2 assimilation into leaves increasing the risk of CS (Damour et al., 2010; Plaut et al., 2012). The response of G_s to drought varies across the isohydric-anisohydric continuum of hydraulic strategies (Martínez-Vilalta et al., 2014). For this hydraulic strategy continuum, the canopy scale (G_s) simulation has been adapted based on models developed by (Buckley et al., 2003) and (Gao et al., 2002) as follows:

$$G_s = (1 - PLC)/(VPD * p)(SWP - \Psi_l) \quad (4.\ 6)$$

where Ψ_l (MPa) is the leaf water potential (LWP), VPD (mb) is the vapor pressure deficit of the canopy and p is a coefficient. Eq. 6 indicates that mortality may increase when drought causes a sustained decrease in the soil water potential, while an increase in VPD can potentially be considered the greatest threat to survival because increasing global temperatures are driving a chronic increase in the VPD despite concurrent increases in specific humidity (Williams et al., 2013).

In TRIPLEX1.0, gross primary productivity (GPP, in t ha^{-1}) is calculated as a function of the received photosynthetically active radiation (PAR) modified by the leaf area index (LAI), forest age (f_a), monthly mean air temperature (f_t), soil drought (f_w) and the percentage of frost days within a period of a month (f_d). k is a conversion constant (Peng et al., 2002). Stomatal conductance (G_s) is used as a limiting factor of GPP.

$$GPP = kI_m LAI f_a f_t f_w f_d G_s \quad (4.\ 7)$$

We adapted the original NSC submodel from the RHESSys process-based model ((Tague et al., 2013) and then integrated this model into the TRIPLEX-Mortality model to estimate dynamic NSC pools (Fig. 4. S1). The NSC pool maintains a net balance between carbohydrate allocation and consumption. Under normal conditions, it is assumed that a portion of carbohydrates (α, see Table 2. S1) is allocated to the NSC pool until the total NSC reaches a threshold ($P_{threshold}$, see Table 2. S1) percentage of the total aboveground biomass (Fisher et al., 2010; Genet et al., 2009; Gruber et

al., 2012). The remaining carbohydrate is then transferred to the structural carbon pool. During drought events, in conjunction with a rapid decline in productivity, if the ratio of leaves to aboveground carbon falls below 0.05, a value that derives from (Callaway et al., 1994) and (Tague et al., 2013) or if the climate moisture index is less than -20, trees will access the NSC pool to maintain respiration requirements and restore their hydraulic function and leaf biomass.

$$NSC = NPP * \alpha - C_m - C_s \quad (4.\ 8)$$

where C_m represents the carbohydrate consumption from NSC to support basic metabolism, and C_s is the carbohydrate consumption from NSC that is transferred to structural carbon.

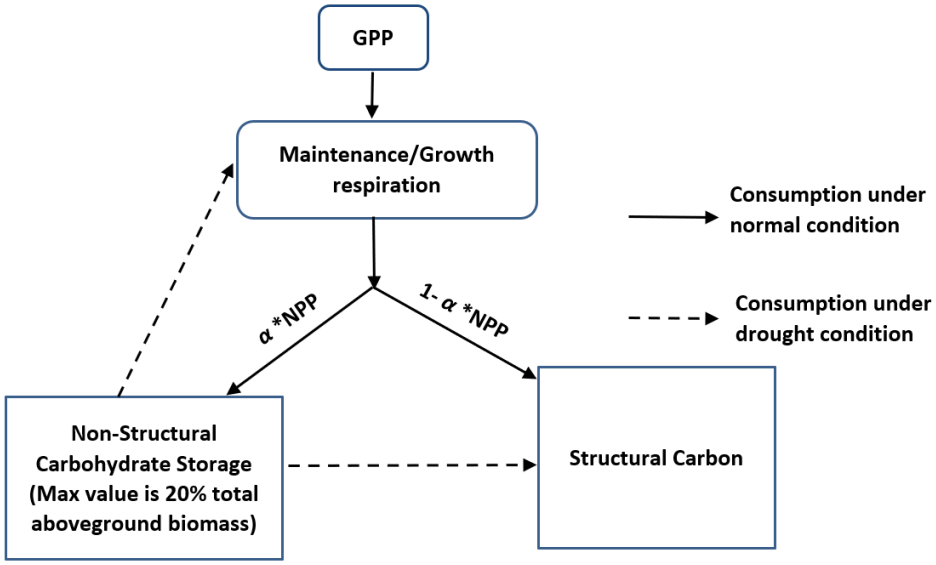

Figure 4. S1. The new carbon allocation mechanisms provided in the TRIPLEX-Mortality model. GPP, NPP and α represent gross primary production, net primary productivity and a percentage for the net primary productivity transfer to the non-structural carbon pool.

4.8.2. Forest stand, soil information

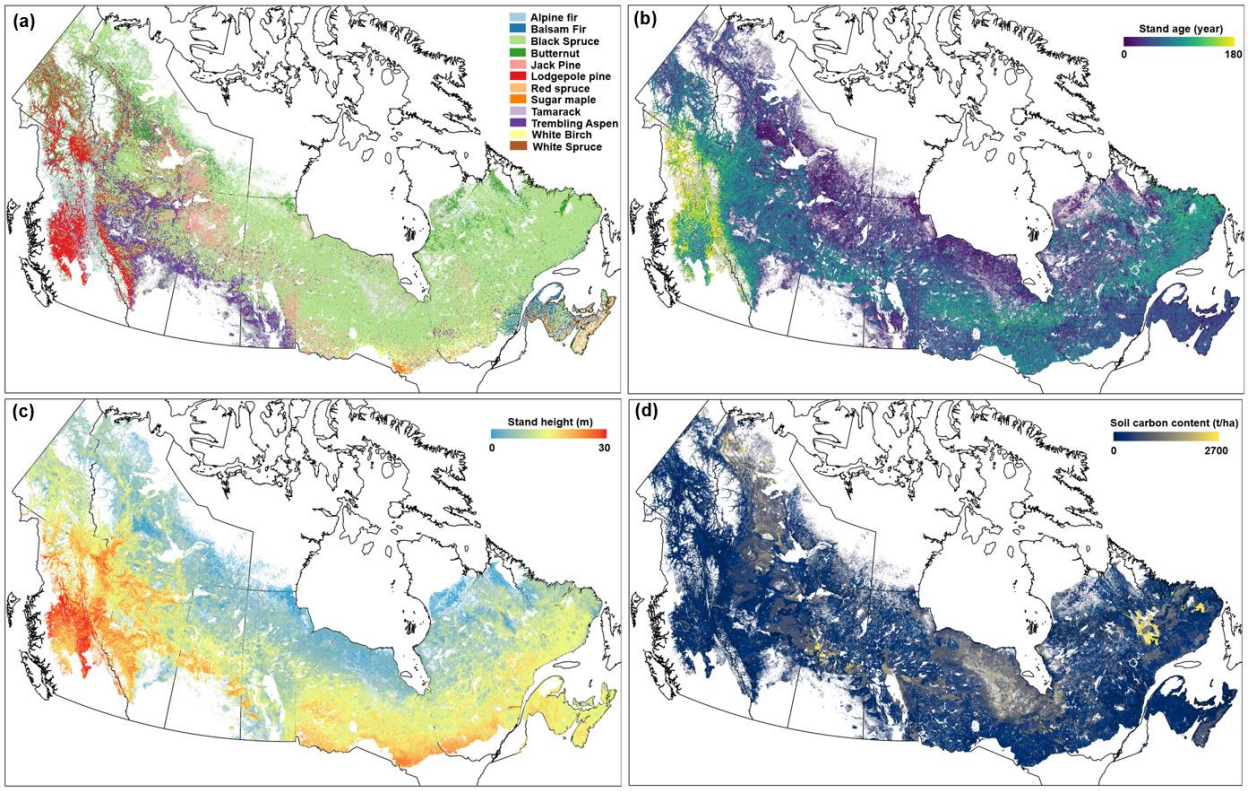

Figure 4. S2. The dominate tree species in each simulation grid (a). Forest stand age of the study area in each simulation grid (b). Forest stand height of the study area in each simulation grid (c). Soil carbon content of the study area (d). Data derived from Beaudoin et al., (2014).

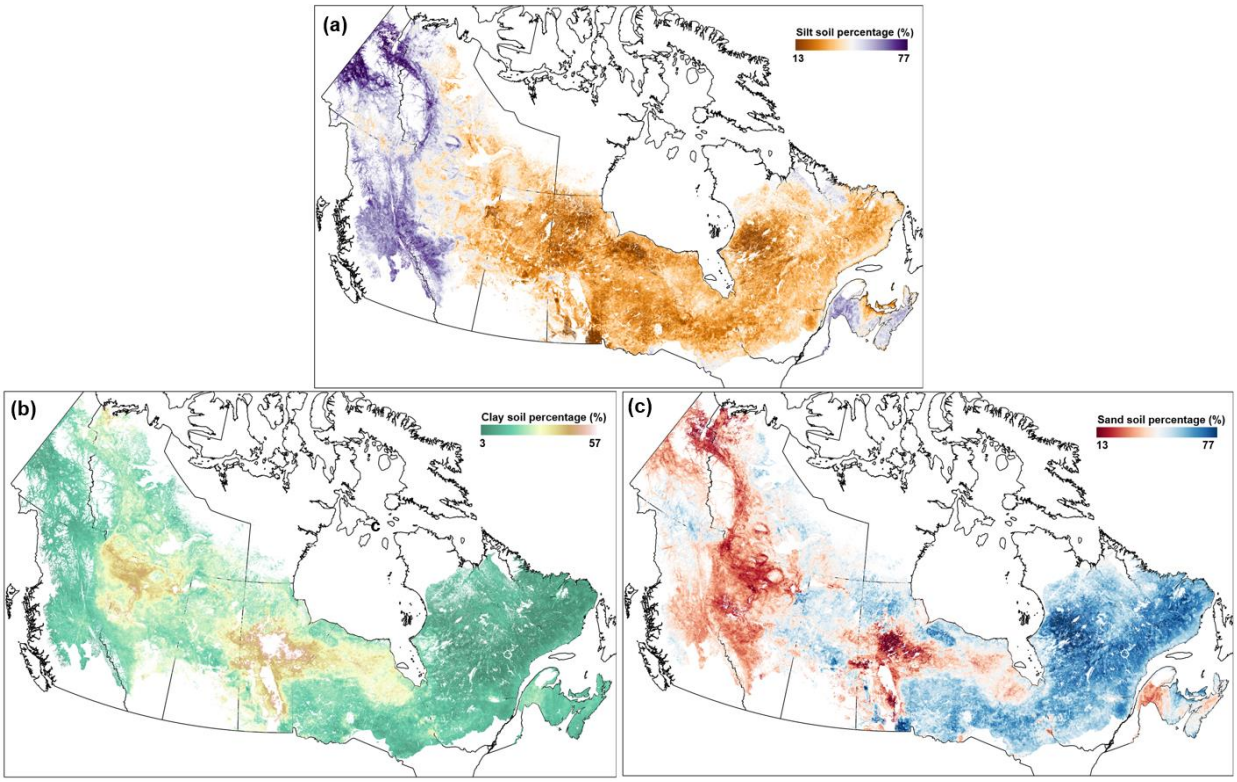

Figure 4. S3. Soil texture map of the study area. Silt soil percentage (a). Clay soil percentage (b). Sand soil percentage (d). Data derived from Tarnocai & Lacelle., (1996) and Batjes et al., (2012)

4.8.3. Nonlinear mixed-effects model

The rate of tree mortality was regressed as a function of drought indices (i.e., CMI) to test for significant trends. We used the following nonlinear mixed-effects model:

$$y = A1 + \frac{A2 - A1}{1 + 10^{(LOGx0 - x)p}} \quad (4.\ 9)$$

where y is tree mortality rate, and x represents the CMI values. $A1$, $A2$, $LOGx0$, and p are model parameters.

Table 4. S1. Fixed effects of the linear mixed models (Eq. S4. 9) that describe the relationships between the rate of tree mortality and drought indices under each climate change scenario.

Scenarios	$A1$	$A2$	$LOGx0$	p	P value	R^2

SSP1	0.00541	0.08819	18.6546	-0.0767	< 0.05	0.61
SSP2	0	0.1	16.6232	-0.0594	< 0.05	0.64
SSP3	0	0.1	15.4189	-0.0498	< 0.05	0.60
SSP5	0.0111	0.08181	-169.405	-0.0174	< 0.05	0.71

4.9. References

Adams, H. D., Williams, A. P., Xu, C., Rauscher, S. A., Jiang, X., & McDowell, N. G. (2013). Empirical and process-based approaches to climate-induced forest mortality models. *Frontiers in Plant Science*, *4*(November), 1–5. https://doi.org/10.3389/fpls.2013.00438

Allen, C. D., Macalady, A. K., Chenchouni, H., Bachelet, D., McDowell, N., Vennetier, M., Kitzberger, T., Rigling, A., Breshears, D. D., Hogg, E. H. (Ted., Gonzalez, P., Fensham, R., Zhang, Z., Castro, J., Demidova, N., Lim, J. H., Allard, G., Running, S. W., Semerci, A., & Cobb, N. (2010). A global overview of drought and heat-induced tree mortality reveals emerging climate change risks for forests. *Forest Ecology and Management*, *259*(4), 660–684. https://doi.org/10.1016/j.foreco.2009.09.001

Batjes, N. H. (2012). *ISRIC-WISE derived soil properties on a 5 by 5 arc-minutes global grid (ver. 1.2)*. ISRIC-World Soil Information.

Beaudoin, A., Bernier, P. Y., Guindon, L., Villemaire, P., Guo, X. J., Stinson, G., Bergeron, T., Magnussen, S., & Hall, R. J. (2014). Mapping attributes of Canada's forests at moderate resolution through kNN and MODIS imagery. *Canadian Journal of Forest Research*, *44*(5), 521–532. https://doi.org/10.1139/cjfr-2013-0401

Berner, L. T., Law, B. E., & Hudiburg, T. W. (2017). Water availability limits tree productivity, carbon stocks, and carbon residence time in mature forests across the western US. *Biogeosciences*, *14*(2), 365–378. https://doi.org/10.5194/bg-14-365-2017

Brandt, J. P., Flannigan, M. D., Maynard, D. G., Thompson, I. D., & Volney, W. J. A. (2013). An introduction to Canada's boreal zone: Ecosystem processes, health, sustainability, and environmental issues. *Environmental Reviews*, *21*(4), 207–226. https://doi.org/10.1139/er-2013-0040

Breshears, D. D., Carroll, C. J. W., Redmond, M. D., Wion, A. P., Allen, C. D., Cobb, N. S., Meneses, N., Field, J. P., Wilson, L. A., Law, D. J., McCabe, L. M., & Newell-Bauer, O. (2018). A Dirty Dozen Ways to Die: Metrics and Modifiers of Mortality Driven by Drought and Warming for a Tree Species. *Frontiers in Forests and Global Change*, *1*(October).

https://doi.org/10.3389/ffgc.2018.00004

Buckley, T. N., Mott, K. A., & Farquhar, G. D. (2003). A hydromechanical and biochemical model of stomatal conductance. *Plant, Cell and Environment*, *26*(10), 1767–1785. https://doi.org/10.1046/j.1365-3040.2003.01094.x

Callaway, R. M., DeLucia, E. H., & Schlesinger, W. H. (1994). Biomass allocation of montane and desert ponderosa pine: An analog for response to climate change. *Ecology*, *75*(5), 1474–1481. https://doi.org/10.2307/1937470

Choat, B., Brodribb, T. J., Brodersen, C. R., Duursma, R. A., López, R., & Medlyn, B. E. (2018). Triggers of tree mortality under drought. *Nature*, *558*(7711), 531–539. https://doi.org/10.1038/s41586-018-0240-x

Cook, B. I., Mankin, J. S., Marvel, K., Williams, A. P., Smerdon, J. E., & Anchukaitis, K. J. (2020). Twenty-First Century Drought Projections in the CMIP6 Forcing Scenarios. *Earth's Future*, *8*(6), 1–20. https://doi.org/10.1029/2019EF001461

Cruz, J. L., Alves, A. A. C., LeCain, D. R., Ellis, D. D., & Morgan, J. A. (2016). Elevated CO2 concentrations alleviate the inhibitory effect of drought on physiology and growth of cassava plants. *Scientia Horticulturae*, *210*, 122–129. https://doi.org/10.1016/j.scienta.2016.07.012

D'Orangeville, L., Houle, D., Duchesne, L., Phillips, R. P., Bergeron, Y., & Kneeshaw, D. (2018). Beneficial effects of climate warming on boreal tree growth may be transitory. *Nature Communications*, *9*(1), 1–10. https://doi.org/10.1038/s41467-018-05705-4

Damour, G., Simonneau, T., Cochard, H., & Urban, L. (2010). An overview of models of stomatal conductance at the leaf level. *Plant, Cell and Environment*, *33*(9), 1419–1438. https://doi.org/10.1111/j.1365-3040.2010.02181.x

De Kauwe, M. G., Medlyn, B. E., Ukkola, A. M., Mu, M., Sabot, M. E. B., Pitman, A. J., Meir, P., Cernusak, L., Rifai, S. W., Choat, B., Tissue, D. T., Blackman, C. J., Li, X., Roderick, M., & Briggs, P. R. (2020). Identifying areas at risk of drought-induced tree mortality across South-Eastern Australia. *Global Change Biology*, *26*(10), 5716–5733. https://doi.org/10.1111/gcb.15215

Fisher, J. B., Sitch, S., Malhi, Y., Fisher, R. A., Huntingford, C., & Tan, S.-Y. (2010). Carbon cost of plant nitrogen acquisition: A mechanistic, globally applicable model of plant nitrogen uptake, retranslocation, and fixation. *Global Biogeochemical Cycles*, *24*(1). https://doi.org/10.1029/2009gb003621

Gao, Q., Zhao, P., Zeng, X., Cai, X., & Shen, W. (2002). A model of stomatal conductance to quantify the relationship between leaf transpiration, microclimate and soil water stress. *Plant,*

Cell and Environment, *25*(11), 1373–1381. https://doi.org/10.1046/j.1365-3040.2002.00926.x

Genet, H., Bréda, N., & Dufrêne, E. (2009). Age-related variation in carbon allocation at tree and stand scales in beech (Fagus sylvatica L.) and sessile oak (Quercus petraea (Matt.) Liebl.) using a chronosequence approach. *Tree Physiology*, *30*(2), 177–192. https://doi.org/10.1093/treephys/tpp105

Gruber, A., Pirkebner, D., Florian, C., & Oberhuber, W. (2012). No evidence for depletion of carbohydrate pools in Scots pine (Pinus sylvestris L.) under drought stress. *Plant Biology*, *14*(1), 142–148. https://doi.org/10.1111/j.1438-8677.2011.00467.x

Gustafson, E. J., & Sturtevant, B. R. (2013). Modeling Forest Mortality Caused by Drought Stress: Implications for Climate Change. *Ecosystems*, *16*(1), 60–74. https://doi.org/10.1007/s10021-012-9596-1

Hartmann, H. (2015). Carbon starvation during drought-induced tree mortality – are we chasing a myth? In *Journal of Plant Hydraulics* (Vol. 2, Issue 0, p. 005). https://doi.org/10.20870/jph.2015.e005

Hogg, E. H., Barr, A. G., & Black, T. A. (2013). A simple soil moisture index for representing multi-year drought impacts on aspen productivity in the western Canadian interior. *Agricultural and Forest Meteorology*, *178–179*, 173–182. https://doi.org/10.1016/j.agrformet.2013.04.025

Hogg, E. H., Brandt, J. P., & Michaelian, M. (2008). Impacts of a regional drought on the productivity, dieback, and biomass of western Canadian aspen forests. *Canadian Journal of Forest Research*, *38*(6), 1373–1384. https://doi.org/10.1139/X08-001

Humphrey, V., Zscheischler, J., Ciais, P., Gudmundsson, L., Sitch, S., & Seneviratne, S. I. (2018). Sensitivity of atmospheric CO2 growth rate to observed changes in terrestrial water storage. *Nature*, *560*(7720), 628–631. https://doi.org/10.1038/s41586-018-0424-4

Kannenberg, S. A., Schwalm, C. R., & Anderegg, W. R. L. (2020). Ghosts of the past: how drought legacy effects shape forest functioning and carbon cycling. *Ecology Letters*, *23*(5), 891–901. https://doi.org/10.1111/ele.13485

Korzukhin, M. D., Ter-Mikaelian, M. T., & Wagner, R. G. (1996). Process versus empirical models: which approach for forest ecosystem management? *Canadian Journal of Forest Research*, *26*(5), 879–887.

Kurz, W. A., Dymond, C. C., Stinson, G., Rampley, G. J., Neilson, E. T., Carroll, A. L., Ebata, T., & Safranyik, L. (2008). Mountain pine beetle and forest carbon feedback to climate change.

Nature, *452*(7190), 987–990. https://doi.org/10.1038/nature06777

Kurz, W. A., Stinson, G., Rampley, G. J., Dymond, C. C., & Neilson, E. T. (2008). Risk of natural disturbances makes future contribution of Canada's forests to the global carbon cycle highly uncertain. *Proceedings of the National Academy of Sciences of the United States of America*, *105*(5), 1551–1555. https://doi.org/10.1073/pnas.0708133105

Liu, Q., Peng, C., Schneider, R., Cyr, D., Liu, Z., Zhou, X., & Kneeshaw, D. (2021). TRIPLEX-Mortality model for simulating drought-induced tree mortality in boreal forests: Model development and evaluation. *Ecological Modelling*, *455*. https://doi.org/10.1016/j.ecolmodel.2021.109652

Liu, Z., Peng, C., De Grandpré, L., Candau, J. N., Work, T., Huang, C., & Kneeshaw, D. (2019). Simulation and Analysis of the Effect of a Spruce Budworm Outbreak on Carbon Dynamics in Boreal Forests of Quebec. *Ecosystems*, *22*(8), 1838–1851. https://doi.org/10.1007/s10021-019-00377-7

Liu, Z., Peng, C., De Grandpré, L., Candau, J. N., Work, T., Zhou, X., & Kneeshaw, D. (2020). Aerial spraying of bacterial insecticides to control spruce budworm defoliation leads to reduced carbon losses. *Ecosphere*, *11*(1). https://doi.org/10.1002/ecs2.2988

Luo, Y., & Chen, H. Y. H. (2013). Observations from old forests underestimate climate change effects on tree mortality. *Nature Communications*, 1–6. https://doi.org/10.1038/ncomms2681

Luo, Y., & Chen, H. Y. H. (2015). Climate change-associated tree mortality increases without decreasing water availability. In *Ecology Letters* (Vol. 18, Issue 11, pp. 1207–1215). https://doi.org/10.1111/ele.12500

Ma, Z., Peng, C., Zhu, Q., Chen, H., Yu, G., Li, W., Zhou, X., Wang, W., & Zhang, W. (2012). Regional drought-induced reduction in the biomass carbon sink of Canada's boreal forests. *Proceedings of the National Academy of Sciences*, *109*(7), 2423–2427. https://doi.org/10.1073/pnas.1111576109

Martínez-Vilalta, J., Poyatos, R., Aguadé, D., Retana, J., & Mencuccini, M. (2014). A new look at water transport regulation in plants. *New Phytologist*, *204*(1), 105–115. https://doi.org/10.1111/nph.12912

McDowell, N., Fisher, R., Chonggang, X., Sperry, J. S., Boutz, A., Dickman, L., Gehres, N., Limousin, J. M., Macalady, A., Pangle, R. E., Rasse, D. P., Ryan, M. G., Sevanto, S., Waring, R. H., Williams, A. P., Yepez, E. A., & Pockman, W. T. (2013). Evaluating theories of drought-induced vegetation mortality using a multimodel – experiment framework. *New Phytologist*, *200*, 304–321. https://doi.org/10.1111/nph.12465

McDowell, N. G. (2011). Mechanisms Linking Drought, Hydraulics, Carbon Metabolism, and Vegetation Mortality. *Plant Physiology*, *155*(3), 1051–1059. https://doi.org/10.1104/pp.110.170704

McDowell, N. G., Sapes, G., Pivovaroff, A., Adams, H. D., Allen, C. D., Anderegg, W. R., Arend, M., Breshears, D. D., Brodribb, T., Choat, B., & Cochard, H. (2022). Mechanisms of woody-plant mortality under rising drought, CO2 and vapour pressure deficit. *Nature Reviews Earth & Environment*, *3*(5), 294–308. https://doi.org/10.1038/s43017-022-00272-1

McDowell, N. G., & Sevanto, S. (2010). The mechanisms of carbon starvation: how, when, or does it even occur at all? *New Phytologist*, *186*(2), 264–266. https://doi.org/https://doi.org/10.1111/j.1469-8137.2010.03232.x

McDowell, N. G., Williams, A. P., Xu, C., Pockman, W. T., Dickman, L. T., Sevanto, S., Pangle, R., Limousin, J., Plaut, J., Mackay, D. S., Ogee, J., Domec, J. C., Allen, C. D., Fisher, R. A., Jiang, X., Muss, J. D., Breshears, D. D., Rauscher, S. A., & Koven, C. (2016). Multi-scale predictions of massive conifer mortality due to chronic temperature rise. *Nature Climate Change*, *6*(3), 295–300. https://doi.org/10.1038/nclimate2873

McDowell, N., Pockman, W. T., Allen, C. D., David, D., Cobb, N., Kolb, T., Plaut, J., Sperry, J., West, A., Williams, D. G., & Yepez, E. A. (2008). Mechanisms of plant survival and mortality during drought: why do some plants survive while others succumb to drought? *New Phytologist*, *178*(4), 719–739. https://doi.org/10.1111/j.1469-8137.2008.02436.x

Michaelian, M., Hogg, E. H., Hall, R. J., & Arsenault, E. (2011). Massive mortality of aspen following severe drought along the southern edge of the Canadian boreal forest. *Global Change Biology*, *17*(6), 2084–2094. https://doi.org/10.1111/j.1365-2486.2010.02357.x

Mitchell, P. J., O'Grady, A. P., Pinkard, E. A., Brodribb, T. J., Arndt, S. K., Blackman, C. J., Duursma, R. A., Fensham, R. J., Hilbert, D. W., Nitschke, C. R., Norris, J., Roxburgh, S. H., Ruthrof, K. X., & Tissue, D. T. (2016). An ecoclimatic framework for evaluating the resilience of vegetation to water deficit. *Global Change Biology*, *22*(5), 1677–1689. https://doi.org/10.1111/gcb.13177

Neufeld, H. S., Grantz, D. A., Meinzer, F. C., Goldstein, G., Crisosto, G. M., & Crisosto, C. (1992). Genotypic variability in vulnerability of leaf xylem to cavitation in water-stressed and well-irrigated sugarcane. *Plant Physiology*, *100*(2), 1020–1028. https://doi.org/https://doi.org/10.1104/pp.100.2.1020

O'Neill, B. C., Tebaldi, C., Van Vuuren, D. P., Eyring, V., Friedlingstein, P., Hurtt, G., Knutti, R., Kriegler, E., Lamarque, J. F., Lowe, J., Meehl, G. A., Moss, R., Riahi, K., & Sanderson, B. M. (2016). The Scenario Model Intercomparison Project (ScenarioMIP) for CMIP6.

Geoscientific Model Development, *9*(9), 3461–3482. https://doi.org/10.5194/gmd-9-3461-2016

O'sullivan, O. S., Heskel, M. A., Reich, P. B., Tjoelker, M. G., Weerasinghe, L. K., Penillard, A., Zhu, L., Egerton, J. J. G., Bloomfield, K. J., Creek, D., Bahar, N. H. A., Griffin, K. L., Hurry, V., Meir, P., Turnbull, M. H., & Atkin, O. K. (2017). Thermal limits of leaf metabolism across biomes. *Global Change Biology*, *23*(1), 209–223. https://doi.org/10.1111/gcb.13477

Oleson, K. W., Lawrence, D. M., Bonan, G. B., Flanner, M. G., Kluzek, E., Lawrence, P. J., Levis, S., Swenson, S. C., & Thornton, P. E. (2010). *Technical description of version 4.0 of the Community Land Model (CLM)*. papers2://publication/uuid/6858EE7A-C77E-4439-832D-CEC2791FBEBA

Pammenter, N., & Van der Willigen, C. (1998). A mathematical and statistical analysis of the curves illustrating vulnerability of xylem to cavitation. *Tree Physiology*, *18*, 589–593. https://doi.org/https://doi.org/10.1093/treephys/18.8-9.589

Pan, Y., Birdsey, R. A., Fang, J., Houghton, R., Kauppi, P. E., Kurz, W. A., Phillips, O. L., Shvidenko, A., Lewis, S. L., Canadell, J. G., Ciais, P., Jackson, R. B., Pacala, S. W., McGuire, A. D., Piao, S., Rautiainen, A., Sitch, S., & Hayes, D. (2011). A large and persistent carbon sink in the world's forests. *Science*. https://doi.org/10.1126/science.1201609

Parton, W. ., Scurlock, J. ., Ojima, D. ., Gilmanov, T. ., Scholes, R. ., & Schimel, D. . (1993). Observations and modeling of biomass and soil organic matter dynamics for the grassland biome worldwide. *Global Biogeochemical Cycles*, *7*, 785–809. https://doi.org/https://doi.org/10.1029/93GB02042

Parton, W. J., Schimel, D. S., Cole, C. V., & Ojima, D. S. (1987). Analysis of Factors Controlling Soil Organic Matter Levels in Great Plains Grasslands. *Soil Science Society of America Journal*, *51*(5), 1173–1179. https://doi.org/10.2136/sssaj1987.03615995005100050015x

Peng, C., Liu, J., Dang, Q., Apps, M. J., & Jiang, H. (2002). TRIPLEX: A generic hybrid model for predicting forest growth and carbon and nitrogen dynamics. *Ecological Modelling*, *153*(1–2), 109–130. https://doi.org/10.1016/S0304-3800(01)00505-1

Peng, C., Ma, Z., Lei, X., Zhu, Q., Chen, H., Wang, W., Liu, S., Li, W., Fang, X., & Zhou, X. (2011). A drought-induced pervasive increase in tree mortality across Canada's boreal forests. *Nature Climate Change*, *1*(9), 467–471. https://doi.org/10.1038/nclimate1293

Peng, C., Zhou, X., Zhao, S., Wang, X., Zhu, B., Piao, S., & Fang, J. (2009). Quantifying the response of forest carbon balance to future climate change in Northeastern China: Model validation and prediction. *Global and Planetary Change*, *66*(3–4), 179–194.

https://doi.org/10.1016/j.gloplacha.2008.12.001

Phillips, O. L., Phillips, O. L., Aragão, L. E. O. C., Lewis, S. L., Fisher, J. B., Lloyd, J., López-gonzález, G., Malhi, Y., Monteagudo, A., Peacock, J., Quesada, C. A., Heijden, G. Van Der, Almeida, S., Amaral, I., Arroyo, L., Aymard, G., Baker, T. R., Bánki, O., Blanc, L., … Keeling, H. (2009). Drought Sensitivity of the Amazon Rainforest. *Science*, *323*, 1344–1348. https://doi.org/10.1126/science.1164033

Piao, S., Wang, X., Ciais, P., Zhu, B., Wang, T., & Liu, J. (2011). Changes in satellite-derived vegetation growth trend in temperate and boreal Eurasia from 1982 to 2006. *Global Change Biology*, *17*(10), 3228–3239. https://doi.org/10.1111/j.1365-2486.2011.02419.x

Plaut, J. A., Yepez, E. A., Hill, J., Pangle, R., Sperry, J. S., Pockman, W. T., & Mcdowell, N. G. (2012). Hydraulic limits preceding mortality in a piñon-juniper woodland under experimental drought. *Plant, Cell and Environment*, *35*(9), 1601–1617. https://doi.org/10.1111/j.1365-3040.2012.02512.x

Pugh, T. A. M., Lindeskog, M., Smith, B., Poulter, B., Arneth, A., Haverd, V., & Calle, L. (2019). Role of forest regrowth in global carbon sink dynamics. *Proceedings of the National Academy of Sciences of the United States of America*, *116*(10), 4382–4387. https://doi.org/10.1073/pnas.1810512116

Rosner, S., Johnson, D. M., Voggeneder, K., & Domec, J.-C. (2019). The conifer-curve: fast prediction of hydraulic conductivity loss and vulnerability to cavitation. *Annals of Forest Science*, *76*(3), 1–15. https://doi.org/10.1007/s13595-019-0868-1

Seidl, R., & Rammer, W. (2017). Climate change amplifies the interactions between wind and bark beetle disturbances in forest landscapes. *Landscape Ecology*, *32*(7), 1485–1498. https://doi.org/10.1007/s10980-016-0396-4

Sperry, J. S., & Tyree, M. T. (1988). Mechanism of Water Stress-Induced. *Plant Physiology*, *88*(3), 581–587. https://doi.org/10.1104/pp.88.3.581

Sun, J., Peng, C., McCaughey, H., Zhou, X., Thomas, V., Berninger, F., St-Onge, B., & Hua, D. (2008). Simulating carbon exchange of Canadian boreal forests. II. Comparing the carbon budgets of a boreal mixedwood stand to a black spruce forest stand. *Ecological Modelling*, *219*(3–4), 276–286. https://doi.org/10.1016/j.ecolmodel.2008.03.031

Tague, C. L., McDowell, N. G., & Allen, C. D. (2013). An integrated model of environmental effects on growth, carbohydrate balance, and mortality of Pinus ponderosa forests in the southern Rocky Mountains. *PLoS ONE*, *8*(11), e80286. https://doi.org/10.1371/journal.pone.0080286

Tarnocai, C., & Lacelle., B. (1996). Soil organic carbon of Canada map. *Eastern Cereal and Oilseed Research Centre, Agriculture and Agri-Food Canada, Research Branch, Ottawa, Ontario, Canada*.

Toms, J. D., & Lesperance, M. . (2003). Piecewise regression: a tool for identifying ecological thresholds. *Ecology*, *84*(8), 2034–2041. https://doi.org/https://doi.org/10.1890/02-0472

Trenberth, K. E., Dai, A., Schrier, G. Van Der, Jones, P. D., Barichivich, J., Briffa, K. R., & Sheffield, J. (2014). Global warming and changes in drought. *Nature Climate Change*, *4*(1), 17–22. https://doi.org/10.1038/NCLIMATE2067

Van Mantgem, P. J., Nathan L, S., John C, B., Lori D, D., Jerry F, F., Peter Z, F., Mark E, H., Andrew J, L., Jeremy M, S., Alan H, T., & Thomas T, V. (2009). Widespread increase of tree mortality rates in the western United States. *Science*, *323*(5913), 521–524. https://doi.org/10.1126/science.1165000

Vicente-Serrano, S. M., Quiring, S. M., Peña-Gallardo, M., Yuan, S., & Domínguez-Castro, F. (2020). A review of environmental droughts: Increased risk under global warming? *Earth-Science Reviews*, *201*(September 2019), 102953. https://doi.org/10.1016/j.earscirev.2019.102953

Wang, W., Peng, C., Kneeshaw, D. D., Larocque, G. R., Song, X., & Zhou, X. (2012). Quantifying the effects of climate change and harvesting on carbon dynamics of boreal aspen and jack pine forests using the TRIPLEX-Management model. *Forest Ecology and Management*, *281*, 152–162. https://doi.org/10.1016/j.foreco.2012.06.028

Wang, X., Piao, S., Ciais, P., Li, J., Friedlingstein, P., Koven, C., & Chen, A. (2011). Spring temperature change and its implication in the change of vegetation growth in North America from 1982 to 2006. *Proceedings of the National Academy of Sciences of the United States of America*, *108*(4), 1240–1245. https://doi.org/10.1073/pnas.1014425108

Wang, Y., Hogg, E. H., Price, D. T., Edwards, J., & Williamson, T. (2014). Past and projected future changes in moisture conditions in the Canadian boreal forest. *Forestry Chronicle*, *90*(5), 678–691. https://doi.org/10.5558/tfc2014-134

Williams, A. P., Allen, C. D., Alison K. Macalady, Daniel Griffi, Connie A.Woodhouse, & David M. Meko. (2012). Temperature as a potent driver of regional forest drought stress and tree mortality. *Nature Climate Change*, *3*(3), 292–297. https://doi.org/10.1038/nclimate1693

Williams, A. P., Allen, C. D., Macalady, A. K., Griffin, D., Woodhouse, C. A., Meko, D. M., Swetnam, T. W., Rauscher, S. A., Seager, R., Grissino-Mayer, H. D., Dean, J. S., Cook, E. R., Gangodagamage, C., Cai, M., & Mcdowell, N. G. (2013). Temperature as a potent driver of

regional forest drought stress and tree mortality. *Nature Climate Change*, *3*(3), 292–297. https://doi.org/10.1038/nclimate1693

Williams, J. W., & Jackson, S. T. (2007). Novel climates, no-analog communities, and ecological surprises. *Frontiers in Ecology and the Environment*, *5*(9), 475–482. https://doi.org/10.1890/070037

Zhang, G., Zhang, Y., Dong, J., & Xiao, X. (2013). Green-up dates in the Tibetan Plateau have continuously advanced from 1982 to 2011. *Proceedings of the National Academy of Sciences of the United States of America*, *110*(11), 4309–4314. https://doi.org/10.1073/pnas.1210423110

Zhang, J., Chu, Z., Ge, Y., Zhou, X., Jiang, H., Chang, J., Peng, C., Zheng, J., Jiang, B., Zhu, J., & Yu, S. (2008). TRIPLEX model testing and application for predicting forest growth and biomass production in the subtropical forest zone of China's Zhejiang Province. *Ecological Modelling*, *219*(3–4), 264–275. https://doi.org/10.1016/j.ecolmodel.2008.07.016

Zhou, X., Peng, C., Dang, Q. L., Chen, J., & Parton, S. (2005). Predicting forest growth and yield in northeastern Ontario using the process-based model of TRIPLEX1.0. *Canadian Journal of Forest Research*, *35*(9), 2268–2280. https://doi.org/10.1139/x05-149

Zhou, X., Peng, C., Dang, Q. L., Sun, J., Wu, H., & Hua, D. (2008). Simulating carbon exchange in Canadian Boreal forests. I. Model structure, validation, and sensitivity analysis. *Ecological Modelling*, *219*(3–4), 287–299. https://doi.org/10.1016/j.ecolmodel.2008.07.011

CHAPTER V

GENERAL CONCLUSIONS AND FUTURE DIRECTIONS

5.1. Summary of findings

Given the critical role of Canada's boreal forest in the global carbon budget, quantifying and predicting drought-induced tree mortality and its impacts on this forest's biomass carbon sink capacity is a particular concern under a changing climate. My doctoral work on this subject found that (1) recent knowledge on the mechanisms that cause drought-induced mortality can be integrated into a process-based tree mortality model (TRIPLEX-Mortality), suggesting the TRIPLEX-Mortality model is reliable in the simulation of drought-induced tree mortality and associated impacts on carbon dynamics; (2) From 1970 to 2020, nearly 43% of Canada's forest areas experienced significant increases in tree mortality, most of these areas are located in western Canada. This increase in tree mortality resulted in a significant carbon loss (0.46 ± 0.09 PgC $year^{-1}$). Such findings highlight the significant impacts of drought on Canada's boreal forest dynamics; (3) In the future (2050-2100), climate change will increase the risk of drought-induced tree mortality ($4.2\% \pm 0.4\%$~$7.2\% \pm 0.4\%$) and the associated loss of biomass carbon sink (0.7 ± 0.06 Pg C $year^{-1}$ ~1.29 ± 0.05 Pg C $year^{-1}$). If future climate change follows the high-end climate pathway, not only western but eastern Canada's boreal forest is at significant risk to lose its role as a carbon sink.

5.1.1. The TRIPLEX-Mortality model development and validation

To the best of our knowledge, this study represents the first successful integration of two important physiological tree mortality mechanisms: hydraulic failure (HF) and carbon starvation (CS) into a new process-based model (TRIPLEX-Mortality) at a stand level in Canada's boreal forests. Results from model validation indicate that observed and simulated mortality rates were highly correlated (R^2=0.79; P<0.01; IA=0.94), offering high confidence in applying this model across the boreal forest. To future better the application of this new model, I identified the sensitivity parameters of the model and indicated that the shape parameter (c) for calculating percentage loss of conductivity

(PLC) was the most sensitive parameter when simulating tree mortality. Further application of the model should focus on the calibration of this parameter. Overall, the TRIPLEX-Mortality model intends to contribute to the scientific modeling community by providing a new, groundbreaking approach and contribution to future Earth System Model development under a changing climate.

5.1.2. Drought-induced tree mortality and corresponding impacts on biomass carbon sink capacity of Canada's boreal forests from 1970 to 2020

Modelling results demonstrate that since 1970, droughts have triggered a widespread increase (slope = 0.03%, $P < 0.05$, $R^2 = 0.55$) in tree mortality rates (average=2.7% year^{-1}) across Canada's boreal forests, these accelerate after 2002, and indicate that this increase in tree mortality is a dominant contributing factor to large carbon biomass losses (0.46 ± 0.09 PgC year^{-1}) across Canada's boreal forests. This result thus suggests that previous studies that did not account for the impacts of drought-induced tree mortality on C likely overestimated the biomass carbon sink capacity of Canada's boreal forests. The projected ongoing increase in drought events could potentially have a considerable negative impact on vegetation productivity and health, while also resulting in a reduction in the boreal forest carbon sink potential globally, which would result in accelerated positive feedback that will affect both regional and global climate conditions.

5.1.3. Forecasting drought-induced tree mortality and its impacts on carbon dynamics in Canada's boreal forest by the end of the twenty-first century

I combined the state-of-the-art and validated tree mortality model TRIPLEX-Mortality with the latest, climate model projections in CMIP6, as well as other soil and forest information, to forecast the likelihood of drought-induced tree mortality and its impacts on Canada's boreal forest carbon dynamics by the end of the twenty-first century (2050-2100). I estimated that overall annual tree mortality would be around 4.1%~ 7.1% across the low to high forcing climate change pathways (i.e., from SSP1-2.6 to SSP5-8.5). These results indicate great uncertainty in drought-induced tree mortality under future climate change and a huge risk for forest ecosystem health if future climate change follows the high forcing pathway (i.e., SSP5-8.5). In addition, mortality rates tend to increase in all climate change scenarios and increase with increasing radiative forcing in SSP scenarios (i.e., from SSP1 to SSP5), peaking in SSP5-8.5 scenarios (increases trend with 0.008%

year^{-1} for SSP1 and with 0.05% year^{-1} for SSP5). The spatial extent of increased drought-induced tree mortality increases under the higher forcing and warming scenarios, especially for the western region of Canada. This increased mortality can result in a huge reduction (0.74 ± 0.05 PgC year^{-1} ~ 1.28 ± 0.05 PgC year^{-1}) in the biomass carbon sink capacity of Canada's boreal forests. Similar to the mortality, the spatial extent of reduction in biomass carbon sink loss increases under the higher forcing and warming scenarios, especially for the western region of Canada. If future climate change follows the high-end forcing pathway (SSP5-8.5 scenario), the eastern region of Canada's boreal forest also has a significant risk to lose its role as a carbon sink.

5.2. Uncertainties and future directions

Our approaches and efforts to model drought-induced tree mortality represent the first step toward a new generation of process models of TRIPLEX that are capable of integrating key tree mortality processes into the state-of-the-art model for Canada's boreal forests. Field measurements and mechanistic models made it possible to represent the coupling between carbon and hydraulic states of trees during drought over both short and long-time scales, allowing mechanistically constrained model parameterization and large scaling potential (De Kauwe et al., 2020; McDowell et al., 2022). Nevertheless, some modeling challenges remain for those processes that are currently represented in the TRIPLEX-Mortality model, partly due to the poor understanding of the interactive mechanisms of drought-induced mortality (Choat et al., 2018; McDowell et al., 2013). For example, there are much feedbacks between carbohydrates and hydraulic dynamics that can accelerate or buffer mortality during drought. In theory, simulated PLC and NSC should capture many of these feedbacks regardless of the spatial or temporal scale of the simulation. However, rigorously quantifying the interdependencies of these mechanisms is a huge challenge (McDowell et al., 2013). In addition, the stomatal behavior of isohydry and anisohydric plant is very different under drought conditions (McDowell et al., 2008). This results in significant differences in carbon and water dynamics in these two plants under the same drought intensities. And the identification of isohydry and anisohydric properties of many plant species still requires effort. Although the stomatal conductance model of the TRIPLEX-Mortality model takes into account these effects to the extent possible. However, to accurately simulate the internal carbon and water dynamics of different vegetation under drought conditions, and to quantify the contribution of the two main mechanisms (i.e., HF and CS) to tree mortality still requires the academic community to continue

to make progress in identifying isohydry and anisohydric properties of plant and related tree mortality mechanisms. Moreover, some other processes associated with drought-induced tree mortality need to be better represented in models. For example, drought-induced water stress not only affects ecosystem functions during drought events, but it can also cause a lag effect in vegetation that can last for years (Kannenberg et al., 2020). This phenomenon, commonly referred to as the "drought legacy effect," has yet to be fully captured by the model, resulting in uncertainties in simulated tree mortality. Such uncertainties in drought-induced tree mortality rates may also cause uncertainties in simulated biomass carbon loss. In addition, processes such as vegetation regeneration, which have yet to be integrated into the model, may also offset mortality to some extent, leading to uncertainties in drought-induced tree mortality and corresponding impacts on biomass carbon sink capacity.

To improve the ability of our process-based TRIPLEX-Mortality model in simulating drought-induced mortality, several processes need to be added, such as changes in canopy leaf area during drought events, coupling hydraulic architecture with stomatal conductance, and determining the dependence of plant water status on soil water potential vs on vapor pressure deficit (VPD) (Choat et al., 2018; Hendrik & Maxime, 2017; Oogathoo et al., 2020). First, during drought events, many forest trees attempt to avoid the influence of drought stress on plant water content by leaf shedding (Limousin et al., 2010; Vilagrosa et al., 2003). However, due to the complex dynamics involved in leaf shedding, models poorly capture this effect (Dahlin et al., 2017). Second, despite recent progress in modelling relationships between hydraulic architecture and stomatal conductance under drought conditions (Mackay et al., 2015), non-stomatal limitations to photosynthesis during drought should be incorporated into models to better simulate drought-induced mortality (Hendrik & Maxime, 2017). In addition, the relationship between soil and the status of plant water is a key component of the HF pathway. However, many models only simulate soil water content by using the single water bucket technique, which does not fully capture these relationships. Future models need to incorporate vertical gradients into soil moisture potential, root distribution and soil-root resistance alterations caused by soil drying (Christoffersen et al., 2016; De Kauwe et al., 2015). Finally, on the carbon side, models require an improved understanding of carbohydrate storage regulation under drought condition. NSC content is a net product of GPP and multiple sinks, including storage, respiration, growth, and defense, and linking each of these allocations through

empirical and model-based studies is essential for mortality simulation (McDowell et al., 2013). In my study, relationships between mortality in conjunction with hydraulic risk (PLC) or carbon dynamics (NSC) were fitted based on mortality observations. However, observed tree mortality rates only cover a range of mortality rates (from permanent sampling plots) between 0 to 40%. This may generate uncertainties in plots where mortality is greater than 40%. The uncertainty sources of this study may potentially be due to the using empirical thresholds for PLC and NSC owning the lack of in situ observed PLC and NSC data. Another source of uncertainty is the absence of acclimation in our model. This is mainly due to the lack of knowledge of what parameters acclimate and at what rate under future climate change (McDowell et al., 2022). In model prediction, the values of key parameters are based on historical and empirical values, which may cause uncertainty of the model simulation results under future climate change conditions.

Despite the abovementioned limitations and challenges, I remain confident that our TRIPLEX-Mortality model, which has integrated advanced physiological mechanisms and has been well calibrated and validated against observed data at a stand scale provides useful and meaningful results. The TRIPLEX-Mortality model offers a quantitative understanding and a new tool for simulating drought-induced mortality dynamics and shows great potential in predicting the impacts of drought-induced mortality on carbon sinks and sources across Canadian boreal forests under past and future climate change conditions.

5.3. Concluding remarks

My Ph.D. study has led to the groundbreaking development of a new process-based model (TRIPLEX-Mortality) for simulating and forecasting drought-induced tree mortality and corresponding impacts on carbon dynamics in Canada's boreal forests under a changing climate. The TRIPLEX-Mortality model has filled in research gaps in our understanding of increasing tree mortality on large-scale carbon dynamics. This helps us to better understand how climate change will affect tree mortality and forest ecosystem biomass carbon dynamics and to reduce the uncertainties in the estimation of terrestrial ecosystem carbon sinks. Furthermore, this work could help forest managers and policy-makers to maintain the sustainability of forest resources and reduce the potential risk of boreal forests converting from carbon sinks to sources in a changing world.

5.4. References

Choat, Brendan., Brodribb, T. J., Brodersen, C. R., Duursma, R. A., López, Rosana., & Medlyn, B. E. (2018). Triggers of tree mortality under drought. Nature, 558(7711), 531–539. https://doi.org/10.1038/s41586-018-0240-x

Christoffersen, B. O., Gloor, M., Fauset, S., Fyllas, N. M., Galbraith, D. R., Baker, T. R., Kruijt, B., Rowland, L., Fisher, R. A., Binks, O. J., Sevanto, S., Xu, C., Jansen, S., Choat, B., Mencuccini, M., McDowell, N. G., & Meir, P. (2016). Linking hydraulic traits to tropical forest function in a size-structured and trait-driven model (TFS v.1-Hydro). Geoscientific Model Development, 9(11), 4227–4255. https://doi.org/10.5194/gmd-9-4227-2016

Dahlin, K. M., Ponte, D. Del, Setlock, E., & Nagelkirk, R. (2017). Global patterns of drought deciduous phenology in semi-arid and savanna-type ecosystems. Ecography, 40(2), 314–323. https://doi.org/10.1111/ecog.02443

De Kauwe, M. G., Medlyn, B. E., Ukkola, A. M., Mu, M., Sabot, M. E. B., Pitman, A. J., Meir, P., Cernusak, L. A., Rifai, S. W., Choat, B., Tissue, D. T., Blackman, C. J., Li, X., Roderick, M., & Briggs, P. R. (2020). Identifying areas at risk of drought-induced tree mortality across South-Eastern Australia. Global Change Biology, 26(10), 5716–5733. https://doi.org/10.1111/gcb.15215

De Kauwe, M. G., Zhou, S. X., Medlyn, B. E., Pitman, A. J., Wang, Y. P., Duursma, R. A., & Prentice, I. C. (2015). Do land surface models need to include differential plant species responses to drought? Examining model predictions across a mesic-xeric gradient in Europe. Biogeosciences, 12(24), 7503–7518. https://doi.org/10.5194/bg-12-7503-2015

Hendrik, D., & Maxime, C. (2017). Assessing drought-driven mortality trees with physiological process-based models. Agricultural and Forest Meteorology, 232, 279–290. https://doi.org/10.1016/j.agrformet.2016.08.019

Kannenberg, S. A., Schwalm, C. R., & Anderegg, W. R. L. (2020). Ghosts of the past: how drought legacy effects shape forest functioning and carbon cycling. Ecology Letters, 23(5), 891–901. https://doi.org/10.1111/ele.13485

Limousin, J. M., Longepierre, D., Huc, R., & Rambal, S. (2010). Change in hydraulic traits of Mediterranean Quercus ilex subjected to long-term throughfall exclusion. Tree Physiology, 30(8), 1026–1036. https://doi.org/10.1093/treephys/tpq062

Mackay, D. S., Roberts, D. E., Ewers, B. E., Sperry, J. S., McDowell, N. G., & Pockman, W. T. (2015). Interdependence of chronic hydraulic dysfunction and canopy processes can improve integrated models of tree response to drought. Water Resources Research, 51(8), 6156–6176.

https://doi.org/10.1002/2015WR017244

McDowell, N., Fisher, R., Chonggang, X., Sperry, J. S., Boutz, A., Dickman, L., Gehres, N., Limousin, J. M., Macalady, A., Pangle, R. E., Rasse, D. P., Ryan, M. G., Sevanto, S., Waring, R. H., Williams, A. P., Yepez, E. A., & Pockman, W. T. (2013). Evaluating theories of drought-induced vegetation mortality using a multimodel – experiment framework. New Phytologist, 200, 304–321. https://doi.org/10.1111/nph.12465

McDowell, N., Pockman, W. T., Allen, C. D., David, D., Cobb, N., Kolb, T., Plaut, J., Sperry, J., West, A., Williams, D. G., & Yepez, E. A. (2008). Mechanisms of plant survival and mortality during drought: why do some plants survive while others succumb to drought? New Phytologist, 178(4), 719–739. https://doi.org/10.1111/j.1469-8137.2008.02436.x

McDowell, N. G., Sapes, G., Pivovaroff, A., Adams, H. D., Allen, C. D., Anderegg, W. R., Arend, M., Breshears, D. D., Brodribb, T., Choat, B., & Cochard, H. (2022). Mechanisms of woody-plant mortality under rising drought, CO2 and vapour pressure deficit. Nature Reviews Earth & Environment, 3(5), 294–308. https://doi.org/10.1038/s43017-022-00272-1

Oogathoo, S., Houle, D., Duchesne, L., & Kneeshaw, D. (2020). Vapour pressure deficit and solar radiation are the major drivers of transpiration of balsam fir and black spruce tree species in humid boreal regions, even during a short-term drought. Agricultural and Forest Meteorology, 291(2019), 108063. https://doi.org/10.1016/j.agrformet.2020.108063

Vilagrosa, A., Bellot, J., Vallejo, V. R., & Gil-Pelegrín, E. (2003). Cavitation, stomatal conductance, and leaf dieback in seedlings of two co-occurring Mediterranean shrubs during an intense drought. Journal of Experimental Botany, 54(390), 2015–2024. https://doi.org/10.1093/jxb/erg221